

1-1-2006

## Performance of plate fin compact heat exchangers

Ibrahim Mohamed Khalil  
*University of Nevada, Las Vegas*

Follow this and additional works at: <https://digitalscholarship.unlv.edu/rtds>

---

### Repository Citation

Khalil, Ibrahim Mohamed, "Performance of plate fin compact heat exchangers" (2006). *UNLV Retrospective Theses & Dissertations*. 2058.  
<http://dx.doi.org/10.25669/xiz7-i3d7>

This Thesis is protected by copyright and/or related rights. It has been brought to you by Digital Scholarship@UNLV with permission from the rights-holder(s). You are free to use this Thesis in any way that is permitted by the copyright and related rights legislation that applies to your use. For other uses you need to obtain permission from the rights-holder(s) directly, unless additional rights are indicated by a Creative Commons license in the record and/or on the work itself.

This Thesis has been accepted for inclusion in UNLV Retrospective Theses & Dissertations by an authorized administrator of Digital Scholarship@UNLV. For more information, please contact [digitalscholarship@unlv.edu](mailto:digitalscholarship@unlv.edu).

# PERFORMANCE OF PLATE FIN COMPACT HEAT EXCHANGERS

by

Ibrahim Mohamed Khalil

Bachelor of Science in Mechanical Engineering  
Alexandria University, Alexandria  
July 2000

A thesis submitted in partial fulfillment  
of the requirements for the

**Master of Science Degree in Engineering**  
**Department of Mechanical Engineering**  
**Howard R. Hughes College of Engineering**

**Graduate College**  
**University of Nevada, Las Vegas**  
**December 2006**

UMI Number: 1441715

### INFORMATION TO USERS

The quality of this reproduction is dependent upon the quality of the copy submitted. Broken or indistinct print, colored or poor quality illustrations and photographs, print bleed-through, substandard margins, and improper alignment can adversely affect reproduction.

In the unlikely event that the author did not send a complete manuscript and there are missing pages, these will be noted. Also, if unauthorized copyright material had to be removed, a note will indicate the deletion.

**UMI<sup>®</sup>**

---

UMI Microform 1441715

Copyright 2007 by ProQuest Information and Learning Company.

All rights reserved. This microform edition is protected against unauthorized copying under Title 17, United States Code.

ProQuest Information and Learning Company  
300 North Zeeb Road  
P.O. Box 1346  
Ann Arbor, MI 48106-1346

Copyright by Ibrahim Mohamed Khalil 2006  
All Rights Reserved



## **Thesis Approval**

The Graduate College  
University of Nevada, Las Vegas

This Thesis prepared by **Ibrahim M. Khalil**

Entitled

### **Performance of Plate Fin Compact Heat Exchangers**

was approved in partial fulfillment of the requirements for the degree of

### **Master of Science in Mechanical Engineering**

By the undersigned on October 20, 2006

Robert Boehm, Examination Committee Chair

Samir.F. Moujaes, Examination Committee Member

Yi-Tung Chen, Examination Committee Member

Moses Karakouzian, Graduate Faculty Representative

A handwritten signature in black ink, appearing to be "Robert Boehm", written over a horizontal line.

Dean of the Graduate College

Thesis Approval Form  
Provided by the Graduate College

## ABSTRACT

### **Performance of Plate Fin Compact Heat Exchangers**

by

Ibrahim Mohamed Khalil

Dr. Robert F. Boehm, Examination Committee Chair  
Professor of Mechanical Engineering  
University of Nevada, Las Vegas

Heat exchangers design includes the consideration of both the heat transfer rates between two fluids and the pumping power required to overcome fluid friction and push the fluids through the heat exchangers. In gas flow heat exchangers, the friction power limitations force the designer to select moderately low mass velocities. Low mass velocities with low thermal conductivities will result in low heat transfer rate per unit of the surface area. Thus a large surface area is a typical characteristic of a gas flow heat exchanger.

The problem of a large required area can be solved by using large area density which will lead to *compact heat exchangers*. The main target of this study is to provide full explanation of previous comparison methods of compact heat exchangers surfaces (plain, strip, louvered, wavy, pin, perforated and vortex) used in plate fin compact heat exchangers and to generalize these methods in order to identify the advantages and disadvantages of each type of geometry based on required size, entropy generation, pumping power, weight, and cost.

## TABLE OF CONTENTS

ABSTRACT.....	iii
LIST OF FIGURES.....	vi
LIST OF TABLES .....	vii
NOMENCLATURE.....	viii
ACKNOWLEDGMENTS.....	x
CHAPTER 1 INTRODUCTION AND BACKGROUND.....	1
1.1 Compact Heat Exchangers Surfaces .....	2
1.1.1 Plain Fin Geometry .....	2
1.1.2 Strip Fin Geometry.....	2
1.1.3 Louvered Fin Geometry .....	2
1.1.4 Wavy Fin Geometry .....	3
1.1.5 Pin Fin Geometry .....	3
1.1.6 Perforated Fin Geometry.....	4
1.1.7 Vortex Generator Geometry.....	4
1.2 Compact Heat Exchangers Design Procedures.....	8
1.3 Heat Transfer and Flow Friction Design Data .....	10
1.4 Core Geometry Relations.....	10
1.5 Objective of the Study.....	11
1.6 Geometry Characteristics .....	11
CHAPTER 2 REVIEW OF CURRENT METHODOLOGIES FOR DESIGN PLATE FIN HEAT EXCHANGER.....	19
2.1 Basic Concepts of Heat Exchangers .....	19
2.1.1 Direct Test Data .....	19
2.1.2 Surface Selection.....	20
2.2 Design Procedures.....	22
2.3 Entropy Generation .....	22
2.4 Vortex Generators .....	23
2.5 Minimum Weight of Compact Heat Exchangers .....	24
2.6 Compact Heat Exchanger Theories.....	24
2.7 Ranking of Compact Heat Exchangers .....	25
CHAPTER 3 PLATE FIN COMPACT HEAT EXCHANGERS SIZING AND COMPARISON.....	26
3.1 Sizing Procedures Overview .....	26
3.2 Problem Data.....	26



3.3	Assumptions for Heat Transfer Analysis .....	27
3.4	Calculation Steps.....	30
3.5	Entropy Generation .....	45
3.6	Combination of Different Surfaces .....	51
3.7	Minimum Weight of CHE's.....	52
3.8	Pumping Power Calculation.....	52
CHAPTER 4 DATA AND RESULTS ANALYSIS .....		53
4.1	Sizing Data Analysis and Comparison.....	53
4.2	Results Validation .....	63
4.3	Entropy Generation .....	68
4.3.1	Strip Fins .....	68
4.3.2	Louvered Fins.....	70
4.3.3	Wavy Fin .....	72
4.3.4	Plain Fin .....	73
4.3.5	Vortex Generator.....	74
4.4	Pumping Power .....	76
4.4.1	Plain Fin Surfaces .....	76
4.4.2	Louvered Fin Surfaces .....	77
4.4.3	Wavy Fin Surfaces .....	77
4.4.4	Perforated and Vortex Generator Surfaces .....	77
4.4.5	Strip Fin Surfaces.....	78
4.5	Combination Between Two Different Surfaces .....	79
4.6	Final Surface Ranking.....	80
CHAPTER 5 CONCLUSIONS AND RECOMMENDATIONS .....		81
5.1	Sizing Results.....	82
5.2	Entropy Generation .....	83
5.3	Minimum Weight.....	83
5.4	Future Work and Recommendations.....	84
APPENDIX A CHARACTERISTIC CURVES OF HIGH PERFORMANCE SURFACES OF PLATE FIN HEAT EXCHANGERS .....		85
APPENDIX B MATHCAD CODE.....		121
B.1	Sizing of Surface 11.94 T Plain .....	121
BIBLIOGRAPHY .....		137
VITA.....		142

## LIST OF FIGURES

Figure 1.1a	Plain Fin Surface .....	4
Figure 1.1b	Strip Fin Surface .....	5
Figure 1.1c	Louvered Fin Surface .....	5
Figure 1.1d	Wavy Fin Surface.....	5
Figure 1.1e	Pin Fin Surface .....	6
Figure 1.1f	Perforated Generator Surface .....	6
Figure 1.1g	Vortex Fin Surface .....	6
Figure 1.2	Methodology of Heat Exchanger Design .....	8
Figure 1.3	Symmetric Pair of Longitudinal Vortices .....	13
Figure 1.4a	Schematic of Plate Fin Heat Exchanger.....	15
Figure 1.4b	Compact Heat Exchanger Surface with Fins in the Form of V.G.....	15
Figure 1.4c	Rectangular Winglets Elements .....	15
Figure 1.5	Comparison of Vortex Surfaces with Louvered and Strip Surfaces .....	16
Figure 1.6	Eight Periodic WVG Fin Plate Heat Exchanger Elements .....	17
Figure 1.7	Nusselt Number and Friction Factor Enhancement .....	17
Figure 4.1	Volume Comparison of Different Types of Plain Surfaces .....	63
Figure 4.2	Volume Comparison of Different Types of Louvered Surfaces .....	63
Figure 4.3	Total Area Comparison of Different Types of Surfaces .....	64
Figure 4.4	Envelop for Best Plain-Fin Surface Performance .....	65
Figure 4.5	Envelop for Best Louvered-Fin Surface Performance .....	65
Figure 4.6	Area Goodness Factor ( $j/f$ ) of Different Types of Surfaces .....	66
Figure 4.7	Entropy Generation Factor for the First Group of Strip Surfaces .....	67
Figure 4.8	Entropy Generation Factor for the Second Group of Strip Surfaces .....	68
Figure 4.9	Entropy Generation Factor for Louvered Surfaces .....	70
Figure 4.10	Entropy Generation Factor for Wavy Surfaces .....	71
Figure 4.11	Entropy Generation Factor for Vortex Surface .....	73
Figure 5.1	Frontal Area Comparison of Various Geometries .....	81

## LIST OF TABLES

Table 1.1	Different Types of Geometries.....	7
Table 3.1	Problem Formulation .....	27
Table 4.1	Frontal and Free Flow Area for Plain Surfaces.....	54
Table 4.2	Volume and Dimensions of Plain Fin Surfaces .....	55
Table 4.3	Frontal and Free Flow Area for Louvered Surfaces.....	56
Table 4.4	Volume and Dimensions of Louvered Fin Surfaces .....	57
Table 4.5	Frontal and Free Flow Area for Strip Surfaces .....	58
Table 4.6	Volume and Dimensions of Strip Fin Surfaces.....	59
Table 4.7	Frontal and Free Flow Area for Wavy Surfaces .....	60
Table 4.8	Volume and Dimensions of Wavy Fin Surfaces .....	60
Table 4.9	Frontal and Free Flow Area for Pin Surfaces.....	61
Table 4.10	Volume and Dimensions of Pin Fin Surfaces .....	61
Table 4.11	Frontal and Free Flow Area for Perforated and V. G. Surfaces.....	62
Table 4.12	Volume and Dimensions of Perforated and V.G Surfaces.....	62
Table 4.13	Ascending Order for Strip Geometry .....	69
Table 4.14	Ascending Order for Louvered Geometry .....	70
Table 4.15	Ascending Order for Wavy Geometry .....	72
Table 4.16	Ascending Order for Plain Geometry .....	72
Table 4.17	Entropy Generation Classification of Different Surfaces .....	73
Table 4.18	Entropy Generation Ascending Order for Best 30 Surfaces .....	74
Table 4.19	Pumping Power Requirements on Both Sides for Plain Surfaces.....	75
Table 4.20	Pumping Power Requirements on Both Sides for Louvered Surfaces.....	76
Table 4.21	Pumping Power Requirements on Both Sides for Wavy Surfaces .....	76
Table 4.22	Pumping Power Requirements on Both Sides for Perforated, V.G .....	76
Table 4.23	Pumping Power Requirements on Both Sides for Strip Surfaces .....	77
Table 4.24	The Effect of Combination of Two Different Surfaces.....	78
Table 4.25	Performance Aspects of Conventional High Performance Surfaces.....	79

## NOMENCLATURE

$A$	Total transfer area of one side of exchanger, ft <sup>2</sup> or m <sup>2</sup>
$a$	Plate thickness, ft or m
$Ab$	Base plate area, ft <sup>2</sup> or m <sup>2</sup>
$Ac$	Free-flow area of one side, ft <sup>2</sup> or m <sup>2</sup>
$Af$	Total fin area on one side, ft <sup>2</sup> or m <sup>2</sup>
$Afr$	Frontal area of one side, ft <sup>2</sup> or m <sup>2</sup>
$Ar$	The ratio of fin area to total heat transfer area on one side
$b$	Plate spacing, ft or m
$Cc$	Flow stream capacity rate of cold side fluid
$Ch$	Flow stream capacity rate of cold side fluid
$cp$	Specific heat at constant pressure
$Dh$	Hydraulic diameter of any internal passage, ft or m
$f$	Mean friction factor
$fo$	Mean friction factor for reference surface
$G$	Flow stream mass velocity, kg/m <sup>2</sup> s
$h$	Convective heat transfer coefficient, w/ m <sup>2</sup> K
$j$	Colburn factor
$jo$	Colburn factor for reference surface
$k$	Thermal conductivity, w/mK
$Kc$	Contraction loss coefficient at entrance
$Ke$	Expansion loss coefficient at exit
$L$	Flow length on one side, ft or m
$l$	Fin length from root to center, ft or m
$Lstack$	No flow length, ft or m
$m$	Correction factor for friction factor
$N$	Entropy factor
$n$	Correction factor for colburn factor
$nf$	Number of fins per meter
$NTU$	Number of heat transfer units
$Nu$	Nusselt Number

$P_{cc}$	Pumping power on cold side, w
$P_{hh}$	Pumping power on hot side, w
$Pr$	Prandtl number
$Q$	Heat transfer rate, w
$Re$	Reynolds number
$Re_o$	Reynolds number for reference surface
$r_h$	Hydraulic radius, ft or m
$S_p$	Entropy generation rate per unit exchanger length
$St$	Stanton number
$T$	Absolute temperature, K
$T_i$	Inlet temperature, K
$T_w$	Wall temperature, K
$U$	Overall thermal conductance, w/m <sup>2</sup> K
$V$	Total exchanger volume, $ft^3, m^3$
VG	Vortex generator
$W$	Mass flow rate, kg/s
WVG	Wing vortex generator
$W_s$	Weight of one side of the heat exchanger, kg
$\alpha$	Ratio of total area on one side to total exchanger volume
$\beta$	Ratio of total area on one side to volume between plates
$\beta^*$	Angle of attack for vortex element
$\Delta P$	Pressure drop on one side, kPa
$\delta$	Fin thickness, ft or m
$\varepsilon$	Exchanger Effectiveness
$\eta_f$	Fin Efficiency
$\eta_o$	Total surface effectiveness
$\sigma$	Ratio of free-flow to frontal area of one side of exchanger
$\mu$	Dynamic viscosity, Pa s
$\rho$	Density, Kg/m <sup>3</sup>

## ACKNOWLEDGMENTS

First, I would like to thank Almighty Allah for His Help. This work, and every other task I accomplished, was completed with Allah's blessings first; my humble efforts come second. Prophet Mohamad (PBUH) said: "He who doesn't thank people doesn't thank Allah," (Abu Dawud, Book 41: 4793). Below I express my appreciation and gratitude to the people who have helped me complete this work.

I would like to start by thanking my parents, Mohamed Khalil and Hamed Hafez. They helped me more than anyone can imagine. Mr. Mohamed Khalil is a true example for giving without limits. He taught me manners. Mrs. Hamed Hafez enlightened my life by her mercy. I would never forget their support in my life.

I would like to thank my aunt Assmaa Hafez for her unforgettable favor in my life.

I would also like to thank Dr. Robert Boehm for guiding me in the development of this work and answering all my questions. Really I do appreciate his attitude towards me.

I would also like to thank our department chair Dr. Mohammed Trabia for his help and guidance during my study.

Special gratitude is expressed to my grandmother Soaad Mustafa for raising me and for her encouragement. May her soul rest in paradise.

Finally, I would like to thank my twin sister Eman and my brothers Akram and Eslam.

## CHAPTER 1

### INTRODUCTION AND BACKGROUND

The importance of compact heat exchangers (CHEs) has been recognized in aerospace, automobile, gas turbine power plant, and other industries for the last 50 years or more. This is due to several factors, such as packaging constraints, sometimes high performance requirements, low cost, and the use of air or gas as one of the fluids in the exchanger. For nearly two decades, the additional driving factors for heat exchanger design have been reducing energy consumption for operation of heat exchangers and process plants, and minimizing the capital investment (Hesselgreaves, 2001).

The use of plate heat exchangers and other CHEs has been increasing due to some of the inherent advantages mentioned above. In addition, CHEs offer the reduction of floor space, decrease in fluid inventory in closed system exchangers, use as multifunctional units, and tighter process control with liquid and phase-change working fluids.

Heat transfer and flow friction single-phase design correlations are given for the most commonly used modern heat transfer surfaces in CHEs. The main design considerations for compact heat exchangers are surface size, shape, weight and pumping power.

## 1.1 Compact Heat Exchangers Surfaces

The following sub-sections briefly explain the different geometries of CHE's (Kays and London, 1984). The heat transfer enhancement mechanism for each type of geometry will be explained as well.

### 1.1.1 Plain Fin Geometry

The plain fin surfaces include rectangular passages, triangular passages, and passages with rounded and reentry corners and characterized by long uninterrupted flow passages used to increase the total surface area as shown in Figure 1.a (Hall, 2003). Plain surfaces considered in this study are shown in Table 1.1.

The semi-descriptive method of designating plain fin surfaces refers to the number of fin per inch transverse to the flow direction. Thus surface 19.86 has 19.86 fins per inch. The number given for plain surface denotes for the number of fins per inch and the suffix T denotes for triangular flow passage.

### 1.1.2 Strip Fin Geometry

The strip fin surfaces are similar in principle to the louvered fin surfaces, the only difference being that the short sections of fins are aligned entirely with the flow direction. With the strip fin configuration it is feasible to have very short flow length fins and thus very high heat transfer coefficients as shown in Figure 1.b (Hall, 2003). The designation scheme for the strip fin surfaces is essentially the same as that used for the louvered surfaces. Strip surfaces considered in this study are shown in Table 1.1.

### 1.1.3 Louvered Fin Geometry

The louvered fin surfaces are characterized by fins that have been cut and bent out into the flow stream at frequent intervals. The purpose of louvering is to break the boundary layers so as to yield higher heat transfer than are possible with plain fins under



the same flow conditions as shown in Figure 1.c (Hall, 2003). The louvered fin surfaces are designated by two figures. The first refers to the length of the louvered fin in the flow direction, the second to the fins per inch transverse to the flow. Thus surface 3/8–11.1 has 3/8 in louvers and 11.1 fins per inch. Louvered surfaces considered in this study are shown in Table1.1.

#### 1.1.4 Wavy Fin Geometry

The wavy fin surfaces are also high-performance surfaces with performance quite similar to the louvered and strip-fin surfaces. The change in flow direction induced by the fins, caused boundary-layer separation with effects similar to complete fin interruption as shown in Figure.1.d (Hall, 2003). The wavy-fin surfaces are designated by two figures, giving the number of fins per-inch and the wavelength, followed by the letter W. Thus surface 11.5 – 3/8 W has 11.5 fins per inch and a complete wave every 3/8 in. Wavy surfaces considered in this study are shown in Table1.1.

#### 1.1.5 Pin Fin Geometry

Pin fin surfaces are another example of the plate-fin system, where the purpose is to achieve very high heat transfer coefficients by maintaining thin boundary layers on the fins as shown in Figure 1.e (Hall, 2003). By constructing the fins from small diameter wire, the effective flow length of the fins can be very small indeed. The pin-fin surfaces are characterized by quite high friction factors attributable primarily to form drag associated with the boundary layer separation, that occurs on the pins. Nevertheless, the very high heat transfer coefficients attainable often more than offset the high friction factors when the final heat exchanger design is considered.

The designation scheme for the pin fin surfaces is not descriptive. Pin surfaces considered in this study are shown in Table1.1.

### 1.1.6 Perforated Fin Geometry

Perforated fin surface is designated simply by the number of fins per inch transverse to the flow and the letter P as shown in Figure 1.f (Stevens, 2001). Holes cut out of the fins again provide boundary layer interruption. The friction factors for this surface are quite low (promising surface). Perforated surface considered in this study is shown in Table1.1.

### 1.1.7 Vortex Generator Geometry

Vortex generator surface depends on generating longitudinal vortices that enhances thermal mixing and increasing the heat transfer coefficient as shown in Figure 1.g (Brockmeier, 1993).

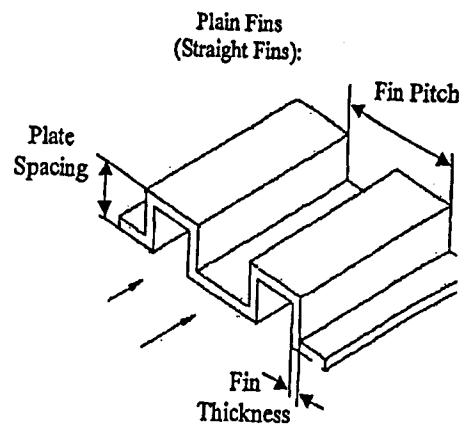


Figure 1.a Plain Fin Surface (Hall, 2003)

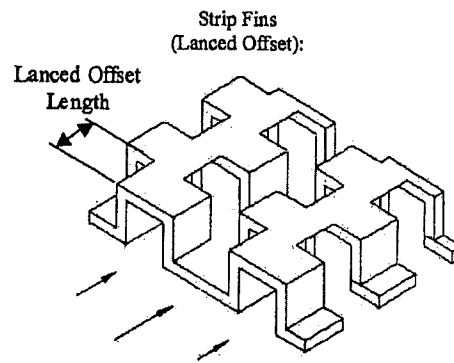


Figure 1.b Strip Fin Surface (Hall, 2003)

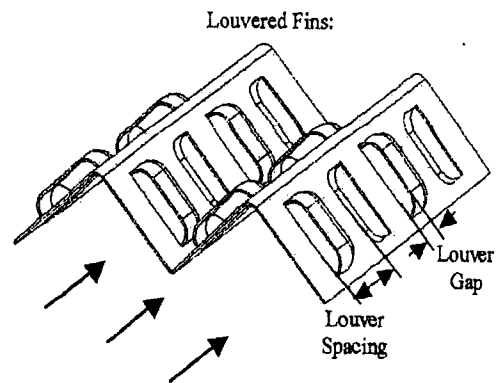


Figure 1.c Louvered Fin Surface (Hall, 2003)

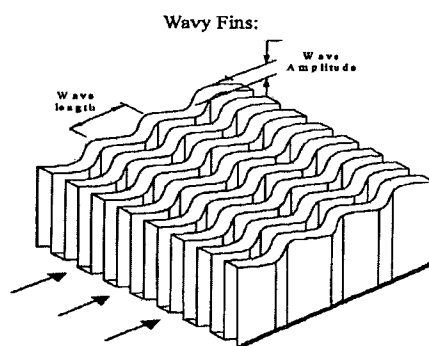


Figure 1.d Wavy Fin Surface (Hall, 2003)

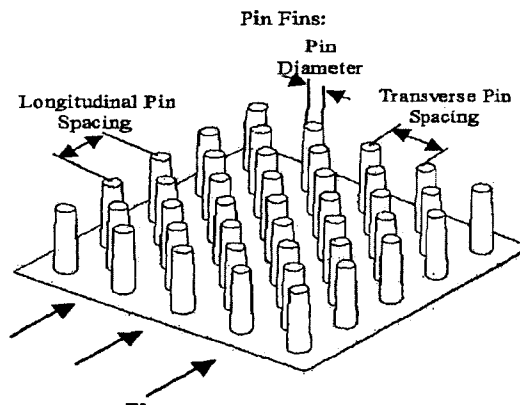


Figure.1.e Pin Fin Surface (Hall, 2003)

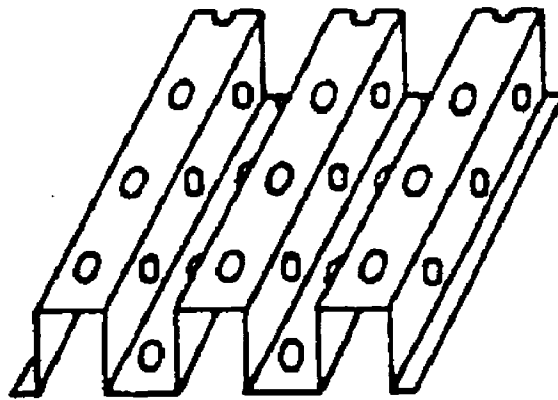


Figure 1.f Vortex Generator Surface (Brockmeier, 1993)

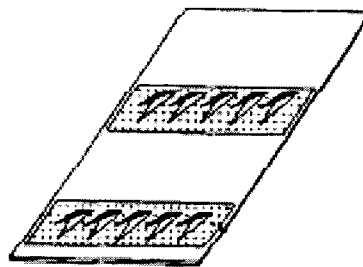


Figure 1.g Perforated Fin Surface (Stevens, 2001)

Table 1.1 Different Types of Geometries

Surfaces Analyzed						
Plain	Strip	Louvered	Wavy	Pin	Perforated	Vortex
2.0	1/4s-11.1	3/8-6.06	11.44-3/8	AP-1	13.95 (P)	Vortex Gen.
3.01	1/8-15.2	3/8 a-6.06	11.5-3/8	AP-2		
3.97	1/8-13.95	1/2-6.06	17.8-3/8	PF-4(F)		
5.3	1/8-15.61	1/2 a-6.06		PF-9(F)		
6.2	1/8-19.86	3/8-8.7		PF-10(F)		
9.03	1/9-22.68	3/8 a-8.7				
11.11	1/9-25.01	3/16-11.1				
11.11a	1/9-24.12	1/4-11.1				
14.77	1/10-27.03	1/4 b-11.1				
15.08	1/10-19.35	3/8-11.1				
19.86	1/10-19.74	3/8b-11.1				
10.27T	3/32-12.22	1/2-11.1				
11.94T	1/2-11.9 D	3/4-11.1				
12.00T	1/4-15.4 D	3/4b-11.1				
16.96T	1/6-12.18 D					
25.79T	1/7-15.75D					
30.33T	1/8-16.00D					
46.45T	1/8-16.12D					
	1/8-19.82D					
	1/8-20.06D					
	1/8-16.12T					

The designation scheme for the surfaces considered in Table 1.1 is:

- 19.86 Plain : The surface 19.86 has 19.86 fins per inch
- 1/8-13.95 Strip : The surface 1/8–13.95 has 1/8 in strips and 13.95 fins per inch
- 3/8-11.1 Louvered : The surface 3/8–11.1has 3/8 in louvers and 11.1fins per inch
- 11.5-3/8 Wavy : The surface has 11.5 fins per in and wave length equal 3/8 in
- 13.95 (P) : The number of fins per inch transverse to the flow is13.95

## 1.2 Compact Heat Exchangers Design Procedures

The methodology of achieving optimum heat exchanger design (Kays and London, 1984) is a complex one because so many design factors may contribute in changing the final design as shown in Figure 1.2.

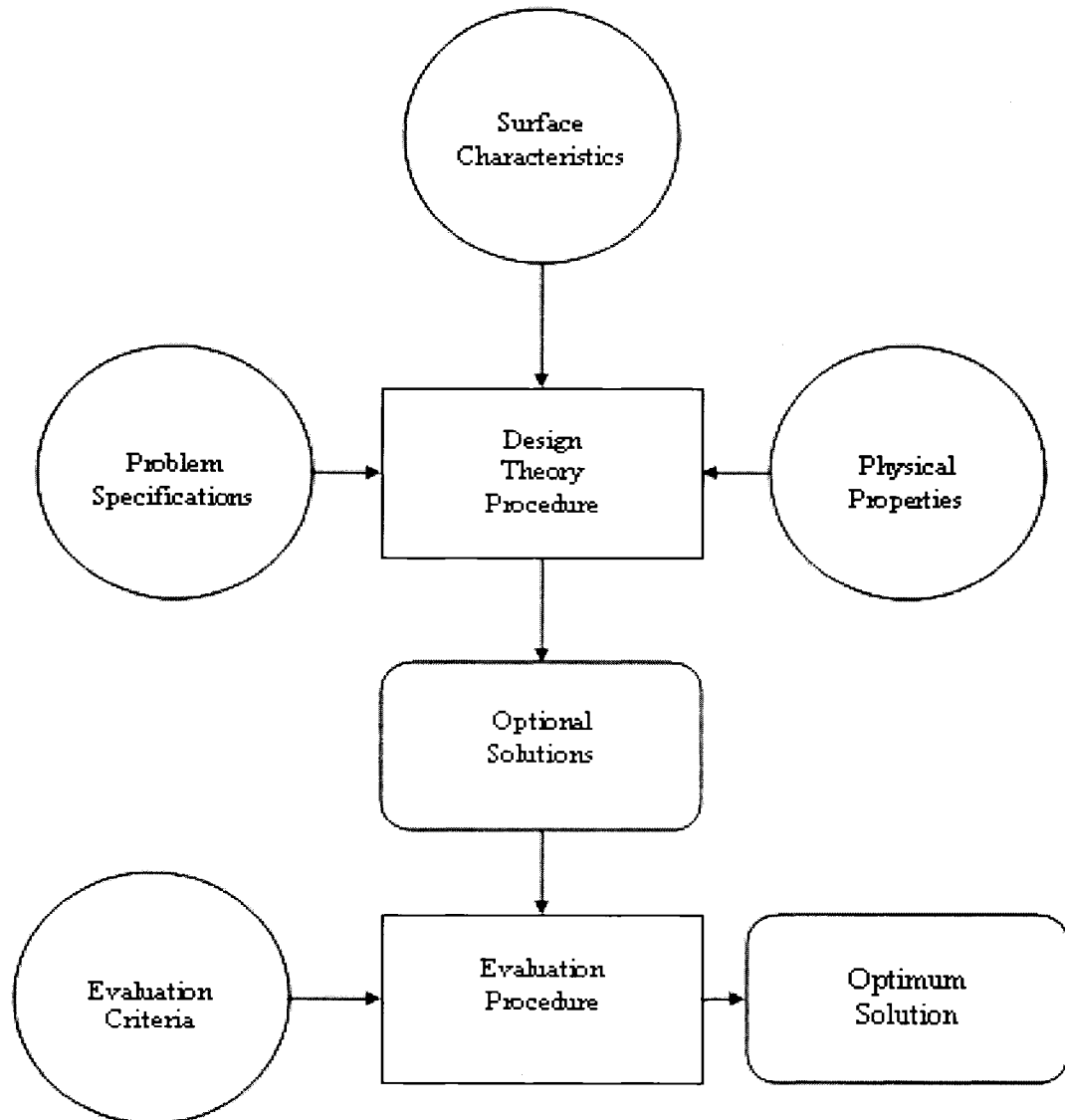


Figure 1.2 Methodology of Heat Exchanger Design (Kays and London, 1984)

Two broad categories of design problem specification are as follow : Given the core geometry, the flow rates, and the entering fluid temperatures, and the rating of the heat exchanger (heat transfer rate and exchanger effectiveness) is required to be determined.

The second category, which is the major subject of this study, is termed the sizing problem in distinction to the rating problem. The purpose of the sizing problem is to specify the size of the core.

In case of a plate fin type heat exchanger, the designer can in principle select the surface configurations for the two fluid sides completely independently. This is one of the virtues of the plate fin construction. Also it is the best heat exchanger type in case both fluids are gases.

The procedure for sizing any one of plate fin heat exchangers is almost inevitably an iterative one and thus lends itself very conveniently to computer implementation. To illustrate such a procedure, a single pass cross flow arrangement will be considered, and it will be assumed that each pass is unmixed.

The two fluids (hot and cold streams) will be designated by subscripts h and c. The two fluid flow rates,  $W_h$  and  $W_c$ , are specified, as well as all four terminal temperatures and the pressure drop for each fluid.

The target of the sizing problem is the determine the three dimensions, the flow length in cold fluid  $L_c$ , the flow length in hot fluid  $L_h$ , and no flow length  $L_{stack}$ , thus the volume of the heat exchanger.

### 1.3 Heat Transfer and Flow Friction Design Data

All direct test data are attached in this thesis in Appendix A. The test data for plain, strip, wavy, louvered, pin, and perforated surfaces were obtained from Kays and London (1984) and test data for vortex generator surface were obtained from Fiebig (1993).

The test data for each surface is the main source of sizing this surface according to the required heat transfer rate, fluid mass flow rates and pressure drop restrictions on each side.

The abscissa on each figure is the Reynolds number that depends directly on mass velocity  $G$ , and the ordinate is used for two parameters: the first is heat transfer parameter ( $j$ ) and the second one is mean friction factor ( $f$ ).

### 1.4 Core Geometry Relations

Some geometrical relations are important in application of the basic heat and flow friction data to the sizing problem in plate fin compact heat exchangers.

The equations below (Kays and London, 1984) give the relations between surface and core factors for one side of the exchanger. Subscript 1 refers to any one side, and 2 refers to the other side. Factors without a subscript are common to both sides.

$$r_h = L \left( \frac{A_c}{A} \right) \quad (1-1)$$

$$\sigma_1 = \left( \frac{A_c}{A_{fr}} \right)_1 = \left( \frac{Ar_h}{LA_{fr}} \right)_1 = \frac{(Ar_h)_1}{V} \quad (1-2)$$

$$\sigma_1 = \frac{b_1 \beta_1 r_{h_1}}{b_1 + b_2 + 2a} \quad (1-3)$$

$$\alpha_1 = \frac{b_1 \beta_1}{b_1 + b_2 + 2a} \quad (1-4)$$



$$A = \alpha L A_{fr} \quad (1-5)$$

$$D_h = \frac{4 A_c L}{A} \quad (1-6)$$

$$A_{c,1} = (\sigma A_{fr})_1 = \left( \frac{A r_h}{L} \right)_1 = \left( \frac{A \sigma}{L \alpha} \right)_1 = (\alpha r_h)_1 \quad (1-7)$$

$$\left( \frac{r_h}{L} \right)_1 = \left( \frac{A_c}{A} \right)_1 = \left( \frac{\sigma}{L \alpha} \right)_1 \quad (1-8)$$

### 1.5 Objective of the Study

The objective of this work focuses around two primary tasks, sizing the compact heat exchanger core to specify the core dimensions for different high performance surfaces, studying entropy generation, and minimum weight and selection of the best surface for specific application.

### 1.6 Geometry Characteristics

The dimensional data given in Appendix A provide all the necessary information required for the basic heat transfer and flow-friction performance applied to the plate-fin surfaces to heat exchanger design. It will be noted that the heat transfer area density is given as  $\beta$  the area per unit of volume between the plates on one flow side.

Extrapolation of the plate fin performance data to surfaces possessing a superficial geometrical similarity but different hydraulic diameter can probably be accomplished without introducing serious uncertainty for moderate changes in hydraulic diameter.

## 1.7 Vortex Generation

Using vortex generators is one of the common methods of heat transfer enhancement. This method depends on creating vortices that enhance the thermal mixing of the flow, hence increasing the local heat transfer and overall heat transfer coefficient. The price of this enhanced heat transfer will be a significant increase in pressure drop and pumping power. Wing-type vortex generator (WVG) can be used as fins or to modify fins and are easily incorporated in to heat exchangers. Different WVGs are evaluated experimentally and numerically with regard to heat transfer enhancement and pressure loss. Detailed data are presented for flow structure, local and global heat transfer and pressure losses (Guntermann, 1992). The high potential of WVGs for compact heat exchangers is very clear from previous studies and current research. Comparison of WVG-fins with offset-strip and louvered fins shows the advantages of WVG's (Brockmeier, 1993). Because of the many geometrical parameters of WVGs, many possibilities for improvements and incorporation into heat exchangers exist.

The requirements for the vortex generators to be used in compact heat exchangers can be deduced from the characteristics of compact heat exchangers. These are summarized with the associated design problems and partial solutions.

Two types of vortex generators are commonly used; The first is transverse vortex generators (TVG) and the second type is longitudinal vortex generators (LVG).

TVGs generate vortex structures with their vortex axes mainly transverse to the primary flow direction, while LVGs generate vortex systems with vortex axes mainly along the primary flow direction. All experimental and theoretical investigations point out that LVGs are preferable to TVGs for compact heat exchangers (Fiebig, 1993).

Wing-type vortex generators (WVG) are easy to incorporate into heat exchangers. The numerous geometrical parameters not only open a large potential, but also afford considerable effort for optimization.

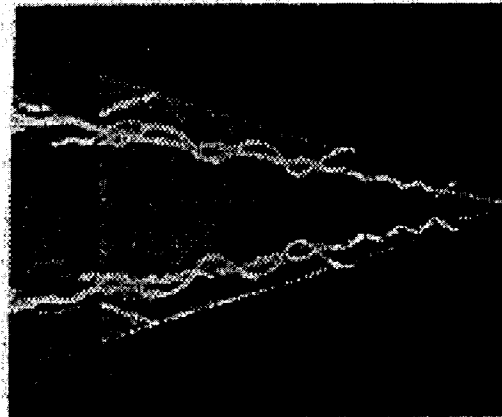


Figure 1.3 Symmetric Pair of Longitudinal Vortices (Fiebig, 1993)

The mechanism for heat transfer enhancement of vortex generators is different from that of offset strip fins and louvered fins. Instead of periodic flow separation, wake recovery and developing laminar boundary layers, they generate swirl or angular rotation of the fluid as shown in Figure 1.3 (Fiebig,1993).

Heat transfer enhancement is always accompanied by additional pressure or flow losses. The price to be paid for heat transfer enhancement is the increased pumping power. The question arises about the acceptable price. To answer the question in terms of heat transfer area, heat exchanger volume or pumping power, a number of criteria have been developed by Cowell (1990), Shah (1978), Webb (1981). They allow the comparative evaluation of different heat transfer surfaces for different objectives.

They will be used for the evaluation of the different heat transfer surfaces in conjunction with the typical heat exchanger design problem.

The enhancement mechanism for longitudinal vortices consists of strong swirling around an axis essentially aligned with the main flow direction. This causes a heavy exchange of core and wall fluid while the enhancement mechanism for transverse vortices requires unsteady flow and implies reserved flow regions.

The following are some facts about vortex generators (Fiebig, 1993):

- WVGs can easily be incorporated into compact heat exchangers. The same manufacturing methods as developed for louvered fins and offset strip fins can be used.
- Delta (triangular) forms are slightly more effective than rectangular forms.
- Winglets give higher heat transfer and pressure loss enhancement than wings.
- Heat transfer and pressure loss enhancement increase with Reynolds number ( $Re \geq 2000$ )
- VGs can generate appreciable heat transfer enhancement (on the average better than 30%), over an area several hundred times the VG area.
- Pressure loss increase is mainly due to form drag of the WVG.
- Transition to turbulence occurs at smaller Reynolds numbers than in plane channel flow, turbulence intensity is increased by VG.
- The two most important dimensionless geometric parameters which control vortex structure, i.e. heat transfer and pressure drop enhancement, are angle of attack and VG primary area.

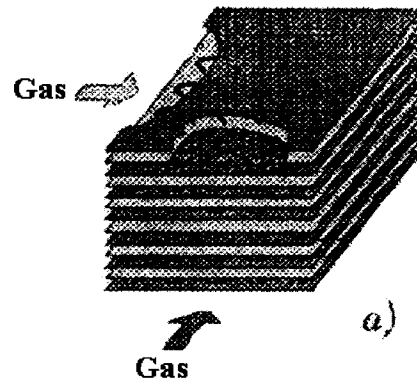


Figure 1.4 a Schematic of Plate Fin Heat Exchanger (Fiebig, 1993)

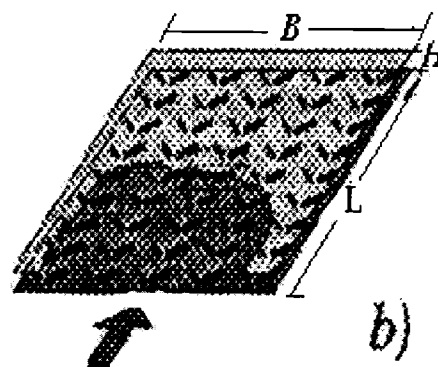


Figure 1.4 b Compact Heat Exchanger Surface with Fins in the Form of Vortex Generator

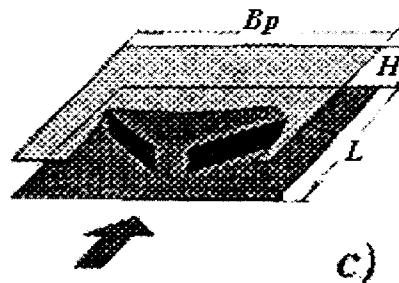


Figure 1.4 c Rectangular Winglets Elements (Fiebig, 1993)

Figure 1.4 a illustrates the construction of cross flow heat exchanger using vortex generators, Figure 1.4 b illustrates one row of the exchanger, Figure 1.4 c shows the vortex generator element (rectangular).

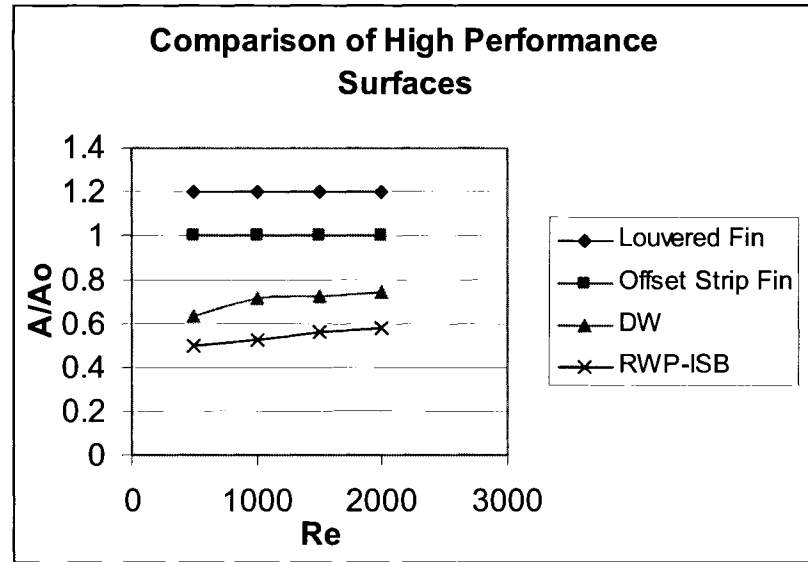


Figure 1.5 Comparison of Vortex Surfaces with Louvered and Strip Surfaces

Figure 1.5 (Fiebig, 1993) compares heat transfer surface requirement for offset-strip fin: 3/32-12.22 and louvered fin: 3/16-11.1 configurations documented in Kays and London (1984) with the delta wing of Brokmeier (1989) and the ISB configuration for  $500 \leq Re \leq 2000$  (Brokmeier, 1993). The offset-strip fin is considered the standard of comparison ( $A_0$ ), with index ( $\circ$ ) for the same mass flow, heat duty, pumping power, hydraulic diameter and temperature.

The offset-strip fin is about 25% better than the louvered fin. It should be noted the experimental data for the offset-strip and louvered fin are compared with numerical data

for the DW-VG of Brockmeier (1989) and ISB-WVG of Guntermann (1992). It might be concluded that WVGs are highly interesting for compact heat exchangers. The ISB configuration needs about 50% less heat transfer surface than the offset-strip fin array and about 25% less than the DW-VG of Brockmeier (1993). Compared to the offset-strip fin and louvered fin, the ISB configuration increases its performance advantage at the lower Reynolds number.

It should, however, be stated the louvered and offset-strip fin configurations can realize much smaller hydraulic diameters than attached WVGs.

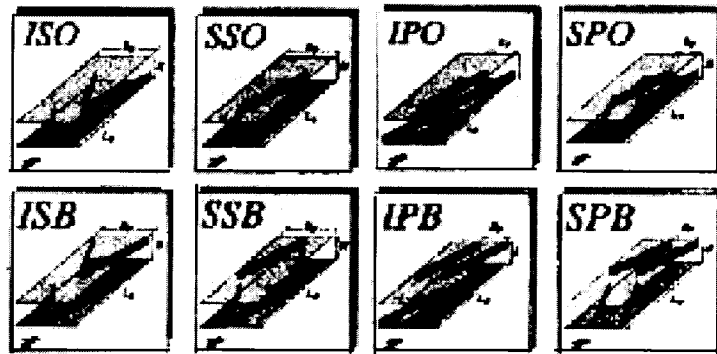


Figure 1.6 Eight Periodic WVG Fin Plate Heat Exchanger Elements.  
First letter: I-in-line and S-Staggered, Second letter. S-Symmetric P-Parallel, Third letter:  
O-One and B-Both sided (Fiebig, 1993)

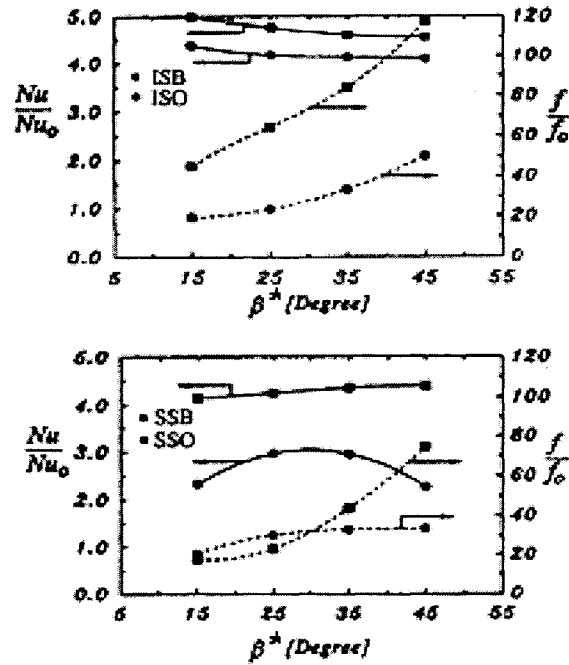


Figure 1.7 Nusselt Number and Friction Factor Enhancement as a Function of Angle of Attack  $\beta^*$  of the Vortex Generator for ISB, ISO, SSB, and SSO WVG Fin Plate Heat Exchanger Elements (Fiebig, 1993)

The heat transfer enhancement is higher of the configurations where the WVGs attachment alternates between both walls. In-line configurations are also better than staggered ones. Symmetric configurations give higher heat transfer but also considerably higher pressure drop enhancement than parallel configurations.

The relative highest value of heat transfer enhancement to pressure loss increase occurs at the lowest angle of attack of  $\beta^* = 15^\circ$ .

From Figure 1.7, it is now clear that the ISB configuration is the best one that can be used in the core of the heat exchanger because it gives high heat transfer rates. However at the same time it causes high pressure drop due to high friction.



## CHAPTER 2

### REVIEW OF CURRENT METHODOLOGIES FOR DESIGN PLATE FIN HEAT EXCHANGER

#### 2.1 Basic Concepts of Heat Exchangers

The gas side heat transfer often limits the thermal performance. The basic concepts of compact heat exchangers are to use high performance surfaces so compact heat exchangers are characterized by high heat duties per unit volume and high heat transfer coefficients.

##### 2.1.1 Direct Test Data

Direct test data for each compact heat exchanger surface is the relation between Colburn factor ( $j$ ) and mean friction factor ( $f$ ) obtained by Kays and London (1984), their 24-year project sponsored by the Office of Naval Research, these are experimental data and cover 132 compact heat transfer surfaces including the plate fin surfaces and tube fin surfaces. While this book is still very widely used worldwide, the most recent design data are from 1967. Because manufacturing technology has progressed significantly since the 1970s, many new and sophisticated forms of heat transfer surfaces have been in use in CHE (Hesselgreaves, 2001). The data of plate fin surfaces are mentioned in Appendix A.

### 2.1.2 Surface Selection

Selection of surface is an important step in the design of a compact heat exchanger because a variety of surfaces are being used in compact heat exchanger applications. There is no such thing as a surface that is best for all applications. The particular application strongly influences the selection of the surface to be used.

The selection criteria for these surfaces are dependent upon the qualitative and quantitative considerations. The qualitative considerations include the designer's experience and judgment, availability of surfaces, manufacturability, maintenance requirements, reliability, safety, cost and the quantitative considerations include performance comparison of surfaces based on surfaces merits.

The following basic categories were identified by Shah (1978):

- Direct comparison of Colburn number  $j$  and friction factor  $f$  values
- Comparison of heat transfer as a function of fluid pumping power
- Miscellaneous comparison methods
- Performance comparison with a reference surface

In Shah's research, over 30 different methods have been suggested in the heat transfer literature for performance comparisons. In all of the comparison methods reviewed, the surface on only one side of the exchanger is considered. Thus in many cases, the best performing surface may not be an optimum heat exchanger surface for a given application. Hence, there is no need to fine tune the selection of a surface individually, and as a result, the selection criteria should be as simple and direct as possible while being meaningful.

A general method for comparison of compact heat transfer surfaces has been recently proposed by Cowell (1990). The method provides compact statements of the relative merits of different heat transfer surfaces by comparing relative pumping powers and relative hydraulic diameters. Also, the relation between several factors of the performance parameters were clarified.

Nunez (1999) developed a thermo hydraulic model that represents the relationship between pressure drop, heat transfer coefficient and exchanger volume. A simple approach to surface selection was based on the concept of volume performance index (VPI): the higher the VPI, the lower the core volume required. Surfaces were compared on the basis of VPI and envelopes for best performance. Simultaneous surface selection and design for full pressure drop utilization could be achieved by using envelopes for best surface performance together with the thermo-hydraulic model.

Taylor (1987) and Shah (1988) used the traditional approach to design the plate fin heat exchangers, and treated the pressure drop as a constraint to see the acceptable pressure drop values for the specified heat duty.

Hesselgreaves (2001) has attempted to provide a treatment that goes beyond dimensionless design data information. In addition to the basic design theory, he includes descriptions of industrial CHEs, specification of a CHE as a part of a system using thermodynamic analysis and broader design considerations for surface size, shape and weight. Heat transfer and flow friction single phase design correlations are given for the most commonly used modern heat transfer surfaces in CHEs, with the emphasis on those surfaces that are likely to be used in the process industries, and some of the operational

considerations including installation, commissioning, operation, and maintenance, including fouling and corrosion.

## 2.2 Design Procedures

Shah and Sekulic (2003) presented the procedures of rating and sizing problems using the mean temperature difference of the fluid on each side of the heat exchanger in order to calculate the fluid properties assuming the uniformity of thermo-physical properties.

Sekulic (2005) offered a very clear methodology for calculating core dimensions of a compact heat exchanger. Considering the analytical complexity of implemented calculations, the most intricate basic flow arrangement situation in a single pass configuration would be a crossflow in which fluids do not mix orthogonal to the respective flow directions. Calculations are executed using an explicit step-by-step routine based on set of known input data is provided in the problem formulation. The procedure follows a somewhat modified thermal design (sizing) procedure derived from the routine advocated in Shah and Sekulic (2003). The main purpose of the calculation sequence is to illustrate the iteration procedures used in commercial software.

The target of this study is to design (to size) a heat exchanger, specifically to determine principal heat exchanger core dimensions (width, length, and height of the specified heat-transfer surfaces).

## 2.3 Entropy Generation

Tagliafico (1996) provided a comparative study of entropy generation of many surfaces scaled by that of a reference configuration (a parallel-plate channel), considering the irreversibility analyses an important factor in determining the operating costs of the heat exchanger.

A possibility to combine hydraulic and heat transfer characteristics is offered by the thermodynamic (second law) analysis developed by Bejan (1987). From this point of view, the entropy generation (irreversibility) in the heat exchanger can be assumed to measure the quality of the performance (London, 1982, Sekulic, 1990, Schenone, 1991).

## 2.4 Vortex Generators

Fiebig (1995) provided a comprehensive study on the use of vortex generators in either tube fin or plate fin compact heat exchangers and showed the recent results from the "Vortices & Heat Transfer" group. He compared the performance of transverse vortex generators and longitudinal vortex generators, described the mechanism of heat transfer enhancement due to using vortex generators and compared the performance of high performance surfaces (louvered, strip) used in plate type compact heat exchangers with two types of vortex generators surfaces. The first vortex characteristics were obtained from Brockmeier (1989) and the second is the ISB configuration (Guntermann, 1992).

Jacobi and Shah (1995) discussed the recent progress of vortex-induced heat transfer enhancement, the theoretical basis for passive and active implementation. They also identified the research needs in the area of vortex-induced heat exchanger enhancement. Also they provided a full coverage for the application of vortex generators in compact heat exchangers.

Jacobi and Shah (1998) studied the behavior of air flow in complex heat exchangers passages with a focus of boundary layer development, turbulence, span wise and stream wise, and wake management. Each of these flow features is discussed for the plain, wavy, and interrupted passages found in contemporary heat exchanger design.

The results obtained may be used to explain the role of these mechanisms in heat transfer enhancement strategies.

Bergeles (1988) estimated that more than 500 papers, reports, and patents were published on heat transfer augmentation.

## 2.5 Minimum Weight of Compact Heat Exchangers

Hesselgreaves (1993) presented a dimensionless analytical method of calculating the size and weight parameters of a simplified plate fin heat exchanger core for a given thermal duty. The thickness of fin material and separating plates which constitute the bulk of the core weight, have lower limits set by pressure containment capability, but it does not necessarily follow that the minimum fin thickness gives the minimum core weight. It is shown that there is a unique fin thickness at which the core weight is a minimum. This optimum fin thickness is shown to be a function of several geometric, material and performance parameters.

## 2.6 Compact Heat Exchanger Theories

Many theories were developed to describe the design and performance of compact heat exchangers starting with Dahlgren and Jenssen (1970), Bergeles and Taborek (1974), Bergeles (1974), Bejan (1978), Sparrow and Liu (1979), Raju and Bansal (1981), Shah and Bergeles (1983), London (1983), Kays and London (1984), Song (1990), Sekulic (1990), Campbell and Rohsenow (1992), Smith (1994). More recent texts such as those of Webb, Hewitt, Bott and Shires (1994), Andrews and Fletcher (1996), Kakac and Liu (1997) have also been referred to extensively in the CHE research.

Much recent knowledge has been accumulated in two proceedings of conferences edited by Shah (1997, 1999), specifically called to promote compact process exchangers.

## 2.7 Ranking of Compact Heat Exchangers

Hall (2003) discussed air-cooled compact heat exchanger design using published data (Kays and London, 1984) contains measured heat transfer and pressure drop data on a variety of circular and rectangular passages. These includes circular tubes, straight fins, louvered fins, strip or lanced offset fins, wavy fins and pin fins.

Soland, Mack, and Rohsenow, (1978), used comparison method converts these  $j$  and  $f$  magnitudes to the base plate area,  $A_b$ ; hence, the effect of the fins is included in the new  $(j_n)$  and  $(f_n)$  based on  $A_b$ . Further, the new Reynolds number will be based on the open flow area,  $A_c$ , as though the fins were not present. This requires that the metal conductivity of the fins be specified in incorporating the effect of the fins into  $j_n$ .

## CHAPTER 3

### PLATE FIN COMPACT HEAT EXCHANGERS SIZING AND COMPARISON

#### 3.1 Sizing Procedures Overview

This chapter offers step-by-step methodology for calculating core dimensions of a compact heat exchanger. Considering the analytical complexity of implemented calculations, the most intricate basic flow arrangement situation in a single-pass configuration would be a crossflow situation in which fluids do not mix orthogonally. The set of known input data is provided in the problem formulation. The procedure follows a somewhat modified sizing procedure derived from the routine advocated in Shah and Sekulic (2003).

The main purpose of the calculation sequence is to illustrate the procedure, usually hidden behind a user-friendly, but content-non-revealing, platform of any existing commercial software package. Such a black-box approach is executed by a computer. This calculation is not intended to focus on a particular design; rather it illustrates the detailed procedure of sizing.

#### 3.2 Problem Data

A task at hand is to design (to size) a heat exchanger. Specifically this is to determine principal heat exchanger core dimensions (width, length, and height of the specified heat-transfer surfaces).



The heat exchanger has to cool a hot-air gas stream, available at an elevated temperature, with a cold-air stream, available at a significantly lower temperature. Terminal states of the both fluid streams are known.

Table 3.1 Problem Formulation (Sekulic, 2006)

Fluid →	Cold fluid			Hot fluid		
Property ↓	Symbol	Unit	Value	Symbol	Unit	Value
Inlet temperature	$T_{c,i}$	K	500	$T_{h,i}$	K	700
Outlet temperature	$T_{c,o}$	K	620	$T_{h,o}$	K	–
Inlet pressure	$P_{c,i}$	kPa	500	$P_{h,i}$	kPa	100
Mass flow	$\dot{m}_c$	kg/s	20	$\dot{m}_h$	kg/s	20
Pressure drop	$\Delta P_c$	kPa	5	$\Delta P_h$	kPa	4.2
Fluid type	Air	–	–	Air	–	–

### 3.3 Assumptions for Heat Transfer Analysis

Determination of the core dimensions assumes an a priori decision regarding selection of heat transfer surface types on both sides of a heat exchanger. This selection is, as a rule, within the realm of an engineer's decisions for any sizing problem; a decision regarding the surface selection will be made at a point when geometric and heat transfer and/or hydraulic characteristics of the core need to be assessed for the first calculation iteration. That decision may always be modified and calculation repeated. The types of heat transfer surfaces will be selected, and data involving geometric, heat transfer, and hydraulic properties will be obtained from a database given in Kays and London (1984).

The assumptions on which the calculation procedure is based are listed and discussed in detail in Shah and Sekulic (2003) as follows:

1. The heat exchanger operates under steady state conditions [i.e., constant flow rates and fluid temperatures (at the inlet and within the exchanger) independent of time].
2. Heat losses to or from the surroundings are negligible (i.e. the heat exchanger outside walls are adiabatic).
3. There are no thermal energy sources or sinks in the exchanger walls or fluids, such as electric heating, chemical reactions, nuclear processes.
4. The temperature of each fluid is uniform over every cross section in counter flow and parallel flow exchangers (i.e., perfect transverse mixing and no temperature gradient normal to the flow direction). Each fluid is considered mixed or unmixed from the temperature distribution viewpoint at every cross section in single-pass cross flow exchangers, depending on the specifications. For a multi pass exchanger the foregoing statements apply to each pass depending on the basic flow arrangement of the passes; the fluid is considered mixed or unmixed between passes as specified.
5. Wall thermal resistance is distributed uniformly in the entire exchanger.
6. Longitudinal heat conduction in the fluids and in the wall is negligible.
7. The individual and overall heat transfer coefficients are constant (independent of temperature, time, and position) throughout the exchanger including the case of phase changing fluids in assumption 6.

8. The specific heat of each fluid is constant throughout the exchanger, so that the heat capacity rate on each side is treated as constant. The other fluid properties are not involved directly in the energy balance and rate equations, but are involved implicitly in  $NTU$  and are treated as constant.
9. For an extended surface exchanger, the overall extended surface efficiency  $\eta_o$  is considered uniform and constant.
10. The heat transfer surface area  $A$  is distributed uniformly on each fluid side in a single pass or multi pass exchanger. In a multi pass unit, the heat transfer surface area is distributed uniformly in each pass, although different passes can have different surface areas.
11. The velocity and temperature at the entrance of the heat exchanger on each fluid side are uniform over the flow cross section. There is no gross flow maldistribution at the inlet.
12. The fluid flow rate is uniformly distributed through the exchanger on each fluid side in each pass so no maldistribution occurs in the exchanger core. Also, no flow stratification, flow bypassing, or flow leakages occur in any stream. The flow condition is characterized by the bulk (or mean) velocity at any cross section.

Assumptions 1 through 5 are necessary in a theoretical analysis of steady state heat exchangers. Assumption 6 essentially restricts the analysis to single-phase flow on both sides or one side with a dominating thermal resistance. For two-phase flows on both sides, many of the foregoing assumptions are not valid since mass transfer in phase change results in variable properties and variable flow rates of each phase, and the heat transfer coefficients may also vary significantly.

### 3.4 Calculation Steps

Design procedure for a sizing problem features two distinct segments of calculation. The first one delivers the magnitude of the thermal size of the core, expressed as a product of the overall heat-transfer coefficient and the heat-transfer area  $UA$ . Determination of this quantity should be based on an application of thermal energy balance [i.e., the heat-transfer rate delivered by one fluid is received by the other; no losses (gains) to (from) the surroundings are present]. Formulation of this balance involves a fundamental analysis of heat-transfer phenomena within the heat exchanger core, which can be summarized through a concept of heat exchangers effectiveness (Kays and London, 1984, Shah and Sekulic, 2003). The resulting design procedure is the "effectiveness number of heat-transfer units" method. The effectiveness is expressed in terms of known inlet and outlet temperatures, and mass flow rates (for known fluids). The unknown temperatures (for some problem formulations) must be determined, and any assumed thermo-physical properties should be re-calculated multiple times (i.e., an iterative procedure is inherent). This feature of the calculation is only one aspect of the design methodology that ultimately leads to an iterative calculation sequence.

The main reason for an iterative procedure is the constraint imposed on pressure drops. The magnitudes of pressure drops must be obtained from the hydraulic part of the design procedure. The hydraulic design of the part of the procedure can not be decoupled from the thermal part, which leads to the calculation of pressure drops after thermal calculations are completed, and hence is followed by a comparison of calculated pressure drops with the imposed limits. As a rule, these limits are not necessarily satisfied after the first iteration.

In Sekulic (2006) routine calculation presentation, determination of the thermal size of the heat exchanger was termed the "targeting the design goal". Each step was separately marked for the purpose of cross-referencing. The second segment of the calculation was devoted to the determination of actual overall dimensions of the core, in a manner to satisfy the required overall heat transfer area and to achieve the overall heat-transfer coefficient to satisfy the required thermal size. This segment was inherently iterative because it required a satisfaction of pressure drop constraints. This segment of calculation was termed "matching geometric characteristics" (MGC) procedure.

Both procedures were organized as a continuous sequence of calculations. The most important comments were given as notes to the respective calculation steps immediately after the equation(s) defining the step. A detailed discussion of numerous aspects of these calculations, and the issue involving relaxation of the assumptions, are provided in Shah and Sekulic (2003).

Some numerical values of the derivative variables presented may differ from the calculated values because of rounding for use elsewhere within the routinely determined data.

$$T_{c,ref} = \frac{T_{c,i} + T_{c,o}}{2} \quad (3.1)$$

$$T_{h,ref} = T_{h,i} \quad (3.2)$$

To initiate the iterative procedure for a sizing problem like the one given in this formulation, a determination of reference temperatures of both fluids is needed. As a first guess, either an arithmetic mean of temperature terminal values or a given temperature value (if single) for each fluid may be selected.

$$C_{p,c} = C_{p,air}(T_{c,ref}) \quad (3.3)$$

$$C_{p,h} = C_{p,air}(T_{h,ref}) \quad (3.4)$$

The specific heat of either of the two fluids is determined at the calculated reference temperatures. Since both fluids are gases in this case, and since both are considered as air, ideal gas thermodynamic properties data will be assumed.

$$C_c = (\dot{m} \times C_p)_c \quad (3.5)$$

$$C_h = (\dot{m} \times C_p)_h \quad (3.6)$$

Heat capacity rates of the fluid streams represent the products of respective mass flow rates and corresponding specific heats, calculated at the estimated reference temperature.

$$C^* = \frac{C_1}{C_2} \quad (3.7)$$

At this point, it is convenient to determine which of the two fluid streams has a larger heat capacity (for a nonbalanced case). The designator 1 denotes the weaker fluid (lower heat capacity) and the designator 2, the stronger fluid (larger heat capacity). The heat capacity rate ratio is not equal to 1; therefore, the heat exchanger operates with nonbalanced fluid streams.

$$\varepsilon = \frac{T_{1,o} - T_{1,i}}{T_{2,i} - T_{1,i}} \quad (3.8)$$

Heat-exchanger effectiveness represents the dimensionless temperature of the weaker fluid ( $C_1 = C_c$ ) (Sekulic, 1990). The current decision on which fluid is weaker was based on the rough estimate, namely, a first iteration of referent temperatures. These are not necessarily the best assumptions, in particular for the hot fluid in this case. So the outlet temperature of the hot fluid must be determined with more precision.

$$T_{h,o} = T_{c,i} (1 - C^* \varepsilon) (T_{h,i} - T_{c,i}) \quad (3.9)$$

The relationship used for determining the outlet temperature of the hot fluid is a straightforward consequence of adopted definitions of the heat-exchanger effectiveness and heat capacity rate ratio, both expressed as functions of terminal temperatures. Therefore having this originally unknown temperature estimated, a new value of the reference temperature for the hot fluid can be determined.

$$T_{h,ref} = \frac{T_{h,i} + T_{h,o}}{2} \quad (3.10)$$

A new value can be obtained of originally unknown outlet temperature of the hot fluid. The criterion for a termination of the iterative procedure may involve either a sufficiently small change of two successive values of this temperature, or a change of the successive values for heat-exchanger effectiveness. In this case, these comparisons indicate that

either no change or a very small change takes place, and the iterative procedure is terminated at this point.

For the crossflow unmixed-unmixed arrangement the relationship between effectiveness and the number of units ( $NTU$ ) (explicit in terms of effectiveness but not explicit in terms of  $NTU$ ) is as follows (Baclic and Heggs, 1985):

$$\varepsilon = \frac{e^{-NTU(1+C^*)} \sum_{n=1}^{\infty} (-1)^n (C^*)^{n/2} I_n(2NTU\sqrt{C^*})}{C^* NTU} \quad (3.11)$$

Therefore, the exact expression for the heat-exchanger effectiveness of an unmixed-unmixed crossflow arrangement used by Sekulic (2006) is algebraically very complex. Graphical representation, as well as tabular data for the crossflow unmixed-unmixed flow arrangement can be found in (Kays and London, 1984, Figure 2-16), this graphical representation is much easier than using Equation (3.11) and it has been used in this study. Figure 2-16 is also attached in Appendix A.

$$UA = NTU \times C_1 \quad (3.12)$$

The product  $UA$ , also termed the "thermal size", is a compounded thermal and physical size of the unit. This size involves the physical size (area of the heat-transfer surface  $A$ ) and heat-transfer size ( $U$  is the overall heat-transfer coefficient). Determination of fluids' thermo-physical properties is required:

- Specific heats  $C_{p,1}, C_{p,2}$
- Viscosities  $\mu_1, \mu_2$
- Thermal conductivities  $k_1, k_2$
- Prandtl numbers  $P_{r,1}, P_{r,2}$
- Densities (inlet)  $\rho_{1,i}, \rho_{2,i}$



- Densities (outlet)  $\rho_{1,o}, \rho_{2,o}$
- Densities (bulk mean)  $\rho_{1,m}, \rho_{2,m}$

The fluid properties are usually determined at arithmetic (or integral) mean values of fluid temperatures. In this calculation, the arithmetic mean values will be adopted from the second iteration. Certain data (temperatures, pressures) are provided in the problem formulation (Table 3.1), and/or devised from the inlet data and known pressure drops. Specific heats and viscosities are based on the mean temperatures. Densities are calculated assuming the ideal-gas assumption. The mean density is based on the following relationship.

$$\rho_{i,m} = \left[ \frac{1}{2} \left( \frac{1}{\rho_i} + \frac{1}{\rho_o} \right) \right]^{-1} \quad (3.13)$$

$$NTU_1 = NTU_c = 2NTU \quad (3.14)$$

$$NTU_2 = NTU_h = C^* NTU_1 \quad (3.15)$$

Distribution of the total dimensions thermal size between two fluid sides is determined in this step. Since both fluids are gases, both thermal resistances are to be assumed as equal in the first iteration. That leads to the given distribution of  $NTU_1$  and  $NTU_2$  versus  $NTU$  (Shah and Sekulic, 2003).

Selection of heat surface type may be one of more than sixty surfaces (Kays and London, 1984). The following data are the specifications of each surface:

- Plate spacing  $b$
- Number of fins  $n_f$
- Hydraulic diameter  $D_h$
- Fin thickness  $\delta$
- Uninterrupted flow length  $l_f$

- Heat-transfer area per volume between passes  $\beta$
- Fin area per total area  $A_f / A$
- Plate thickness  $a$

The sizes and shapes of heat-transfer surfaces are correlated with the heat-transfer and hydraulic characteristics. However, these characteristics in turn are needed to determine the sizes and shapes of the heat-transfer surfaces. This interrelation renders the calculation procedure iterative. A selection of the surface geometry (i.e., selection of both fluid flow area geometries) should be done first. Subsequently, calculation of heat-transfer and fluid flow characteristics may be conducted to establish whether the surfaces selection fits the thermal size distribution and the overall thermal size (but in a manner to satisfy the pressure drop constraints). A variety of different surfaces may be chosen for both fluid sides (Kays and London, 1984). In this research, characteristics of sixty four surfaces were studied in order to calculate the required size of each surface and obtain a comprehensive comparison.

For each surface, the ratio of  $j$  and  $f$  over the wide range of Reynolds numbers (the value of  $j$  and  $f$  depend mainly on Reynolds number) is approximately constant (the average of  $(j/f)$  for  $500 \leq Re \leq 4000$ ). This range of Reynolds number was selected because most of compact heat exchangers work in this range.

$$\left( \frac{j}{f} \right)_{c,h} \approx \text{const} \quad (3.16)$$

Although selection of surface types leads to the known heat-transfer geometries on both fluid sides, the calculation of  $j(Re)$  and  $f(Re)$  parameters (i.e., heat-transfer and friction factors in dimensionless form) cannot be performed straightforwardly at this point. This is because the actual Reynolds numbers for fluid flows are still unknown.

Since this ratio is nearly constant in a wide range of Reynolds numbers, a unique value can be suggested as indicated above. In the first iteration (which will follow) only the value of  $j/f$  (rather than separate  $j$  and  $f$  values) would be needed for calculation of both fluid core mass velocities. Subsequently, these core mass velocities (Eq.3.17) will be used to determine the first iteration of Reynolds numbers, leading to the corresponding values of  $j$  and  $f$ . Subsequently, the second iteration for  $j/f$  can be calculated from known  $j$  and  $f$  values. In this case of the surface 19.86 (Kays and London, 1984),  $j/f$  range is (0.25-0.37) for Re range (500-4000), so the average value would lead to  $j/f \approx 0.30$ .

$$G_c \approx \left[ \left( \frac{j}{f} \right) \left( \frac{\Delta p}{p_{in}} \right) \frac{2 p_{in} \eta_o \rho_m}{NTU \text{Pr}^{2/3}} \right]_c^{1/2} \quad (3.17)$$

$$G_h \approx \left[ \left( \frac{j}{f} \right) \left( \frac{\Delta p}{p_{in}} \right) \frac{2 p_{in} \eta_o \rho_m}{NTU \text{Pr}^{2/3}} \right]_h^{1/2} \quad (3.18)$$

It is generally assumed that the total surface temperature effectiveness for a compact heat-transfer surface (for a good design) must be within the range of 0.7 to 0.9. The high end of this range was assumed for both sides. (i.e.,  $\eta_{o,c} = \eta_{o,h} = 0.9$ , the same geometry was suggested for both surfaces).

In this step, the first estimates of core mass velocities are based on the estimates of  $j/f$  and  $\eta_o$  parameters as discussed. This estimate, as given above, is based on a simplified expression for  $G$  that takes into account the assumptions as follows (Sekulic, 2006):

- Only friction contributes to the pressure drop
- Fouling resistances are neglected
- Thermal resistance of the heat-transfer wall is neglected

- Thermal resistances caused by formations of convective boundary layers on both fluid sides are equal.

$$\text{Re}_c = \frac{G_c D_{h,c}}{\mu_c} \quad (3.19)$$

$$\text{Re}_h = \frac{G_h D_{h,h}}{\mu_h} \quad (3.20)$$

The uncertainties involved with an experimental determination of the Reynolds values, and subsequently  $j$  and  $f$ , are  $\pm 2$ ,  $\pm 14$ , and  $\pm 3$  percent, respectively. So the first estimates for Reynolds numbers must be refined later (in subsequent iterations) up to the margin of  $\pm 2$  percent. One iteration would likely suffice.

This explicit calculation of the refined values for  $j$  and  $f$  is conducted by using  $j(\text{Re})$  and  $f(\text{Re})$  correlations for the selected geometry based on both fluid sides have the same geometry. The values are calculated for Reynolds numbers using (Eq.3.19, 3.20). The values of  $j$  and  $f$  that correspond to the Reynolds number can be easily calculated using the experimentally obtained data listed in Kays and London (1984), Appendix A.

Three iterations (calculation of Reynolds number based on initial guess of  $j$  and  $f$ , then calculated  $j$  and  $f$ ) are enough to result in fast convergence of the correct Reynolds number.

$$T_w = \frac{T_{h,ref} + \frac{NTU_c C^*}{NTU_h} T_{c,ref}}{1 + \frac{NTU_c C^*}{NTU_h}} \quad (3.21)$$

The temperature of the heat-transfer surface wall between the fluids is calculated from a balance equation that relates heat-transfer rates delivered from one fluid to those received by the other. These heat-transfer rates are expressed in terms of fluid-to-wall and

wall-to-fluid temperature differences and the respective thermal resistances on both fluid sides. The wall temperature is needed to perform a correction of thermo-physical properties. This correction is due to temperature gradients between the fluids and the heat-transfer surface wall across the respective boundary layers on both fluid sides.

$$j_{c,corr} = j_c \left( \frac{T_w}{T_{c,ref}} \right)^n \quad (3.22)$$

$$n = 0.3 - \left[ \log_{10} \left( \frac{T_w}{T_{c,ref}} \right) \right]^{1/4} \quad (3.23)$$

The cold air is exposed to heating, and that its flow regime is turbulent. For details of the alternate exponent determination see Shah and Sekulic (2003), table 7.13, p. 531. The conditions to be satisfied are  $1 < T_{w,ref}/T_{c,ref} < 5$ ;  $Pr < 0.9$ .

$$j_{h,corr} = j_h \left( \frac{T_w}{T_{h,ref}} \right)^n = j_h \quad (3.24)$$

The hot fluid experiences cooling conditions. The flow regime is in the laminar region. Therefore, the exponent  $n = 0$  (Shah and Sekulic, 2003, table 7.12, p.531).

$$f_{c,corr} = f_c \left( \frac{T_w}{T_{c,ref}} \right)^m, m = -0.1 \quad (3.25)$$

Cold fluid is heated, and the flow regime is turbulent. The suggested calculation of the exponent in the correction term is valid for the range of temperature ratios as follows:

$$1 < \frac{T_{h,ref}}{T_{c,ref}} < 5$$

In this case, the ratio is 1.07; therefore, the calculation of the exponent  $m$  is performed as indicated. Fluid at the cold side is air; therefore, it is treated as an ideal gas.

$$f_{h,corr} = f_h \left( \frac{T_w}{T_{h,ref}} \right)^m \quad (3.26)$$

For a fluid cooling case and laminar flow, the exponent is equal to 0.81. The conditions to be satisfied are:  $0.5 < T_{h,ref} / T_{h,ref} = 0.94$ ,  $1$ ;  $0.6 < Pr = 0.699 < 0.9$ .

Because the temperature difference in this study is the same as Sekulic (2006), all correction exponents (m, n) are the same.

$$h_c = j_{c,corr} \frac{G_c c_{p,c}}{Pr_c^{2/3}} \quad (3.27)$$

The heat-transfer coefficient for the cold fluid is determined from the definition of the Colburn factor.

$$h_h = j_{h,corr} \frac{G_h c_{p,h}}{Pr_h^{2/3}} \quad (3.28)$$

The heat-transfer coefficient for the hot fluid is determined from definition of the Colburn factor.

$$\eta_{f,c} = \frac{\tanh(ml)_c}{ml_c} \quad (3.29)$$

$$m_c = \sqrt{2h_c / k\delta} \quad (3.30)$$

$$l_c = \frac{b}{2} - \delta \quad (3.31)$$

The thermal conductivity of the fin is assumed to be 200 W/m.K for an alloy at the given temperature. The resulting fin efficiency (Eq.3.29) becomes higher than the actual value. The actual fin efficiency in a brazed heat exchanger throughout the core may be significantly smaller (Zhao et al., 2003).

$$\eta_{f,h} = \frac{\tanh(ml)_h}{ml_h} \quad (3.32)$$

$$m_h = \sqrt{2h_h/k\delta} \quad (3.33)$$

$$l_h = \frac{b}{2} - \delta \quad (3.34)$$

The fin geometry is the same on both fluid sides; therefore, the lengths are the same.

$$\eta_{o,c} = 1 - (1 - \eta_{f,c}) \frac{A_f}{A} \quad (3.35)$$

A detailed discussion of the meaning of the total extended surface efficiency can be found in Shah and Sekulic (2003), p. 289.

$$\eta_{o,h} = 1 - (1 - \eta_{f,h}) \frac{A_f}{A} \quad (3.36)$$

The extended surface efficiencies must differ for both fluid sides even if the same geometry of the fins is used. This is due to the difference in the heat-transfer coefficients.

$$U = \left[ \frac{1}{(\eta_o h)_c} + \frac{A_c/A_h}{(\eta_o h)_h} \right]^{-1} = \left[ \frac{1}{(\eta_o h)_c} + \frac{1}{(\eta_o h)_h} \right]^{-1} \quad (3.37)$$

Because of a high thermal conductivity of wall material, thermal resistance of the wall is neglected in this calculation. Therefore, the overall heat-transfer coefficient is defined by heat-transfer conductance due to convection on both fluid sides only. Again, the heat-transfer surface areas are the same on both fluid sides because the same fin geometry is used.

$$A_c = A_h = \frac{(\dot{m}C_p)_c NTU}{U} \quad (3.38)$$

The heat-transfer surface areas are the same on both fluid sides (same geometries).

$$A_{c,c} = \frac{\dot{m}_c}{G_c} \quad (3.39)$$

The free-flow area on the cold fluid side is determined from the definition of the mass velocity.

$$A_{c,h} = \frac{\dot{m}_h}{G_h} \quad (3.40)$$

The free-flow area on the hot fluid side is determined analogously to the same entity on the cold fluid side.

$$\sigma_c = \sigma_h = \frac{b\beta D_h}{8(b+a)} \quad (3.41)$$

$$A_{fr,c} = \frac{A_{c,c}}{\sigma_c} \quad (3.42)$$

The frontal area on the cold fluid side is determined from the relation between porosity and free-flow area.

$$A_{fr,h} = \frac{A_{c,h}}{\sigma_h} \quad (3.43)$$

The frontal area on the hot fluid side is determined from the relation between porosity and free-flow area.

$$L_c = \frac{D_h A_c}{4A_{c,c}} \quad (3.44)$$

The fluid flow length on the cold fluid side represents the principal core dimension in this direction.

$$L_h = \frac{D_h A_h}{4A_{c,h}} \quad (3.45)$$



The fluid flow length on the hot fluid side represents the principal core dimension in this direction.

$$L_{stack} = \frac{A_{fr,c}}{L_h} \quad (3.46)$$

The core dimension in the third direction (no flow length) can be calculated by using the frontal area of either the cold fluid or the hot fluid. If the calculations were conducted correctly, both values would have to be within the margin of error only as a result of rounding of the numbers. No constraint regarding the aspect ratio (Hesselegreaves, 2001, p.136) of any pair of the core side dimensions is imposed. In case of imposed constraint on the aspect ratio, an additional iterative procedure would be needed. Such a procedure would require a reconsideration of the heat-transfer surface geometry on both fluid sides (the geometries used on both sides may not be the same).

$$\left( \frac{\Delta p}{p_i} \right)_c = \frac{G_c^2}{2(p_{in} p_{in})_c} \left[ (1 - \sigma^2 + K_c) + f \frac{L p_i}{r_h \rho_m} + 2 \left( \frac{\rho_i}{\rho_o} - 1 \right) - (1 - \sigma^2 - K_e) \frac{\rho_i}{\rho_o} \right] \quad (3.47)$$

$$K_{c,c} = f_1 (\sigma_c, Re_c, \text{surface geometry}), K_{e,c} = f_2 (\sigma_c, Re_c, \text{surface geometry})$$

The relative pressure drop calculations require determination of both entrance and exit pressure loss coefficients  $K_c$ ,  $K_e$ . These coefficients can be determined from Kays and London (1984, Figures 5.4, 5.5 p.113-114). The values of pressure drop coefficients depend on surface geometry, porosity and Reynolds number (attached in Appendix A). Fanning friction factors should be determined by accounting for corrections for the reference wall and fluid temperatures. The reference wall temperature may be calculated by taking into account thermal resistances on both fluid sides. In Eq.3.21, the wall temperature is determined in the first approximation without accounting for this factor (thermal resistances on both sides were assumed as equal).

$$\left(\frac{\Delta p}{p_i}\right)_h = \frac{G_h^2}{2(p_{in}p_{in})_h} \left[ (1 - \sigma^2 + K_c) + f \frac{L\rho_i}{r_h\rho_m} + 2\left(\frac{\rho_i}{\rho_o} - 1\right) - (1 - \sigma^2 - K_e) \frac{\rho_i}{\rho_o} \right]_h \quad (3.48)$$

$$K_{c,h} = f_1(\sigma_h, Re_h, \text{surface geometry}), \quad K_{e,h} = f_2(\sigma_h, Re_h, \text{surface geometry})$$

From the input data, an allowed pressure drop is 5 kPa on the cold side and 4.2 kPa on the hot side (Sekulic, 2006). If the imposed condition is not satisfied on any side, this prompts a need to reiterate the calculation with a new value of the mass velocity (in the first iteration, the mass velocity was calculated by using the first approximation based on a weak dependence of  $j/f$  on the Reynolds number).

$$G_c = \frac{\left[ 2(P_{in}\rho_{in} \left( \frac{\Delta P_{Constraint}}{P_i} \right)) \right]_c^{1/2}}{\left[ (1 - \sigma^2 + K_c) + f \frac{L\rho_i}{r_h\rho_m} + 2\left(\frac{\rho_i}{\rho_o} - 1\right) - (1 - \sigma^2 - K_e) \frac{\rho_i}{\rho_o} \right]_c^{1/2}} \quad (3.49)$$

$$G_h = \frac{\left[ 2(P_{in}\rho_{in} \left( \frac{\Delta P_{Constraint}}{P_i} \right)) \right]_h^{1/2}}{\left[ (1 - \sigma^2 + K_c) + f \frac{L\rho_i}{r_h\rho_m} + 2\left(\frac{\rho_i}{\rho_o} - 1\right) - (1 - \sigma^2 - K_e) \frac{\rho_i}{\rho_o} \right]_h^{1/2}} \quad (3.50)$$

The new iteration loop starts with the determination of the set of new mass velocities. These values will be used to calculate the refined values of Reynolds numbers (Eq.3.19, 3.20).

The new mass velocities  $G$  should be calculated from the exact expression for the pressure drop (Eq. 3.49, 3.50), assuming  $G$  values as unknown and the other numerical values in these equations are given. The convergence would be very fast.

$$Re_c = \frac{G_e D_{h,c}}{\mu_c} \quad (3.51)$$

$$\text{Re}_h = \frac{G_h D_{h,h}}{\mu_h} \quad (3.52)$$

Then repeating the procedures from equation 3.22 to 3.50. The pressure drop constraint should be satisfied in order to calculate the final dimensions of the core (Appendix B).

### 3.5 Entropy Generation

The entropy generation (irreversibility) can be used as the quantitative measure of the quality of energy transformation in the heat exchangers (Sekulic, 1990). The analysis of entropy generation (Tagliafico, 1996) only considers the behavior of one fluid in the heat exchanger, the thermal resistance between the other fluid and the exchanger surface is neglected. In real compact-surface heat exchangers with gas on the side under study and liquid on the other side, this assumption can be closely approached. Other assumptions include: The flow is steady in time and hydraulically and thermally fully developed (i.e., the pressure gradient along the main direction of flow and the mean wall-to-fluid temperature difference  $\Delta T$  are constant along the heat exchanger length  $L$ ), thermo-physical properties are constant, and fin efficiency effects, entry/ exit pressure losses are both ignored.

The geometry is defined by the following parameters:

- heat exchanger plate spacing  $b$
- heat exchanger frontal area  $A$
- total heat exchanger volume  $V$
- minimum free flow to frontal area ration  $\sigma$
- hydraulic diameter  $D_h$

The entropy generation rate per unit exchanger length is:

$$S_p = \frac{Q\Delta T}{L \cdot T^2} + \frac{\dot{m}}{\rho T} \left( -\frac{dp}{dx} \right) \quad (3.50)$$

The first term represents the entropy generation rate due to the heat transfer between the wall and the fluid. The second term (in which  $\dot{m}$  is the mass flow rate,  $\rho$  is the density) is due to the irreversibilities caused by fluid friction.

$$\text{Re} = \frac{\dot{m}D_h}{\mu A_c} = \frac{\dot{m}D_h}{\sigma \mu A} \quad (3.51)$$

$$f = \frac{D_h \rho A_c^2}{2\dot{m}^2} \left( -\frac{dp}{dx} \right) \quad (3.52)$$

$$j = \frac{\text{Nu}}{\text{Re} \text{Pr}^{1/3}} \quad (3.53)$$

$$\text{Pr} = \frac{\mu C_p}{k} \quad (3.54)$$

$$\text{Nu} = \frac{Q D_h^2}{4k\Delta T A_c L} = \frac{Q D_h^2}{4k\Delta T \sigma V} \quad (3.55)$$

where  $\mu$ ,  $C_p$  and  $k$  are the dynamic viscosity, specific heat, and the thermal conductivity of the fluid respectively.

Integrating Eq. (3.50) between  $x = 0$  and  $x = L$  leads to:

$$S_p = \left( \frac{Q^2 D_h^2}{4kTi^2 A_c L} \right) \frac{1}{j \text{Re} \text{Pr}^{1/3}} + \left( \frac{2L\mu^3 A_c}{Ti \rho^2 D_h^4} \right) f \text{Re}^3 \quad (3.56)$$

The  $j$  and  $f$  values as a function of  $\text{Re}$  and  $\text{Pr}$  depend on the particular configuration being studied; in this study they have been deduced from the literature data reported by Kays and London (1984).

$$S_{p,o} = \left( \frac{Q^2 D_{ho}}{4kT_i^2 A_{co} L} \right) \frac{1}{j_o \text{Re}_o \text{Pr}^{1/3}} + \left( \frac{2L\mu^3 A_{co}}{Ti\rho^2 D_h^4} \right) f_o \text{Re}_o^3 \quad (3.57)$$

The subscript (o) refers to the reference condition,  $f_o$  and  $j_o$  are obtained from direct test data of the reference surface (Kays and London, 1984).

In order to quantify the thermodynamic impact of the compact geometry with respect to the reference geometry, the entropy generation number  $N$  is introduced:

$$N = S_p / S_{p,o} \quad (3.58)$$

The dimensionless variable  $B$ :

$$B = \frac{\mu^3 k Ti}{8\rho^2 Q^2} \left( \frac{V^2}{b^6} \right) \quad (3.59)$$

$$N = \frac{\left( \frac{1}{4\delta^2 \sigma} \right) \frac{1}{j \text{Re} \text{Pr}^{1/3}} + 16\sigma\delta^4 B \text{Re}^3}{\frac{1}{j_o \text{Re}_o \text{Pr}^{1/3}} + B f_o \text{Re}_o^3} \quad (3.60)$$

where  $\delta = b / D_h$

The constraints considered (Tagliafico, 1996) involve keeping the heat exchanger plate spacing  $b$  and volume  $V$  fixed and assuming the same mass flow rate in and heat transfer  $Q$  for both compact and references configurations. The Reynolds numbers  $\text{Re}$  and  $\text{Re}_o$  are linked through the relationship:

$$\text{Re} = \text{Re}_o / 2\sigma\delta \quad (3.61)$$

Thus for any value  $\text{Re}_o$ ,  $\text{Re}$  is automatically fixed by the constraints.

If the dimensions ( $V$  and  $b$ ), thermo-physical properties ( $\mu, k, \rho$ ), and inlet temperature  $Ti$ , are specified, the parameter  $B$  depends only on heat transfer duty  $Q$ . In conclusion, under the given constrains,  $N$  emerges as a function of the flow rate ( $\text{Re}_o$ ),

heat transfer duty ( $B$ ), and working fluid ( $Pr$ ). In the ranges of variation of the parameters  $Re_o$ ,  $B$ , and  $Pr$ , the entropy generation number  $N$  is a measure of thermodynamic quality of the compact surface geometry. Operating conditions for which  $N$  values are minimized are thermodynamically advantageous.

Calculation of  $N$  values have been performed considering air as working fluid ( $Pr = 0.71$ ), and varying the operational parameters  $B$  within an appropriate range, and  $Re_o$  within the limits for which the performance data are available. It is possible to determine the thermodynamically optimum operating regime of a given compact heat transfer surface, where the optimum corresponds to the working condition for which  $N$  is minimum.

For the highest  $Re_o$  values,  $N$  tends to the pure fluid-flow irreversibility  $Re_o$  limit. In this case friction effects are dominant and the improvement in heat transfer performance is of little value. As  $Re_o$  is reduced,  $N$  values fall into a wide range, depending on operating parameters  $Re_o$  and  $B$  because of the components between flow and heat transfer irreversibilities. The higher the heat transfer duty  $Q$  (or the lower  $B$ ), the greater the importance of entropy production by thermal effects.

As  $Re_o$  is reduced,  $N$  approaches the pure heat transfer irreversibility limit. Very low values of  $N$  can be achieved when the heat transfer performance of the surface under consideration is markedly higher than that of the reference system.

The computed  $N$  values for each particular geometry can be used to directly compare performance under the constraint that mass flow rate ( $Re_o$ ), heat transfer duty ( $B$ ), and overall dimensions ( $W$ ,  $L$ , and  $b$ ) are fixed.

$N$  trends reflect the general considerations previously discussed. Furthermore, decreasing the hydraulic diameter  $D_h$  is advantageous when  $Re_o$  and  $B$  are low (region dominated by wall-fluid  $\Delta T$  irreversibility), and is disadvantageous when  $Re_o$  and  $B$  values are high (region dominated by fluid-friction irreversibility).

Comparisons among surfaces with different plate spacing  $b$  are also possible. A number of criteria can be considered for comparison purposes among surfaces with different  $b$ ; for instance, the entropy generation rates, (Eq.3.56), of different surface configurations can be directly compared assuming the same mass flow rate per unit frontal area and the same heat transfer duty per unit volume ( $Q/V = \text{const.}$ ).

A different constraint involves keeping the mass flow rate  $\dot{m}$  and the heat transfer duty  $Q$ , (as well as  $W$  and  $L$  dimensions), fixed. Under these conditions, the comparison can be developed on the basis of the entropy generation number  $N$ .

Equation 3.59 shows that  $B$  parameter includes the heat transfer duty  $Q$  and a geometric factor,  $V^2/b^6 = (W.L)^2 b^4$ . Keeping  $W$  and  $L$  fixed, the comparison between surfaces with a different  $b$  and the same  $Q$  implies considering different  $B$  values according to the relationship.

$$B = B^* \left( \frac{b^*}{b} \right)^4 \quad (3.62)$$

Where  $(B^*, b^*)$  and  $(B, b)$  refer to the two surfaces to be compared.

Tagliafico (1996) showed  $N$ -curves for six different types of plate-fin surfaces. The selected surfaces were chosen among those reported in Kays and London (1984). The values  $B^* = 10^{-13}$  and  $B^* = 10^{-15}$  are based on  $b^* = 6.35$  mm, (surface 1/4(s)-11.1). The corresponding values of  $B$  (at fixed heat transfer duty  $Q$ ) for the other surfaces can be

calculated from Eq. (3.62). The statement of the thermodynamic performance of surfaces is related to  $N$  values. For  $B^* = 10^{-13}$  and  $Re_o$  less than 10000, the best performance was obtained by strip-fin and wavy-fin surfaces with  $N$  values in the range of 0.02-0.1. Even with  $Re_o$  higher than 10000, the use of strip-fin and wavy-fin surfaces remains advantageous.

As the heat transfer duty  $Q$  is increased, ( $B^* = 10^{-15}$ ), the thermodynamic performance of the surfaces improves, especially for  $Re$  higher than 10000.

In this research, the methodology of thermodynamic analysis for comparing the performance of plate-fin heat transfer surfaces used by Tagliafico (1996) was applied to more than sixty different surfaces in order to get comprehensive results for all surfaces that may be used as a core for compact heat exchangers. The comparison process has been performed under the constraints that heat transfer duty, mass flow rate, and heat exchanger length are fixed and the relative merit of each surface geometry has been linked to its irreversibility level.

It is apparent that the same heat transfer surface may do its job very close to its thermodynamic optimum for certain values of heat transfer and mass flow rates, but perform very far from the optimum when the operational parameters are changed. Therefore, the choice of a suitable surface from the thermodynamic standpoint should be addressed by heat transfer and mass flow rate considerations under the given design constraint.

Finally, the thermodynamic performance of the all studied surfaces turned out to be strongly related to the operating conditions (both heat transfer duty and mass flow rate)



and the results obtained from this research are completely matched with the paper presented by Tagliafico (1996).

### 3.6 Combination of Different Surfaces

Using different surfaces on both sides of the compact heat exchangers will have many effects on the performance and cost of the plate fin compact heat exchangers, These effects are as follows:

- Decreasing the total volume required by more than 50%
- Significant change in the total area required on both sides (this can be used to decrease the area of the expensive surface and increase the area of the cheap surface)
- Increasing the pressure drop by the ratio of 1 to 20%.
- Decreasing the stack length (no flow length)

According to these effects, the use of different surfaces is highly recommended as a method of improving the performance of plate fin compact heat exchangers.

### 3.7 Minimum Weight of CHE's

Most of the compact heat exchangers used in aviation and aerospace involve the use of some plate fin surfaces, which may be straight, corrugated, strip and louvered depending on the available space and other requirements. The use of stainless steel or other low conductivity material of construction carries the penalty of low fin efficiency, which leads to excessive weight if the fin thickness is not correctly chosen.

In aerospace applications, weight saving is of paramount importance. The thickness of the fin and the separating plates material, which constitute the bulk of core weight, has a lower limit set by pressure containment capability, but it does not necessarily follow that the minimum fin thickness gives the minimum core weight.

The formula of weight calculation on one side is reported in Hesselgreaves (2001) as:

$$W_s = \rho_m V (1 - \sigma) \quad (3.63)$$

Where  $\rho_m$  is the material density,  $V$  is the total volume of the exchanger, and  $\sigma$  is the porosity. Equation 3.63 can be multiplied by 2 in order to obtain the whole weight of the heat exchanger based on the both sides have the same geometry.

### 3.8 Pumping Power Calculation

Pumping power can be easily calculated using Eq.3.64

$$P = \frac{\dot{m} \times \Delta P}{\rho} \quad (3.64)$$

Where  $\dot{m}$  is mass flow rate and  $\rho$  is density of the fluid.

## CHAPTER 4

### DATA AND RESULTS ANALYSIS

The goal of this work is to develop a comprehensive comparison of high performance surfaces, giving a full description of previous comparison methods and connecting the results obtained from this study to the selection of the best surface that can be used in air cooled condensers.

#### 4.1 Sizing Data Analysis and Comparison

The sizing results obtained from this study are based on the analysis suggested by Sekulic (2006). These results show the relative core dimensions of plain, louvered, strip, wavy, pin, perforated and vortex generator geometries. Pressure drop satisfaction on both sides is a very important issue, the values of pressure drop constraints are 5 kPa for the cold side and 4.2 kPa for the hot side (Table 3.1). The geometry may give small volume but fails to satisfy the pressure drop on any side (the pressure drop may be higher by 3%). In this case, the geometry will be excluded completely from the selection. The minimum volume of plate fin compact heat exchanger can be obtained by using vortex generator geometry, this geometry proves that it is the best geometry that can be used as a core despite the fact that it requires very high pumping power. The sizing results obtained from this study are shown in Tables 4.1 to 4.10.

Table 4.1 Frontal and Free Flow Area for Plain Surfaces

Geometry	$U, W/m^2 \cdot K$	$A_c, m^2$	$A_h, m^2$	$A_{frc}, m^2$	$A_{cc}, m^2$	$A_{frh}, m^2$	$A_{ch}, m^2$
2.0	72.29	521.579	521.579	0.932	0.381	1.693	0.691
3.01	69.13	542.2	542.2	1.005	0.397	1.933	0.764
3.97	56.003	673.269	673.269	1.125	0.428	2.15	0.817
5.3	89.443	421.553	421.553	0.909	0.369	1.838	0.746
6.2	70.765	532.824	532.824	1.067	0.414	1.994	0.774
9.03	50.745	743.026	743.026	1.13	0.479	2.09	0.886
11.11	84.684	445.264	445.264	1.208	0.426	2.339	0.825
11.11a	70.224	536.928	536.928	1.12	0.433	2.148	0.851
14.77	83.32	452.53	452.53	1.232	0.44	2.486	0.895
15.08	71.382	528.215	528.215	1.168	0.445	2.323	0.885
19.86	87.652	430.166	430.166	1.272	0.417	2.662	0.872
10.27T	70.564	534.336	534.336	1.041	0.414	2.12	0.844
11.94T	66.315	568.315	568.315	1.254	0.44	2.43	0.853
12.00T	66.764	564.754	564.754	1.313	0.461	2.535	0.89
16.96T	59.783	630.702	630.702	1.359	0.446	2.787	0.914
25.79T	87.399	431.44	431.44	1.364	0.398	3.254	0.947
30.33T	89.85	419.642	419.642	1.253	0.416	3.018	1.002
46.45T	116.688	323.126	323.126	1.633	0.402	4.348	1.07

In Table 4.1, it is clear that the best five surfaces based on high conductance  $U$  and low heat transfer area, which also satisfy pressure drop and belong to the plain fin family are:

- Surface 46.45T
- Surface 30.33T
- Surface 19.86
- Surface 25.79T
- Surface 11.11

The surface 5.3 is excluded from this ranking because it failed to satisfy the pressure drop on one side.

Table 4.2 Volume and Dimensions of Plain Fin Surfaces

Geometry	$V, m^3$	$L_c, m$	$L_h, m$	$L_{stack}, m$	$\sigma$	Pressure Drop
2.0	4.617	4.953	2.729	0.342	0.408	Failed on hot side
3.01	3.717	3.698	1.922	0.523	0.395	Satisfied
3.97	3.799	3.375	1.768	0.636	0.38	Satisfied
5.3	1.596	1.756	0.868	1.047	0.406	Satisfied
6.2	1.902	1.782	0.954	1.119	0.388	Satisfied
9.03	2.034	1.801	0.973	1.161	0.424	Satisfied
11.11	0.973	0.805	0.415	2.908	0.353	Satisfied
11.11(a)	1.221	1.09	0.568	1.971	0.387	Satisfied
14.77	0.814	0.66	0.327	3.764	0.36	Satisfied
15.08	0.925	0.792	0.399	2.929	0.381	Failed on cold side
19.86	0.615	0.483	0.231	5.508	0.328	Satisfied
10.27T	1.287	1.236	0.607	1.714	0.398	Satisfied
11.94T	1.161	0.926	0.478	2.621	0.351	Satisfied
12.00T	1.153	0.878	0.455	2.883	0.351	Satisfied
16.96T	0.827	0.609	0.297	4.574	0.328	Satisfied
25.79T	0.426	0.312	0.131	10.407	0.291	Satisfied
30.33T	0.387	0.308	0.128	9.795	0.332	Satisfied
46.45T	0.264	0.162	0.061	26.863	0.246	Satisfied

Table 4.2 shows the dimensions and the volume required by each plain surface that can transfer the same heat duty. The best five surfaces that belong to the plain fin family based on high compactness (large area in small volume) are:

- Surface 46.45T
- Surface 30.33T
- Surface 25.79T
- Surface 16.96T
- Surface 19.86

Table 4.3 Frontal and Free Flow Area for Louvered Surfaces

Geometry	U,W/ m <sup>2</sup> .K	Ac, m <sup>2</sup>	Ah, m <sup>2</sup>	Afrc, m <sup>2</sup>	Acc, m <sup>2</sup>	Afrh, m <sup>2</sup>	Ach, m <sup>2</sup>
3/8-6.06	124.446	302.982	302.982	1.56	0.555	2.917	1.038
3/8(a)-6.06	135.343	278.589	278.589	1.715	0.61	3.234	1.151
1/2-6.06	125.01	301.613	301.613	1.519	0.54	2.839	1.011
1/2(a)-6.06	131.934	285.788	285.788	1.637	0.582	3.098	1.103
3/8-8.7	132.741	284.049	284.049	1.52	0.531	2.87	1.002
3/8(a)-8.7	139.787	269.732	269.732	1.61	0.563	3.008	1.05
3/16-11.1	159.15	236.918	236.918	1.493	0.527	2.928	1.033
1/4-11.1	157.858	238.858	238.858	1.447	0.511	2.797	0.987
1/4(b)-11.1	159.52	236.366	236.366	1.481	0.523	2.777	0.98
3/8-11.1	148.982	253.084	253.084	1.384	0.489	2.702	0.954
3/8(b)-11.1	155.187	242.964	242.964	1.362	0.481	2.626	0.927
1/2-11.1	139.965	269.388	269.388	1.351	0.477	2.537	0.896
3/4-11.1	123.927	304.253	304.253	1.257	0.444	2.457	0.867
3/4(b)-11.1	120.853	311.99	311.99	1.294	0.457	2.506	0.885

In Table 4.3, the best five surfaces based on high conductance U and low heat transfer area, which also satisfy pressure drop that belong to the louvered fin family are:

- Surface 1/4(b)-11.1
- Surface 3/16-11.1
- Surface 3/8(b)-11.1
- Surface 1/2-11.1
- Surface 3/8(a)-6.06

The surfaces 1/4-11.1 and 3/8(a)-8.7 are excluded from this ranking because they failed to satisfy the pressure drop on one side. Failure in satisfying the pressure drop does cancel the geometry selection completely, but this means it causes a slight increase in pressure drop specified in Table 3.1.

Table 4.4 Volume and Dimensions of Louvered Fin Surfaces

Geometry	$V, m^3$	$L_c, m$	$L_h, m$	$L_{stack}, m$	$\sigma$	Pressure Drop
3/8-6.06	0.949	0.608	0.325	4.802	0.356	Satisfied
3/8(a)-6.06	0.872	0.509	0.269	6.366	0.356	Satisfied
1/2-6.06	0.944	0.622	0.332	4.572	0.356	Satisfied
1/2(a)-6.06	0.895	0.546	0.288	5.677	0.356	Satisfied
3/8-8.7	0.742	0.488	0.259	5.876	0.349	Satisfied
3/8(a)-8.7	0.704	0.437	0.234	6.867	0.349	Failed on hot side
3/16-11.1	0.518	0.347	0.177	8.445	0.353	Satisfied
1/4-11.1	0.522	0.361	0.187	7.756	0.353	Failed on hot side
1/4(b)-11.1	0.516	0.349	0.186	7.965	0.353	Satisfied
3/8-11.1	0.553	0.399	0.205	6.764	0.353	Satisfied
3/8(b)-11.1	0.531	0.39	0.202	6.741	0.353	Satisfied
1/2-11.1	0.588	0.436	0.232	5.862	0.353	Satisfied
3/4-11.1	0.665	0.529	0.27	4.646	0.353	Satisfied
3/4(b)-11.1	0.681	0.527	0.272	4.759	0.353	Satisfied

Table 4.4 shows the dimensions and the volume required by each louvered surface that can transfer the same heat duty. The best five surfaces that belong to the louvered fin family based on high compactness (large area in small volume) are:

- Surface 1/2-11.1
- Surface 3/4(b)-11.1
- Surface 1/4(b)-11.1
- Surface 3/8-11.1
- Surface 3/8(b)-11.1

The surface 1/4-11.1 was excluded from high compactness ranking because it failed to satisfy the pressure drop on hot side.

Table 4.5 Frontal and Free Flow Area for Strip Surfaces

Geometry	$U, W/m^2 \cdot K$	$Ac, m^2$	$Ah, m^2$	$A_{frc}, m^2$	$Acc, m^2$	$A_{frh}, m^2$	$A_{ch}, m^2$
1/4(s)-11.1	142.924	263.811	263.811	1.281	0.452	2.522	0.89
1/8-15.2	180.658	208.709	208.709	1.484	0.564	2.782	1.057
1/8-13.95	236.466	159.452	159.452	1.61	0.557	2.973	1.029
1/8-15.61	190.429	198	198	1.396	0.489	2.783	0.974
1/8-19.86	217.454	173.393	173.393	1.893	0.456	3.918	0.944
1/9-22.68	179.139	210.48	210.48	1.353	0.481	2.797	0.996
1/9-25.01	226.08	166.338	166.338	1.518	0.482	3.096	0.981
1/9-24.12	190.357	198.076	198.076	2.469	0.516	4.984	1.042
1/10-27.03	235.35	160.208	160.208	1.421	0.474	2.903	0.97
1/10-19.35	212.618	177.337	177.337	2.061	0.44	4.325	0.921
1/10-19.74	172.998	217.951	217.951	2.78	0.503	5.789	1.048
3/32-12.22	165.542	227.767	227.767	1.347	0.551	2.65	1.084
1/2-11.94D	132.869	283.775	283.775	1.267	0.407	2.611	0.838
1/4-15.4D	146.211	257.864	257.864	1.456	0.445	2.747	0.901
1/6-12.18D	145.169	259.732	259.732	1.155	0.43	1.155	0.834
1/7-15.75D	171.362	220.031	220.031	1.214	0.431	2.5	0.887
1/8-16.00D	208.681	180.683	180.683	1.44	0.462	2.862	0.919
1/8-16.12D	177.177	212.81	212.81	1.615	0.491	3.177	0.966
1/8-19.82D	210.935	178.752	178.752	1.591	0.493	3.213	0.996
1/8-20.06D	206.543	182.553	182.553	1.501	0.46	3.084	0.947
1/8-16.12T	157.882	238.818	238.818	1.586	0.53	3.092	1.033

In Table 4.5, the best five surfaces based on high conductance  $U$  and low heat transfer area, which also satisfy pressure drop that belong to the strip fin family are:

- Surface 1/10-27.03
- Surface 1/9-25.01



- Surface 1/8-19.86
- Surface 1/10-19.35
- Surface 1/8-19.82

Surface 1/8-13.95 was excluded because it did not satisfy the pressure drop (Table3.1).

Table 4.6 Volume and Dimensions of Strip Fin Surfaces

Geometry	$V, m^3$	$L_c, m$	$L_h, m$	$L_{stack}, m$	$\sigma$	Pressure Drop
1/4(s)-11.1	0.576	0.45	0.228	5.607	0.353	Satisfied
1/8-15.2	0.363	0.245	0.131	11.356	0.38	Satisfied
1/8-13.95	0.309	0.192	0.104	15.496	0.346	Failed on hot side
1/8-15.61	0.336	0.241	0.121	11.539	0.35	Satisfied
1/8-19.86	0.277	0.147	0.071	26.783	0.241	Satisfied
1/9-22.68	0.257	0.19	0.092	14.763	0.356	Satisfied
1/9-25.01	0.196	0.129	0.064	23.876	0.317	Satisfied
1/9-24.12	0.287	0.116	0.057	42.967	0.209	Satisfied
1/10-27.03	0.171	0.12	0.059	24.17	0.334	Satisfied
1/10-19.35	0.292	0.141	0.068	30.529	0.213	Satisfied
1/10-19.74	0.367	0.132	0.063	43.863	0.181	Satisfied
3/32-12.22	0.475	0.353	0.179	7.521	0.409	Satisfied
1/2-11.94D	0.5	0.395	0.192	6.608	0.321	Satisfied
1/4-15.4D	0.339	0.233	0.115	12.676	0.306	Satisfied
1/6-12.18D	0.459	0.397	0.205	5.637	0.372	Failed on hot side
1/7-15.75D	0.321	0.264	0.128	9.46	0.355	Satisfied
1/8-16.00D	0.262	0.182	0.092	15.889	0.321	Satisfied
1/8-16.12D	0.272	0.168	0.173	9.344	0.304	Failed on cold side
1/8-19.82D	0.222	0.139	0.069	23.067	0.31	Satisfied
1/8-20.06D	0.222	0.148	0.072	20.883	0.307	Satisfied
1/8-16.12T	0.28	0.177	0.091	17.503	0.334	Satisfied

Table 4.6 shows the dimensions and the volume required by each strip surface that can transfer the same heat duty. The best five surfaces that belong to the strip fin family based on high compactness (large area in small volume) are:

- Surface 1/10-27.03
- Surface 1/9-25.01
- Surface 1/8-20.06
- Surface 1/9-22.68
- Surface 1/8-19.82 (D)

The surface 1/8-16.12 (T) was excluded because it failed to satisfy the pressure drop on the cold side.

Table 4.7 Frontal and Free Flow Area for Wavy Surfaces

Geometry	$U, \text{W/m}^2 \cdot \text{K}$	$A_c, \text{m}^2$	$A_h, \text{m}^2$	$A_{frc}, \text{m}^2$	$A_{cc}, \text{m}^2$	$A_{fth}, \text{m}^2$	$A_{ch}, \text{m}^2$
11.44-3/8	148.577	253.775	253.775	1.426	0.557	2.919	1.141
11.5-3/8	180.494	208.899	208.899	1.486	0.525	3.059	1.083
17.8-3/8	151.872	248.268	248.268	1.387	0.521	2.861	1.076

In Table 4.7, the best wavy fin surface based on high conductance  $U$  and low heat transfer area and satisfies pressure drop is 11.5-3/8 Wavy.

Table 4.8 Volume and Dimensions of Wavy Fin Surfaces

Geometry	$V, \text{m}^3$	$L_c, \text{m}$	$L_h, \text{m}$	$L_{stack}, \text{m}$	$\sigma$	Pressure Drop
11.44-3/8	0.525	0.368	0.18	7.939	0.391	Satisfied
11.5-3/8	0.447	0.3	0.146	10.196	0.354	Satisfied
17.8-3/8	0.351	0.253	0.122	11.32	0.376	Satisfied

Table 4.8 shows the dimensions and the volume required by each wavy surface that can transfer the same heat duty. The best surface that belong to the wavy fin family based on high compactness (large area in small volume) is 17.8-3/8 Wavy.

Table 4.9 Frontal and Free Flow Area for Pin Surfaces

Geometry	$U, \text{W/m}^2 \cdot \text{K}$	$A_c, \text{m}^2$	$A_h, \text{m}^2$	$A_{fr}, \text{m}^2$	$A_{cc}, \text{m}^2$	$A_{frh}, \text{m}^2$	$A_{ch}, \text{m}^2$
AP-1	169.18	222.86	222.86	2.489	0.636	4.355	1.115
AP-2	201.11	187.48	187.48	3.144	0.785	5.377	1.344
PF-3	canceled	cancel	canceled	canceled	cancel	canceled	canceled
PF-4F	229.5	164.29	164.29	2.589	0.727	4.03	1.322
PF-9F	canceled	cancel	canceled	canceled	cancel	canceled	canceled
PF-10F	240.43	156.81	156.81	1.569	0.507	3.005	0.971

Table 4.10 Volume and Dimensions of Pin Fin Surfaces

Geometry	$V, \text{m}^3$	$L_c, \text{m}$	$L_h, \text{m}$	$L_{stack}, \text{m}$	$\sigma$	Pressure Drop
AP-1	0.96	0.386	0.22	11.31	0.256	Failed on hot side
AP-2	0.671	0.214	0.125	25.214	0.25	Failed on hot side
PF-3	canceled	canceled	canceled	canceled	canceled	canceled, Lack of Data
PF-4F	0.828	0.32	0.176	14.723	0.281	Satisfied
PF-9F	canceled	canceled	canceled	canceled	canceled	canceled, Whistling
PF-10F	0.527	0.336	0.175	8.946	0.323	Satisfied

In Table 4.9 and 4.10, the best surface based on high conductance  $U$  and low heat transfer area, high compactness and satisfies pressure drop that belongs to the pin fin family is PF-10 (F) Pin. The surface PF-9 (F) is canceled because of whistling problem at high Reynolds number ( $Re \geq 4000$ ).

Table 4.11 Frontal and Free Flow Area for Perforated and Vortex Generator Surfaces

Geometry	$U, W/m^2 \cdot K$	$A_c, m^2$	$A_h, m^2$	$A_{frc}, m^2$	$A_{cc}, m^2$	$A_{frh}, m^2$	$A_{ch}, m^2$
13.95(P)	157.733	239.043	239.043	1.423	0.399	2.649	0.744
Vortex	355.336	106.11	106.11	1.579	0.51	3.2	1.034

Table 4.12 Volume and Dimensions of Perforated and Vortex Generator Surfaces

Geometry	$V, m^3$	$L_c, m$	$L_h, m$	$L_{stack}, m$	$\sigma$	Pressure Drop
Surface 13.95(P) Perforated	0.533	0.375	0.201	7.079	0.281	Satisfied
Vortex Generator	0.099	0.062	0.031	51.283	0.323	Satisfied

In Table 4.11 and 4.12, the best surface that can be used as a core of heat exchanger is the Vortex Generator, because it gives the highest heat conductance  $U$  and very high compactness, if compared with the other sixty-four surfaces.

## 4.2 Results Validation

In this section, the results obtained from this study will be compared with the previous research results in order to prove the validation of this recent study.

Many studies were performed on the compact heat exchanger sizing in the last two decades. All these studies aimed to compare different surfaces, but only one side of the heat exchanger was studied.

This study represents a complete sizing process for the whole heat exchanger (using different surfaces), assuming the same geometry on both sides.

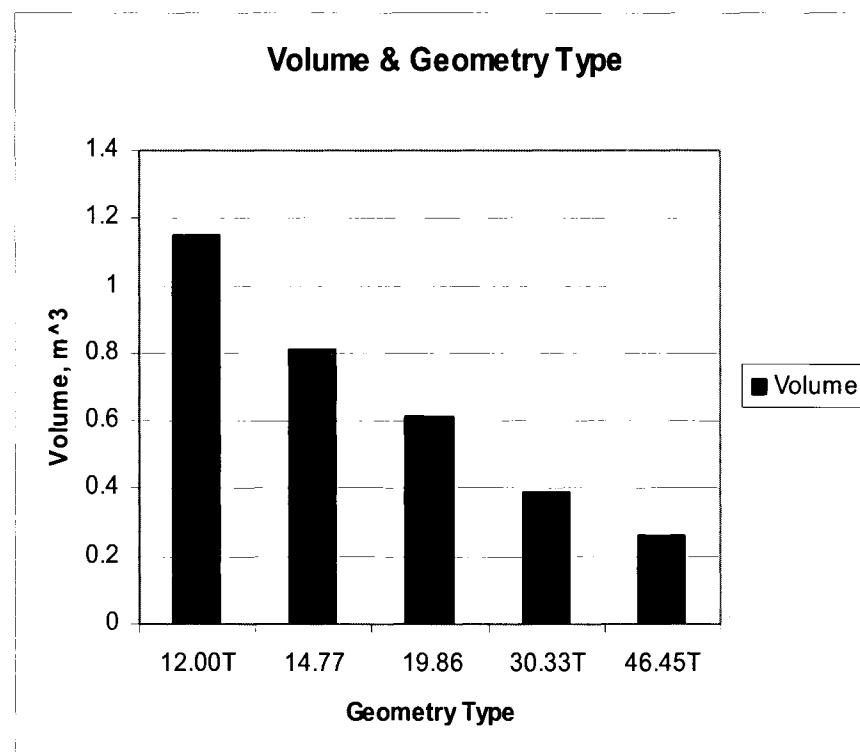


Figure 4.1 Volume Comparison of Different Types of Plain Surfaces

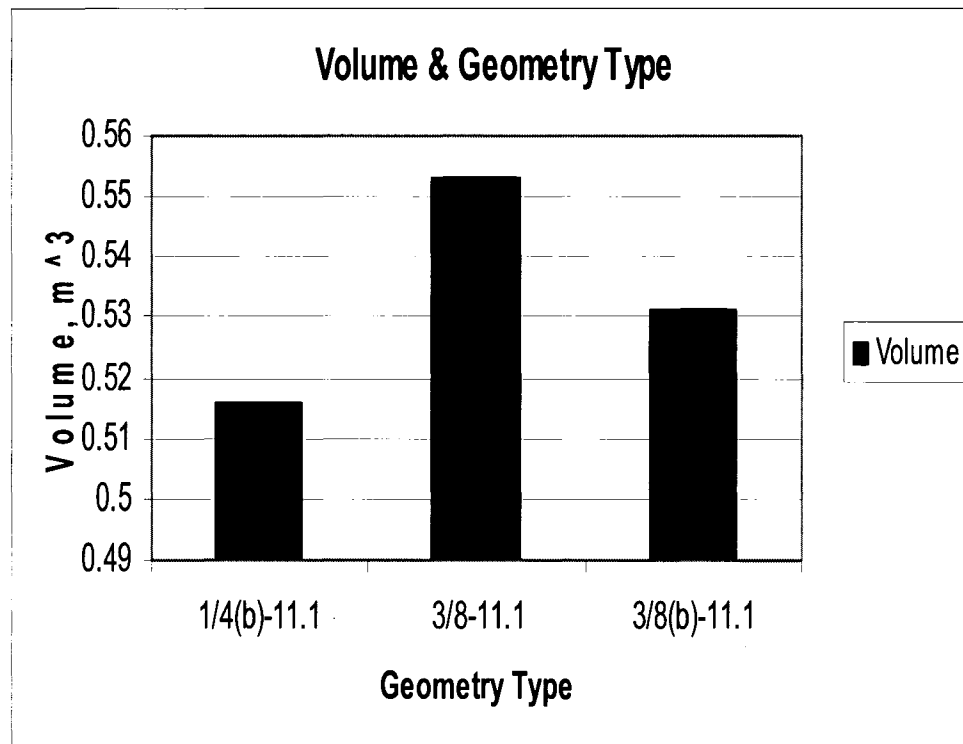


Figure 4.2 Volume Comparison of Different Types of Louvered Surfaces

The results obtained from Figure 4.1 and Figure 4.2 are exactly matched with Nunez (1999), using the volume performance index method.

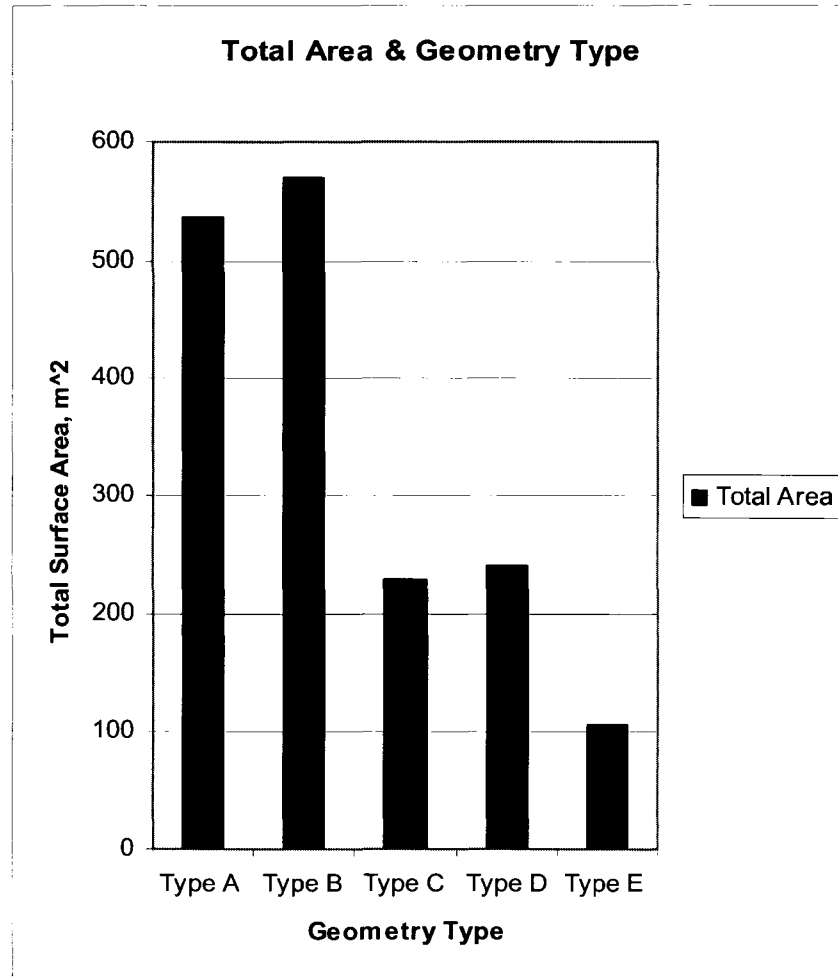


Figure 4.3 Total Area Comparison of Different Types of Surfaces

Figure 4.3 illustrates various types of surfaces: type A is 11.11a plain, type B is 11.94T plain, type C is 3/32-12.22 strip, type D is 3/16-11.1 louvered, and type E is vortex generator geometry. The results represented in Figure 4.3 (obtained from this study) match very well with the results obtained by Brockmeier (1993) using the same designation of the surfaces studied.

There is a very important concept in sizing compact heat exchangers: the dependence of sizing procedures on Reynolds number on both sides. This dependence may lead to different ranking of compact heat exchangers surfaces. All the results obtained from this

research were matched with the previous research of Brockmeier (1993) because both studies used the laminar region in analysis.

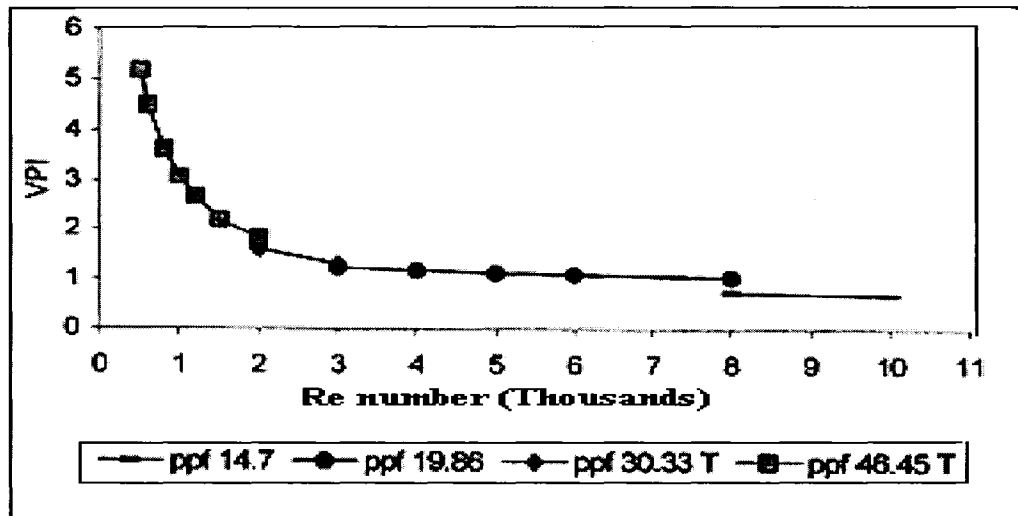


Figure 4.4 Envelop for Best Plain-Fin Surface Performance (Brockmeier, 1993)

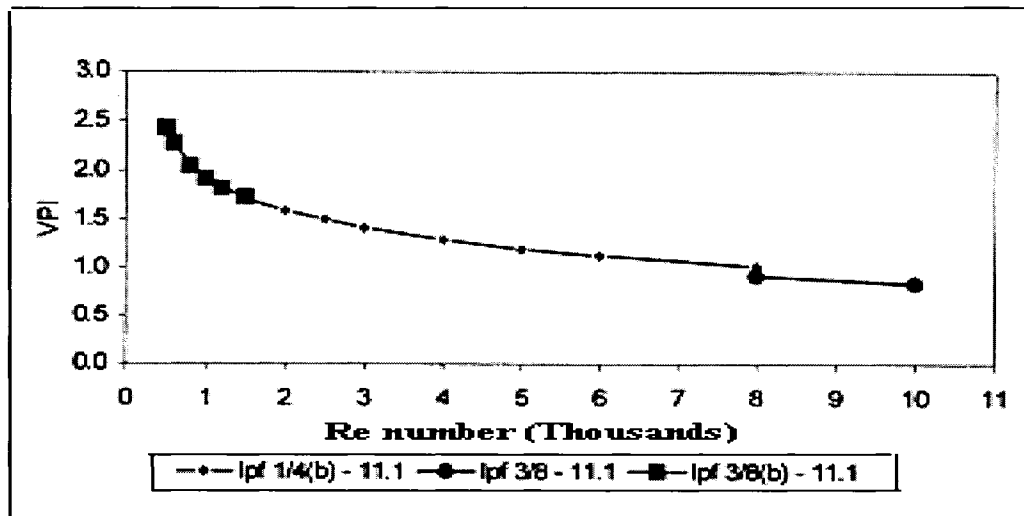


Figure 4.5 Envelop for Best Louvered-Fin Surface Performance (Brockmeier, 1993)



Figures 4.4 and 4.5 illustrate that the best high performance surface that gives small volume and high VPI is not fixed for all heat transfer loads, but it depends mainly on the value of the Reynolds number.

It is very important to explain the concept of volume performance index (VPI) which was applied in Nunez (1999): the higher value of VPI, the smaller the volume of the exchanger and vice versa.

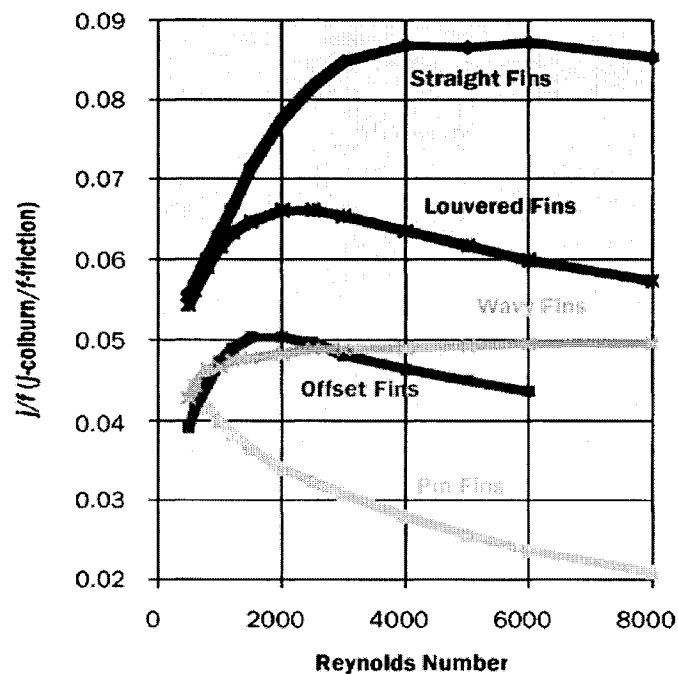


Figure 4.6 Area Goodness Factor ( $j/f$ ) of Different Types of Surfaces (Hall, 2003)

Figure 4.6 represents the relationship between the area goodness factor and Reynolds number. A surface having a higher  $j/f$  factor is good (Shah, 1978) because it will require a lower free flow area and hence a lower frontal area for the exchanger. These facts are presented in Tables 4.1, 4.3, 4.5, 4.7, 4.9, and 4.11.

### 4.3 Entropy Generation

The results obtained in this section are based on using the methodology reported in Tagliafico (1996), using the surface 5.3 plain as the reference surface and the dimensionless variable  $B^* = 10^{-15}$ .

#### 4.3.1 Strip Fins

The entropy generation factor  $N$  is shown in Figures 4.9 and 4.10. It is clear that the strip fin surfaces have a significantly lower entropy generation rate if compared with other surfaces.

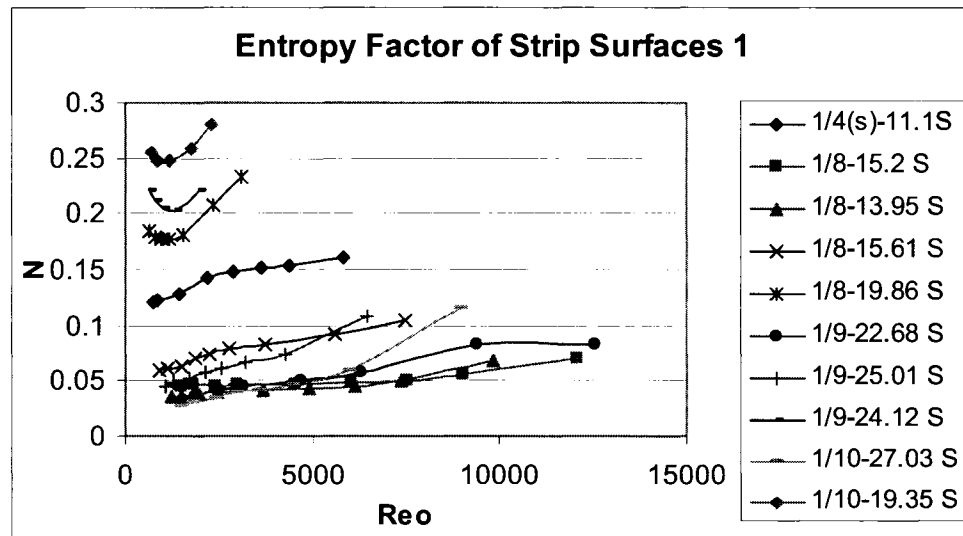


Figure 4.7 Entropy Generation Factor for the First Group of Strip Surfaces

From Figure 4.7, the highly recommended surfaces that produce low entropy generation and belong to the strip family are:

- Surface 1/8-15.2
- Surface 1/8-13.95

- Surface 1/9-22.68

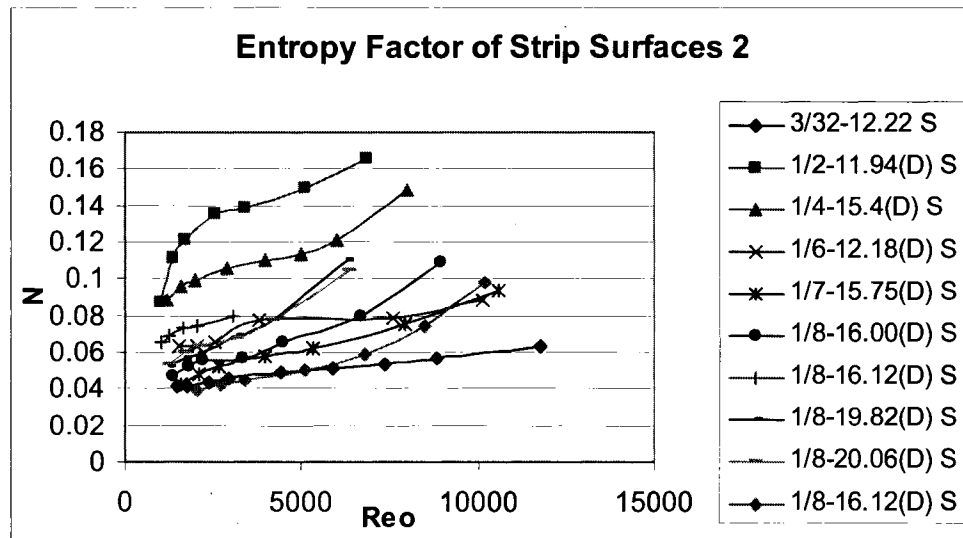


Figure 4.8 Entropy Generation Factor for the Second Group of Strip Surfaces

From Figure 4.8, the highly recommended surfaces that produce low entropy generation and belong to the strip family are:

- Surface 3/32-12.22
- Surface 1/8-16.12
- Surface 1/7-15.75(D)

The ascending order of all strip fin surfaces is represented in Table 4.13. According to Table 4.13, the best five strip surfaces based on low entropy generation rate are:

- Surface 1/8-13.95
- Surface 1/10-27.03
- Surface 3/32-12.22

- Surface 1/8-15.2
- Surface 1/9-22.68

Table 4.13 Ascending Order for Strip Geometry

Ascending order for Strip Geometry	
Surface	Average Entropy Factor
1/8-13.95strip	0.044333
1/10-27.03strip	0.0495
3/32-12.22strip	0.049667
1/8-15.2strip	0.051
1/9-22.68strip	0.053875
1/8-16.12(T)strip	0.058286
1/7-15.75(D)strip	0.061714
1/9-25.01strip	0.064125
1/8-16.00(D)strip	0.066571
1/8-19.82(D)strip	0.070833
1/8-20.06(D)strip	0.071
1/8-16.12(D)strip	0.0722
1/6-12.18(D)strip	0.072667
1/8-15.61strip	0.076444
1/4-15.4(D)strip	0.11025
1/2-11.94(D)strip	0.129714
1/4(s)-11.1strip	0.14125
1/8-19.86strip	0.191286
1/9-24.12strip	0.212
1/10-19.35strip	0.2576

#### 4.3.2 Louvered Fins

As shown in Figure 4.9, the highly recommended louvered surfaces that produce low entropy generation and belong to the louvered family are:

- Surface 3/16-11.1
- Surface 1/4-11.1
- Surface 1/4(b)-11.1

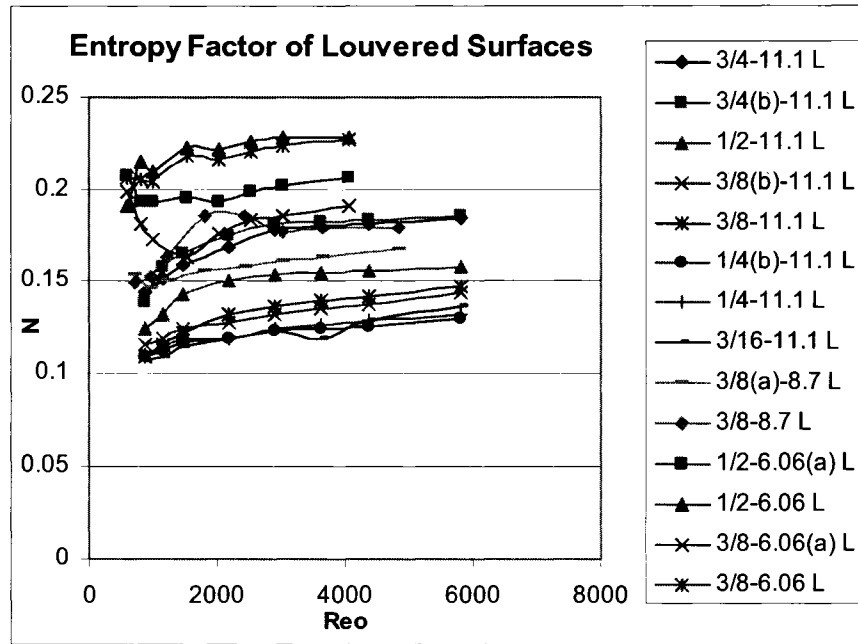


Figure 4.9 Entropy Generation Factor for Louvered Surfaces

Table 4.14 Ascending Order for Louvered Geometry

Ascending order for Louvered Geometry	
Surface	Average Entropy Factor
3/16-11.1Louvered	0.119125
1/4(b)-11.1Louvered	0.119625
1/4-11.1Louvered	0.12125
3/8(b)-11.1Louvered	0.129125
3/8-11.1Louvered	0.13
1/2-11.1Louvered	0.146
3/8(a)-8.7Louvered	0.156625
3/4-11.1Louvered	0.16825
3/4(b)-11.1Louvered	0.17125
3/8-8.7Louvered	0.171375
3/8-6.06(a)Louvered	0.181625
1/2-6.06(a)Louvered	0.19925
3/8-6.06Louvered	0.215125
1/2-6.06Louvered	0.217875

According to Table 4.14, the best five louvered surfaces based on low entropy generation rate are:

- Surface 3/16-11.1
- Surface 1/4(b)-11.1
- Surface 1/4-11.1
- Surface 3/8(b)-11.1
- Surface 3/8-11.1

#### 4.3.3 Wavy Fin

As shown in Figure 4.10, the best surface that produces the lowest entropy generation and belong to the wavy family is surface 17.8-3/8Wavy.

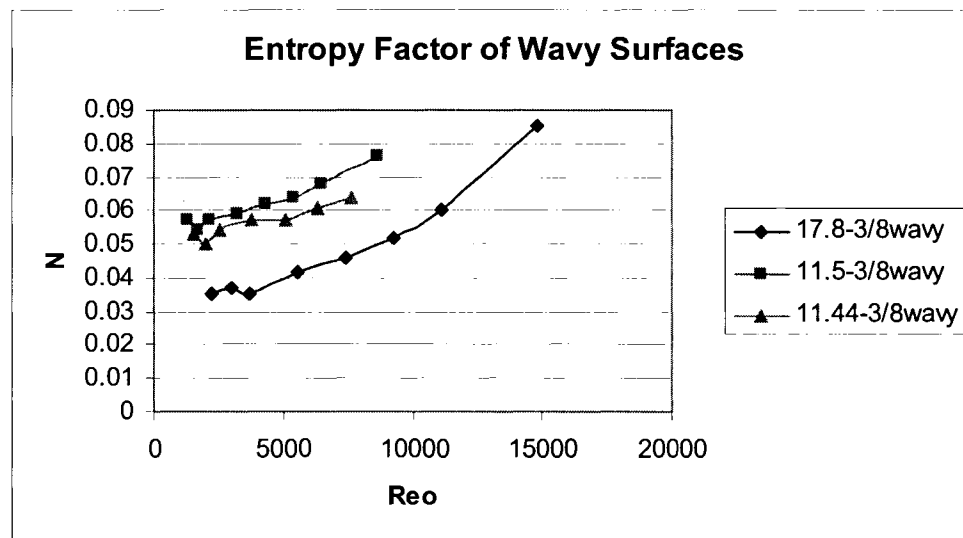


Figure 4.10 Entropy Generation Factor for Wavy Surfaces

Table 4.15 Ascending Order for Wavy Geometry

Ascending order for Wavy Geometry	
Surface	Average Entropy Factor
17.8-3/8 Wavy	0.049
11.44-3/8Wavy	0.056571
11.5-3/8Wavy	0.062125

#### 4.3.4 Plain Fin

Table 4.16 Ascending Order for Plain Geometry

Ascending order for Plain Geometry	
Surface	Average Entropy Factor
30.33T Plain	0.071933
9.03 Plain	0.11374
10.27T Plain	0.120571
15.08 Plain	0.1316125
11.11(a) Plain	0.1425
14.77 Plain	0.146375
19.86 Plain	0.152375
25.79T Plain	0.153571
16.96T Plain	0.192143
46.45T Plain	0.2365
11.1 Plain	0.28425
12.00T Plain	0.28343
11.49 T Plain	0.2898
6.2 Plain	0.378857

According to Table 4.16, the best five plain surfaces based on low entropy generation rate are:

- Surface 30.33T
- Surface 9.03
- Surface 10.27T

- Surface 15.08
- Surface 11.11(a)

#### 4.3.5 Vortex Generator

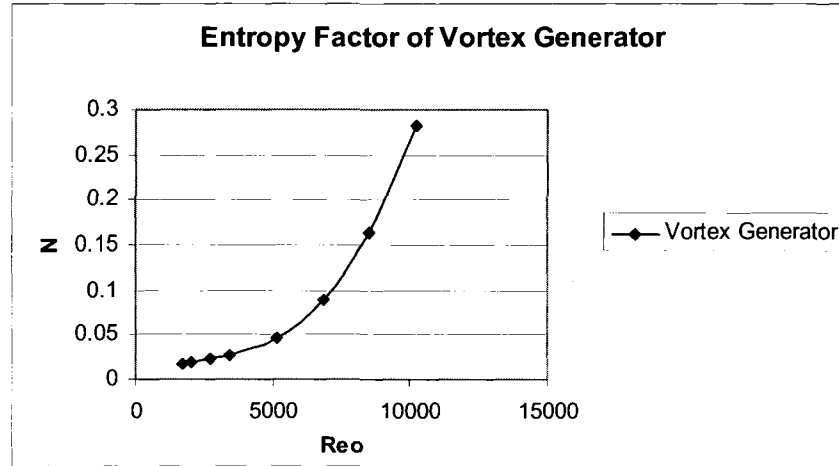


Figure 4.11 Entropy Generation Factor for Vortex Surface

Figure 4.11 shows that the entropy generation rate will increase rapidly when Reynolds number increases so using vortex generator geometry is not recommended in case of very high Reynolds number.

Table 4.17 Entropy Generation Classification of Different Surfaces

Geometry Type	Minimum Entropy	Maximum Entropy	Average Entropy	Min Entropy Surface	Max Entropy Surface
Plain	0.071933	0.37885	0.191978	30.33T	6.2
Strip	0.044333	0.2576	0.096277	1/8-13.95	1/10-19.35
Wavy	0.049	0.062125	0.055898	17.8-3/8	11.5-3/8
Louvered	0.119125	0.217875	0.160464	3/16-11.1	1/2-6.06 L
Vortex	0.083625	0.083625	0.083625	V.G	V.G
Perforated	0.1795	0.1795	0.1795	13.95(P)	13.95(P)



Table 4.17 shows the lower and the higher entropy generation extremes for different surfaces. Pin surfaces were excluded from this table because they cause high pressure drop and most of that type do have sufficient data.

Table 4.18 Entropy Generation Ascending Order for Best 30 Surfaces

Ascending order of all surfaces studied	
Surface	Average Entropy Factor
1/8-13.95strip	0.044333
17.8-3/8wavy	0.049
1/10-27.03strip	0.0495
3/32-12.22strip	0.049667
1/8-15.2strip	0.051
PF-10(F) Pin	0.051143
PF-4F Pin	0.051714
1/9-22.68 Strip	0.053875
11.44-3/8 Wavy	0.05657
AP-2 Pin	0.056571
1/8-16.12T Strip	0.058286
1/7-15.75 (D) Strip	0.061714
11.5-3/8 Wavy	0.062125
1/9-25.01 Strip	0.064125
1/8-16.00(D) Strip	0.066571
1/8-19.82 (D) Strip	0.066571
1/8-19.82 (D) Strip	0.070833
1/8-20.06(D) Strip	0.071
30.33T Plain	0.071933
1/8-16.12(D) Strip	0.0722
1/6-12.18(D) Strip	0.072667
1/8-15.61(D) Strip	0.076444
1/8-20.06(D) Strip	0.0825
Vortex Generator	0.083625
1/4-15.4(D) Strip	0.11025
9.03 Plain	0.113714
3/16-11.1 Louvered	0.119125
1/4(b)-11.11 Louvered	0.119625
10.27T Plain	0.120571
1/4-11.1 Louvered	0.12125

#### 4.4 Pumping Power

The value of pumping power required to push the fluid may be considered one of the valuable criteria for judging the selection of compact heat exchangers, the lower pumping power required to push the same amount of fluid, the better the surface is.

Tables 4.19 to 4.23 illustrate the values of pumping power on both cold and hot sides for various types of examined surfaces. These values are obtained using Eq.3.64.

##### 4.4.1 Plain Fin Surfaces

Table 4.19 Pumping Power Requirements on Both Sides for Plain Surfaces

Geometry	$P_{cc} \cdot 10^5, w$	$P_{hh} \cdot 10^5, w$
Surface 2.0 Plain	Failed on hot side	
Surface 3.01 Plain	0.6489	2.681
Surface 3.97 Plain	1.974	8.487
Surface 5.3 Plain	1.851	7.02
Surface 6.2 Plain	1.15	4.866
Surface 9.03 Plain	1.111	4.903
Surface 11.11 Plain	1.615	6.679
Surface 11.11(a) Plain	1.314	5.707
Surface 14.77 Plain	1.598	7.052
Surface 15.08 Plain	Failed on cold side	
Surface 19.86 Plain	1.771	7.586
Surface 10.27T Plain	1.238	4.887
Surface 11.94T Plain	1.505	5.998
Surface 12.00T Plain	1.487	6.207
Surface 16.96T Plain	1.482	6.94
Surface 25.79T Plain	1.822	7.579
Surface 30.33T Plain	2.37	9.959
Surface 46.45T Plain	3.496	15.93

#### 4.4.2 Louvered Fin Surfaces

Table 4.20 Pumping Power Requirements on Both Sides for Louvered Surfaces

Geometry	$P_{cc} \cdot 10^5, w$	$Phh \cdot 10^5, w$
Surface 3/8-6.06 Louvered	2.02	9.015
Surface 3/8(a)-6.06 Louvered	2.221	9.729
Surface 1/2-6.06 Louvered	2.03	9.012
Surface 1/2(a)-6.06 Louvered	2.073	9.278
Surface 3/8-8.7 Louvered	2.074	10.03
Surface 3/8(a)-8.7 Louvered	Failed on hot side	
Surface 3/16-11.1 Louvered	2.261	10.55
Surface 1/4-11.1 Louvered	Failed on hot side	
Surface 1/4(b)-11.1 Louvered	2.39	10.94
Surface 3/8-11.1 Louvered	2.239	10.05
Surface 3/8(b)-11.1 Louvered	2.29	10.51
Surface 1/2-11.1 Louvered	2.155	9.85
Surface 3/4-11.1 Louvered	2.07	9.167
Surface 3/4(b)-11.1 Louvered	2.02	9.062

#### 4.4.3 Wavy Fin Surfaces

Table 4.21 Pumping Power Requirements on Both Sides for Wavy Surfaces

Geometry	$P_{cc} \cdot 10^5, w$	$Phh \cdot 10^5, w$
Surface 11.44-3/8 Wavy	2.555	10.55
Surface 11.5-3/8 Wavy	2.063	8.63
Surface 17.8-3/8 Wavy	2.42	10.42

#### 4.4.4 Perforated and Vortex Generator Surfaces

Table 4.22 Pumping Power Requirements on Both Sides for Perforated, Vortex Surfaces

Geometry	$P_{cc} \cdot 10^5, w$	$Phh \cdot 10^5, w$
Surface 13.95(P) Perforated	1.542	7.072
Vortex Generator Geometry	3.61	16.24

#### 4.4.5 Strip Fin Surfaces

Table 4.23 Pumping Power Requirements on Both Sides for Strip Surfaces

Geometry	$P_{cc} \cdot 10^5, w$	$P_{hh} \cdot 10^5, w$
Surface 1/4(s)-11.1 Strip	2.212	9.989
Surface 1/8-15.2 Strip	2.368	11.36
Surface 1/8-13.95 Strip	Failed on the hot side	
Surface 1/8-15.61 Strip	3.104	13.81
Surface 1/8-19.86 Strip	3.287	14.18
Surface 1/9-22.68 Strip	3.293	13.81
Surface 1/9-25.01 Strip	3.478	15.08
Surface 1/9-24.12 Strip	3.059	13.95
Surface 1/10-27.03 Strip	3.699	16.39
Surface 1/10-19.35 Strip	3.245	14.16
Surface 1/10-19.74 Strip	4.543	18.87
Surface 3/32-12.22 Strip	2.905	12.86
Surface 1/2-11.94(D) Strip	2.187	8.456
Surface 1/4-15.4(D) Strip	2.241	9.751
Surface 1/6-12.18(D) Strip	Failed on the hot side	
Surface 1/7-15.75(D) Strip	3.262	14.17
Surface 1/8-16.00(D) Strip	2.67	11.85
Surface 1/8-16.12(D) Strip	Failed on the cold side	
Surface 1/8-19.82(D) Strip	2.806	12.37
Surface 1/8-20.06(D) Strip	3.343	14.23
Surface 1/8-16.12(T) Strip	2.463	10.83

From the above results, generally, it is very clear that the plain fin is the best geometry considering the pressure drop and required pumping power, on the other hand the strip fin requires the largest pumping power. The main factor that influences the value of pumping power is the hydraulic diameter. Although plain surfaces require smaller pumping power than other surfaces, the surface 46.45T plain ( $D_h=0.805\text{mm}$ ) requires

more pumping power than most of other surfaces. We conclude that the lower value of hydraulic diameter, the higher expected consumed pumping power. The calculated values for pin surfaces were excluded from this study because most of these surfaces failed to satisfy the pressure drop requirements.

#### 4.5 Combination Between Two Different Surfaces

The combination between two different surfaces inside the compact heat exchanger core is a promising technique that can be used to reduce the total required volume and cost for the same heat transfer load, but in the same time, there will be a significant increase in the pressure drop and consequently the required pumping power as shown in Table 4.24.

Table 4.24 The Effect of Combination of Two Different Surfaces

Geometry Type	Volume	$\Delta P_c$	$\Delta P_h$	Lstack
3/4-11.1 L (Both Sides)	0.665 m <sup>3</sup>	4.39 kPa	4.11 kPa	4.65 m
1/4(s)-11.1 S (Both Sides)	0.576 m <sup>3</sup>	4.38 kPa	4.14 kPa	5.6 m
3/4-11.1L and 1/4(s)-11.1	0.232 m <sup>3</sup>	4.99 kPa	6.07 kPa	1.19 m

Table 4.24 illustrates the value of using different surfaces on both sides of the heat exchanger instead of using the same geometry on the both sides. The surface 3/4-11.1 louvered and 1/4(s)-11.1 strip were selected for this comparison because both of them have the same hydraulic diameter, plate spacing, fin pitch, area density, and the same ratio of fin area to total area. Although this technique is promising, there is 30% increase in pressure drop on the hot side ( $\Delta P_h = 6.07$  kPa instead of 4.2 kPa).

#### 4.6 Final Surface Ranking

The ranking method proposed by (Hall, 2003) will be used in this section in order to get general idea about the various merits of all surfaces studied in this thesis.

Table 4.25 Performance Aspects of Conventional High Performance Surfaces

<b>Fin configuration</b>	<b><math>\Delta P</math></b>	<b>size</b>	<b>weight</b>	<b>cost</b>
Straight	1	5	4	2
Offset	4	2	3	4
Wavy	3	3	2	3
Louver	3	3	3	5
Perforated	1	3	3	3
Vortex	4	1	1	3

The rankings in Table 4.25 are from 1 to 5 with a ranking 1 being the most desirable and a ranking of 5 being the least desirable (based on the thesis results).

A relative comparison of the fin configurations based on all the factors discussed is critical in determining the proper design. All of the parameters are presented as individual design points and the assumption is made that pressure drop is unlimited as well as weight or cost. All of these parameters must be considered to obtain the proper design.

Table 4.25 is an important design tool that guides the designer to the right direction, however, in order to get the optimum design the results obtained for each surface should be considered.

Finally, it is clear that the vortex generator and perforated geometries are attractive for designers of compact heat exchangers. The combination between the above surfaces may lead to obtain very small size with reasonable pumping power.

## CHAPTER 5

### CONCLUSIONS AND RECOMMENDATIONS

The main purpose of sizing process is to obtain an accurate assessment of the surfaces used in the compact heat exchangers. Some surfaces fail to satisfy the pressure drop on one side so these surfaces are excluded from the right selection, also the purpose of studying the entropy generation, pumping power is to refine the selection of the best surface. The best performing surface may not be an optimum heat exchanger surface for a given application. Hence, there is no need to “fine tune” the selection of a surface individually. As a result, the selection criteria should be as simple and direct as possible but meaningful for initial screening and selection of the surfaces.

The main advantage of this thesis is to study the performance of heat exchanger surfaces on both sides, in all of the previous comparison methods reviewed, the surface on only side of the exchanger is considered. However, when this surface is incorporated into a heat exchanger, there are other criteria, not necessarily related to the surface characteristics, that are imposed to optimize a heat exchanger. These criteria are included in this study.

## 5.1 Sizing Results

The sizing results show that the vortex generator geometry is the promising surface to be selected as a core surface because it can transfer the required heat rate with very small volume and it also satisfies the pressure drop requirements. Although this geometry requires significant pumping power due to boundary layer separation, it remains the best selection for the compact heat exchanger designer.

The sizing results obtained are matched with all former comparative research for the selection of the optimum surface. These results give more clear vision of these surfaces, their sizes, pumping power requirements and entropy generation. It was a fact that all highly compact surfaces require large frontal area and small flow length, also they may require high pumping power. This study proves these facts and gives exact ratios of the frontal areas, flow length and pressure drop for more than sixty different geometries.

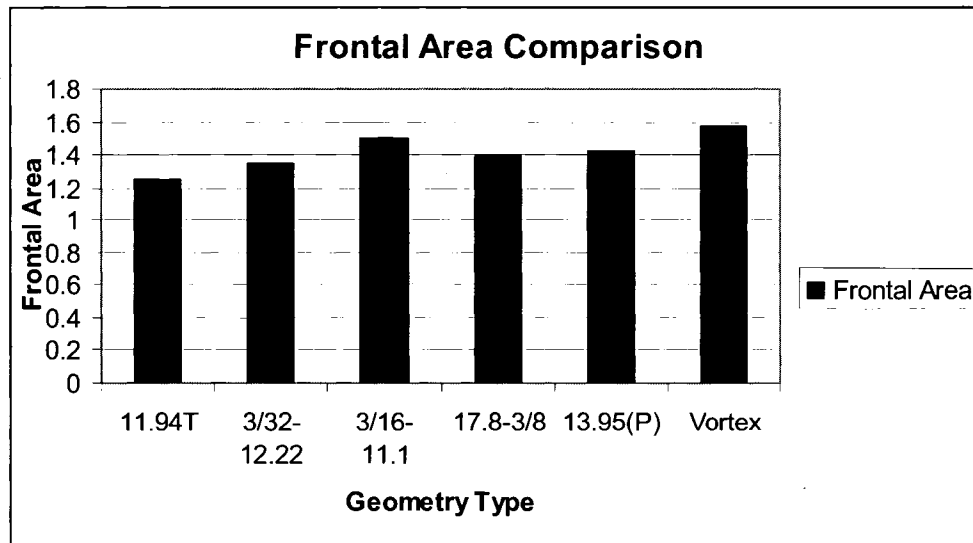


Figure 5.1 Frontal Area Comparison of Various Geometries



## 5.2 Entropy Generation

A thermodynamic analysis for comparing the performance of a number of plate-fin heat transfer surfaces has been generalized to more than sixty geometries. The relative merit of each surface geometry has been linked to its irreversibility level, taking into account both heat transfer and fluid flow friction. Comparison has been performed under the constraint that heat transfer duty, mass flow rate, heat exchanger length, all of which are fixed.

The thermodynamic performance of the most suitable surfaces, among those considered in this research, turned out to be strongly related to the operating conditions (both heat transfer duty and mass flow rate)

## 5.3 Minimum Weight

The analysis of a simplified plate-fin geometry indicates that a minimum weight solution is a function of the performance requirements and material parameters, given basic surface dimensions. This solution corresponds to a unique fin thickness and fin efficiency.

For plate fin surfaces, cores are usually made from sheet stock of a fixed range of thicknesses: rolling fin stock to a special optimum thickness could be uneconomic. It may not be possible to form fins of sufficient dimensional accuracy if they are too thin; if they can be made they might deform unsatisfactorily on brazing. There may also be lower thickness limits set by corrosion requirements. Pressure containment capability often sets a minimum fin thickness, as could stress fatigue requirements.

#### 5.4 Future Work and Recommendations

The direct test data used in this study were published 39 years ago, so many heat transfer enhancement and material development were achieved during this long period.

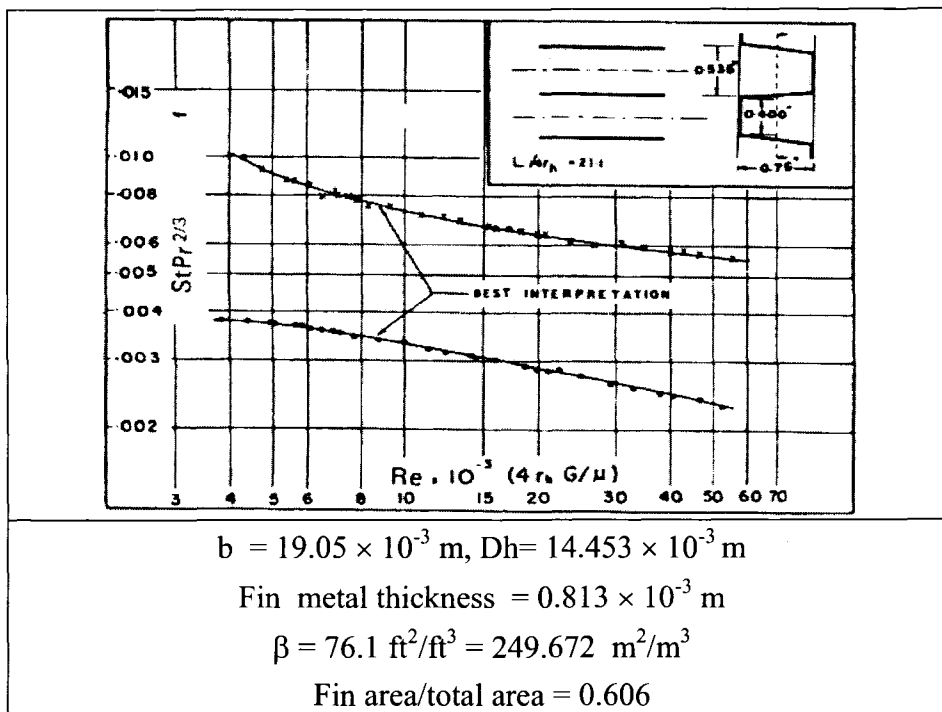
Nowadays there are a lot of very sophisticated compact heat exchangers used in industrial applications which may present a great step in the design of the compact heat exchangers. Printed circuit heat exchangers (PCHE) is one of these sophisticated heat exchangers, originally developed for refrigeration applications, is formed by using a technology adapted from that used for electronic printed circuits, this type is characterized by very high pressure containment capability, high compactness and very high fin efficiency but it requires more weight than the regular plate fin exchanger. The other type is Marbond heat exchangers, giving very low hydraulic diameter, high porosity and very high corrosion resistance. These two types of heat exchangers are commonly used in most of industrial applications but their characteristic curves are unknown. Future work should focus on these types of heat exchangers in order to make fair comparison between all surfaces known used either in academic research and industry.

## APPENDIX A—CHARACTERISTIC CURVES OF HIGH PERFORMANCE SURFACES OF PLATE FIN HEAT EXCHANGERS

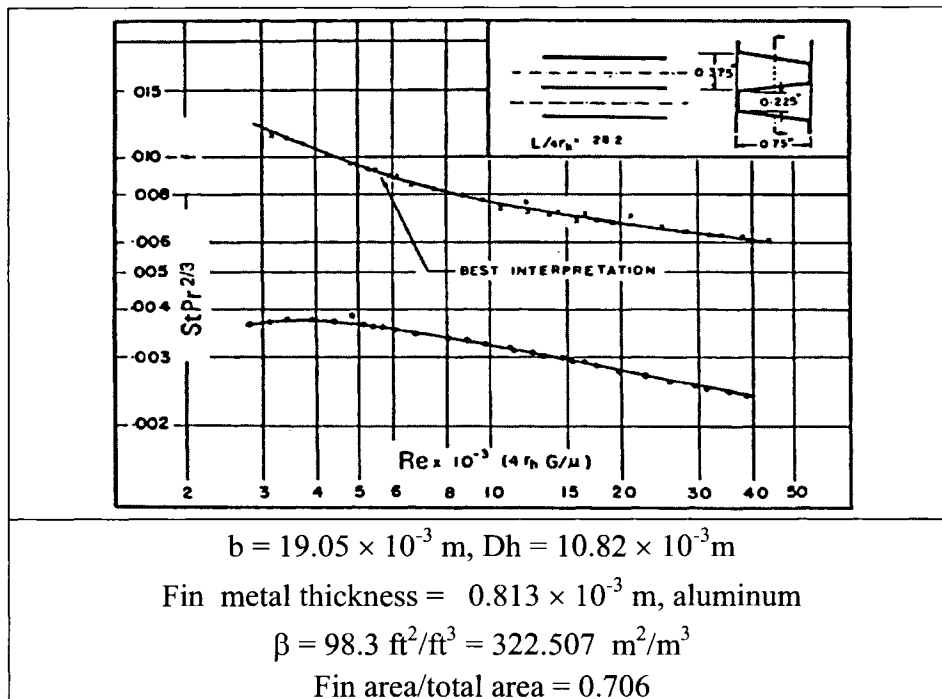
Characteristic curves are the main information needed to design any type of compact heat exchangers surfaces, they are a relation between Colburn factor ( $j$ ) that represents the heat transfer factor and mean friction factor ( $f$ ) factor

### A-1 Characteristic Curves for plain fin surfaces

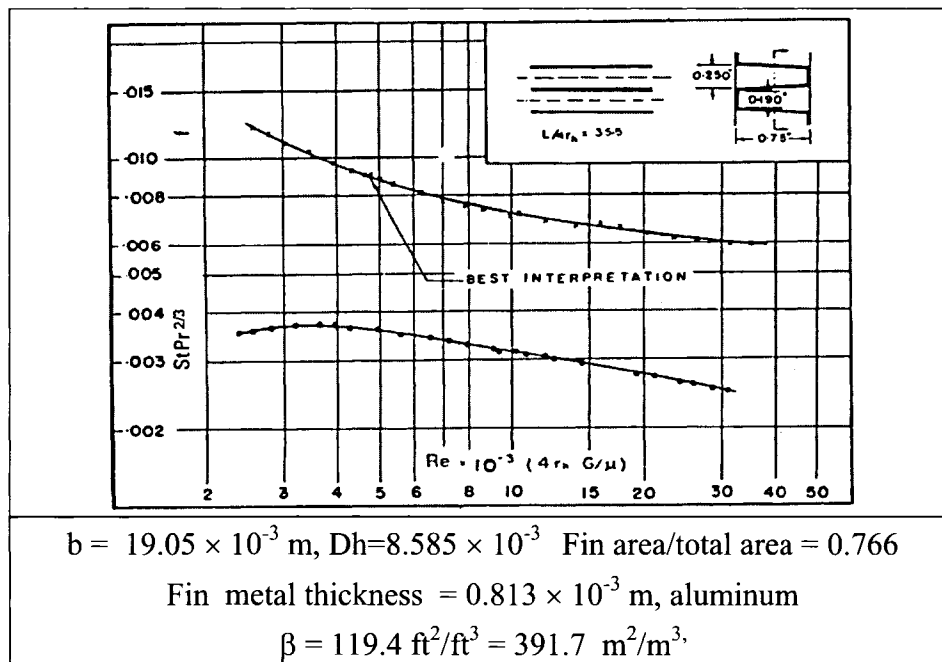
#### 1. Surface 2.0 Plain



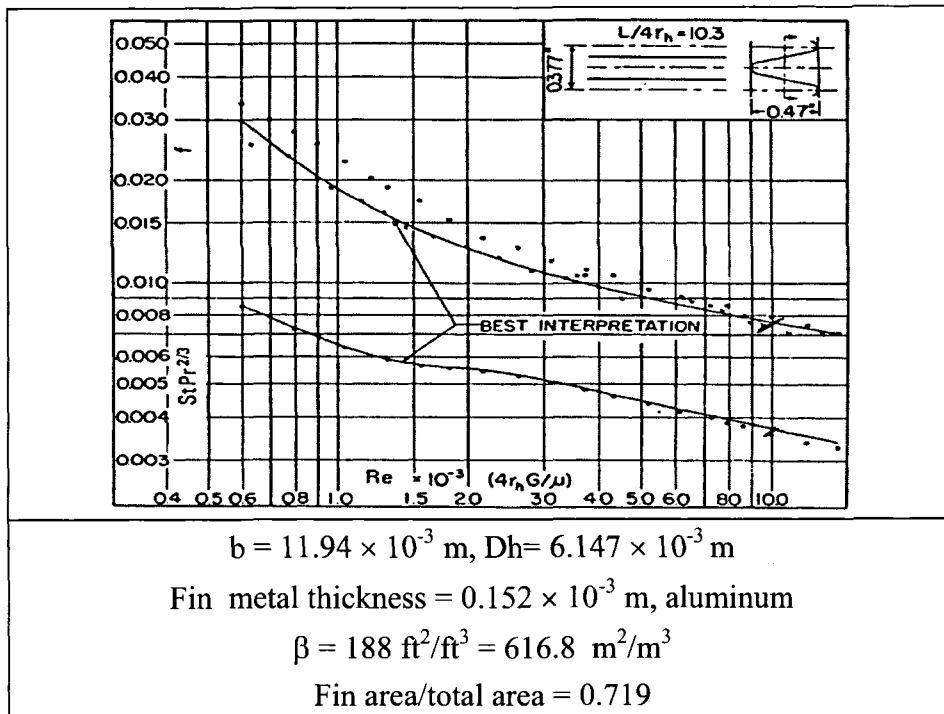
## 2-Surface 3.01 Plain



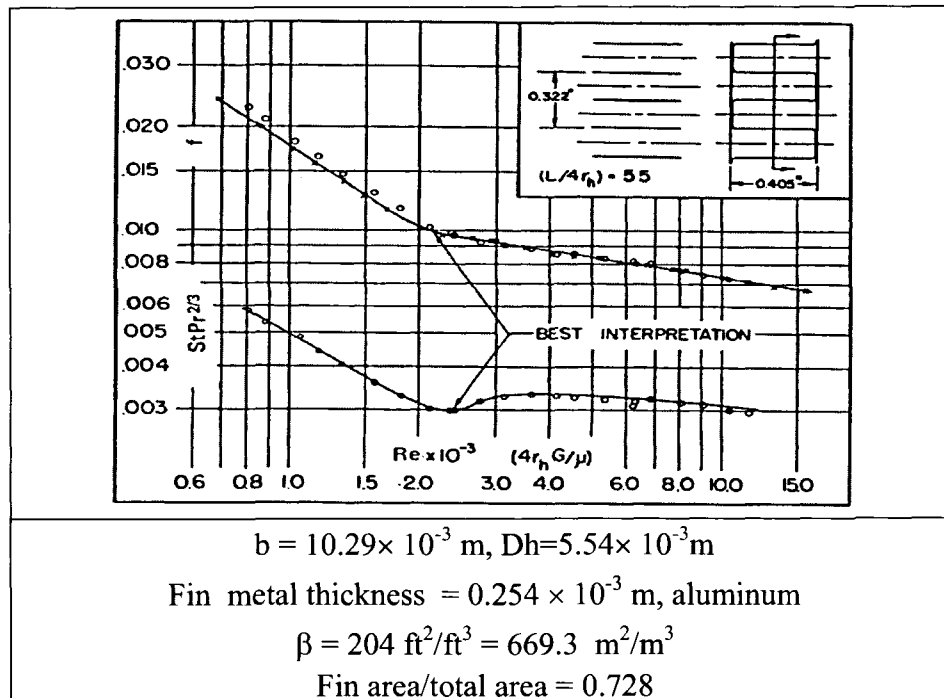
## 3-Surface 3.97 Plain



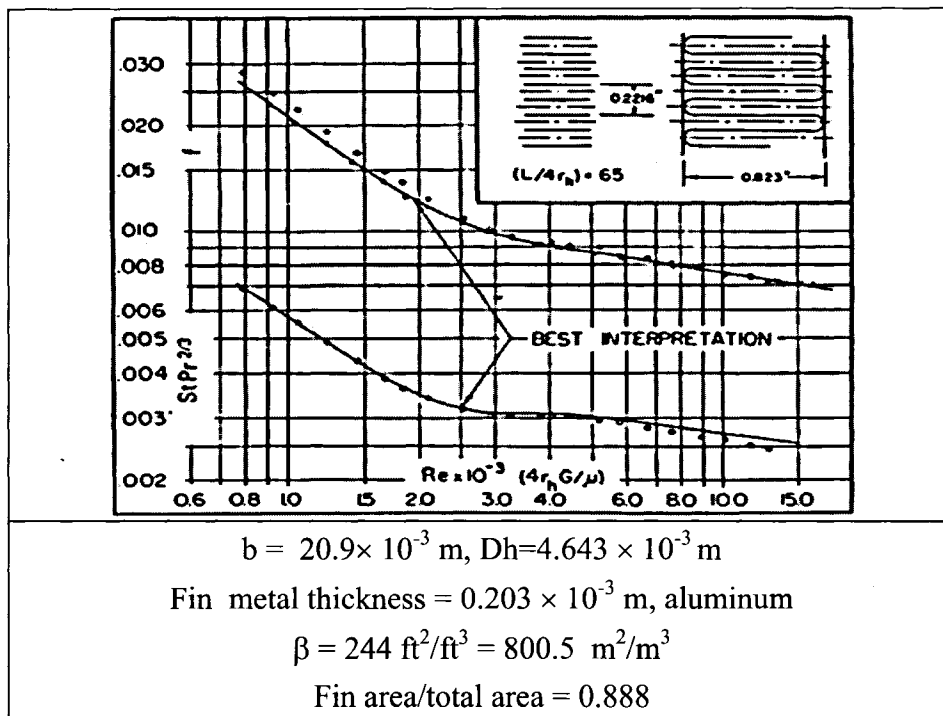
#### 4-Surface 5.3 Plain



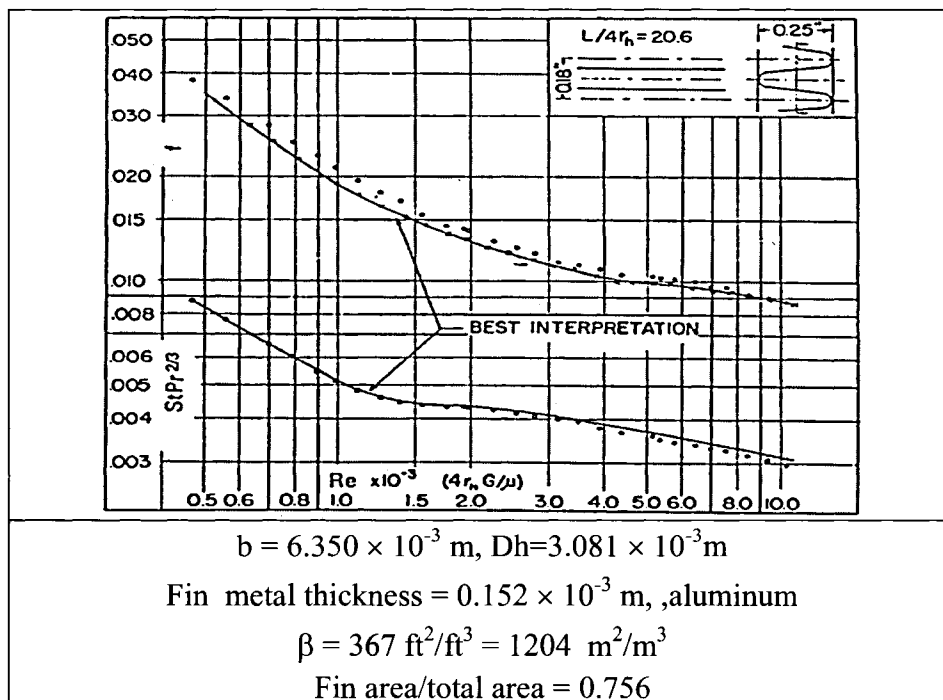
#### 5- Surface 6.2 Plain



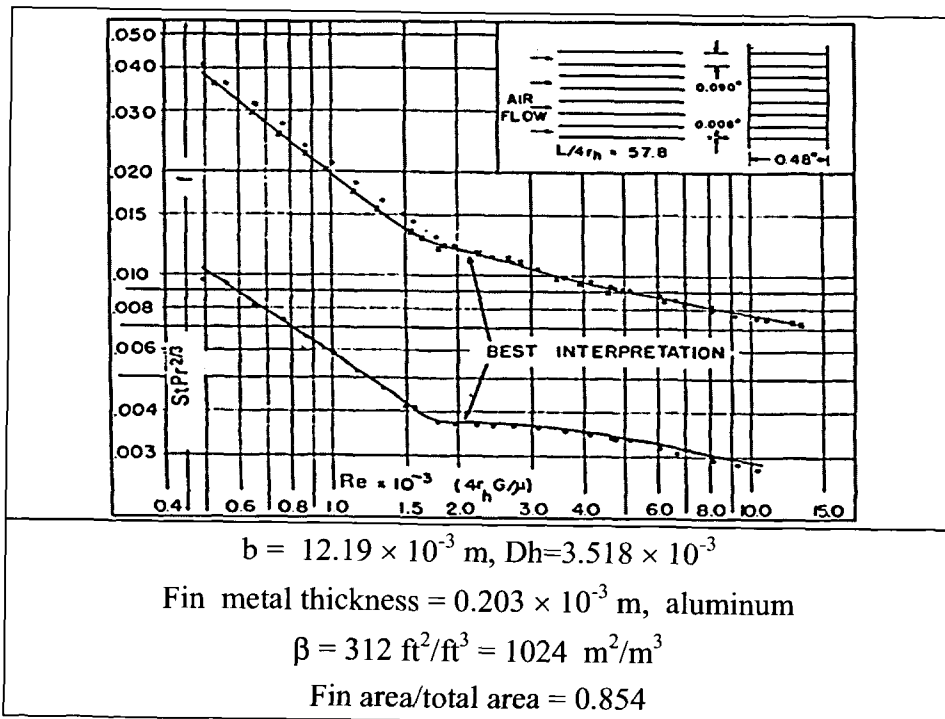
# 6- Surface 9.03 Plain



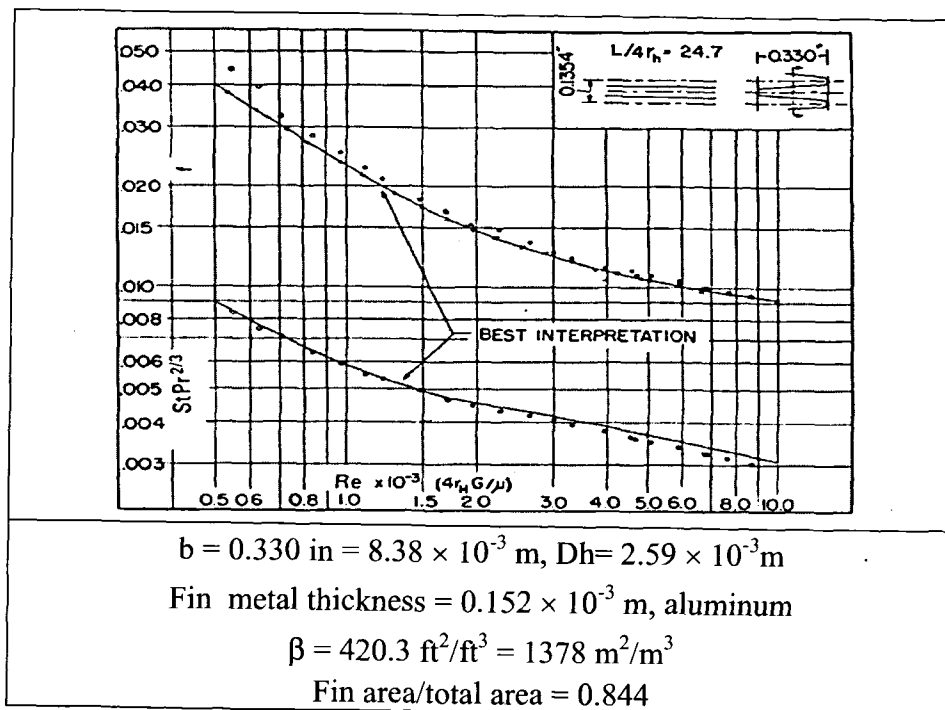
# 7-Surface 11.11



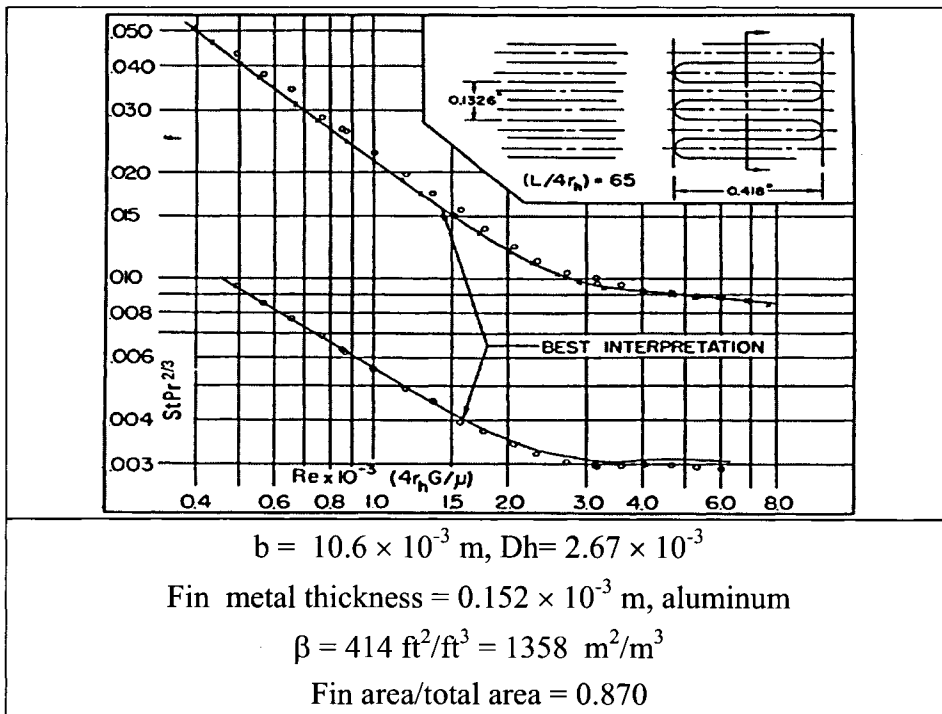
8-Surface 11.11(a) Plain



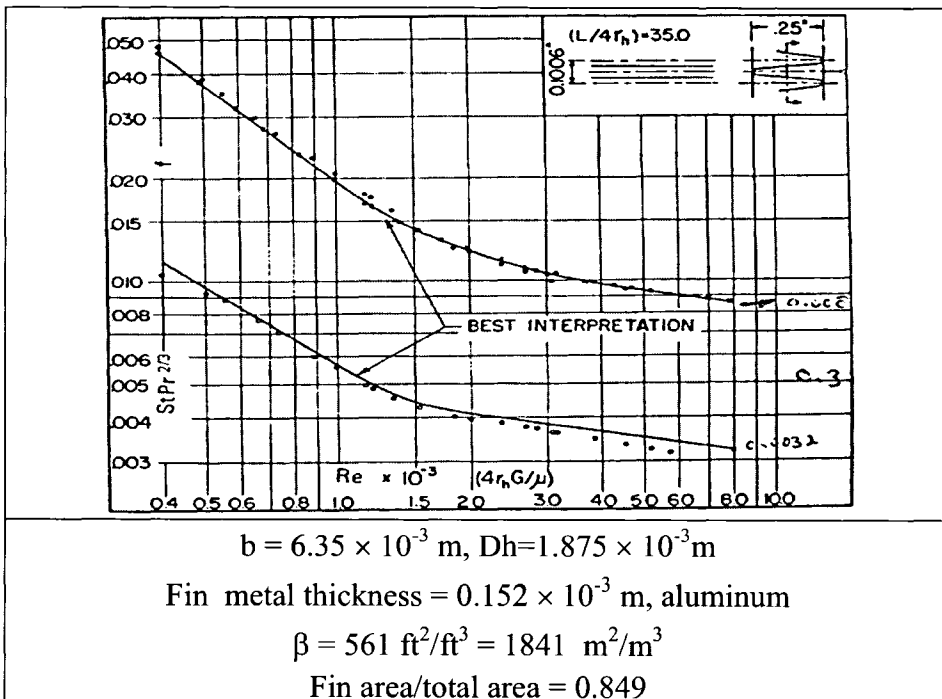
9- Surface 14.77



# 10-Surface 15.08 Plain

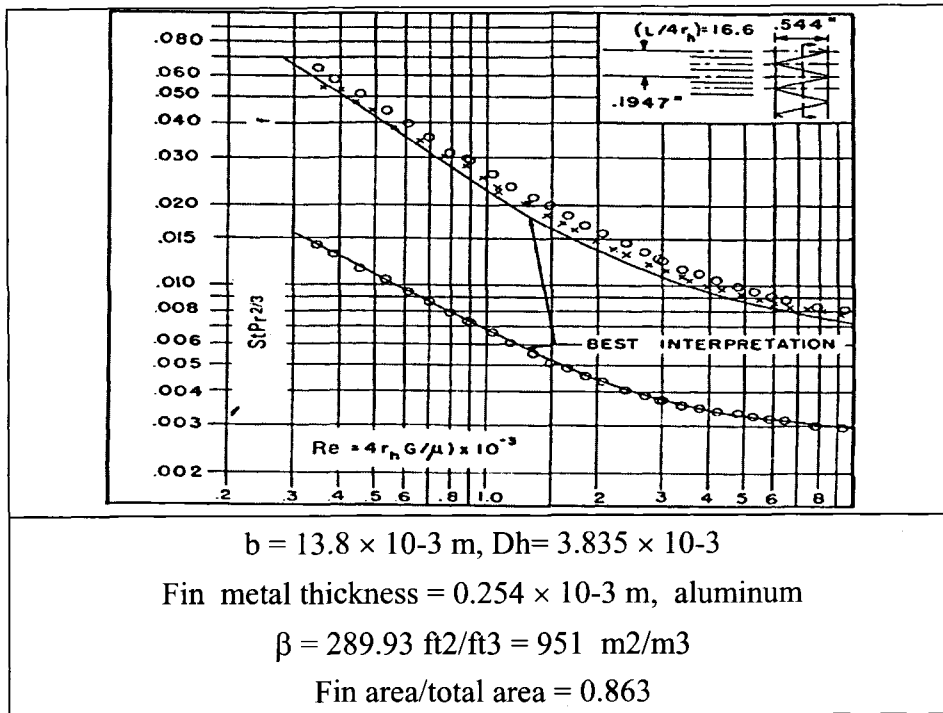


# 11-Surface 19.86 Plain

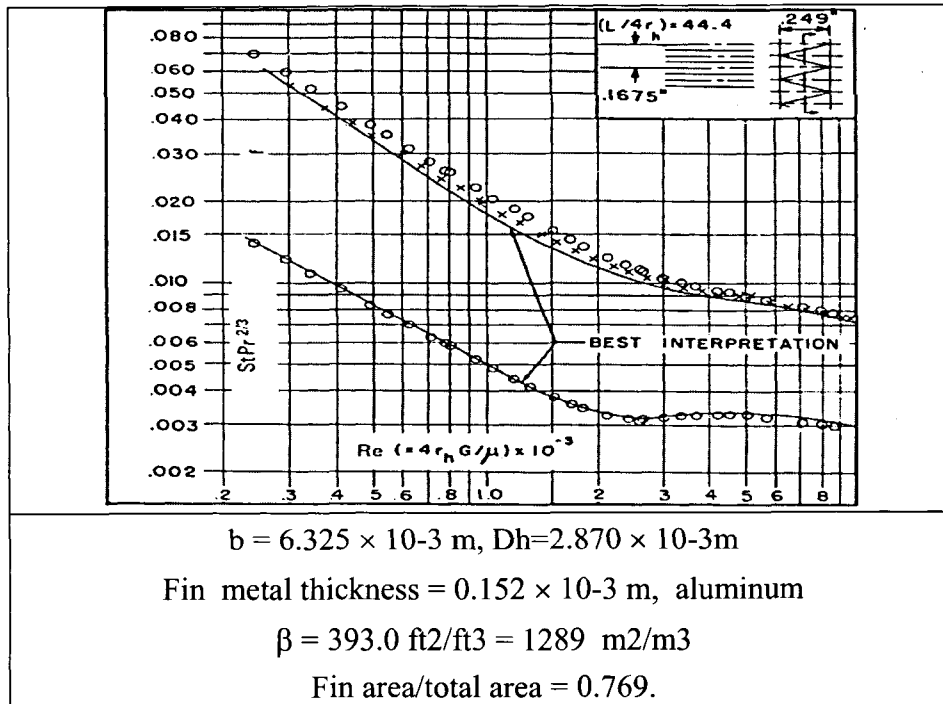




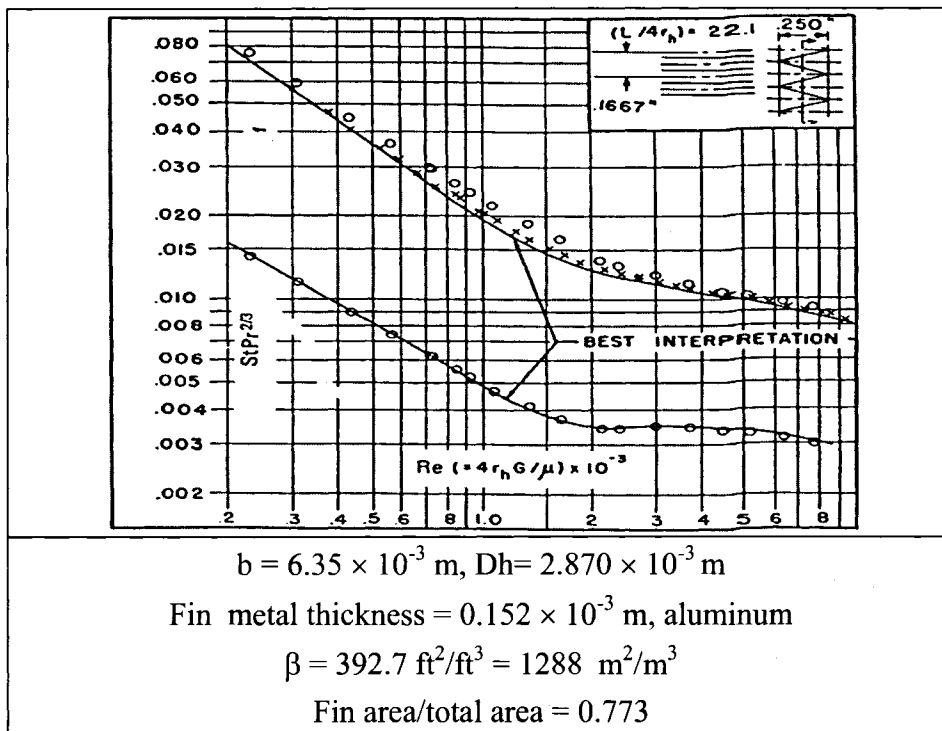
### 12-Surface 10.27 T Plain



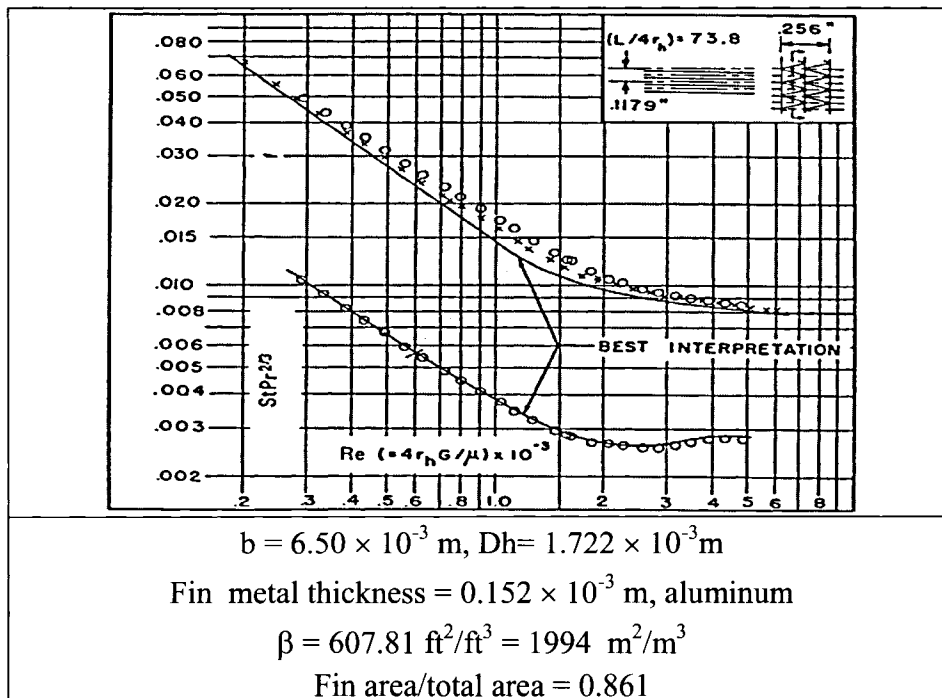
### 13-Surface 11.94 T Plain



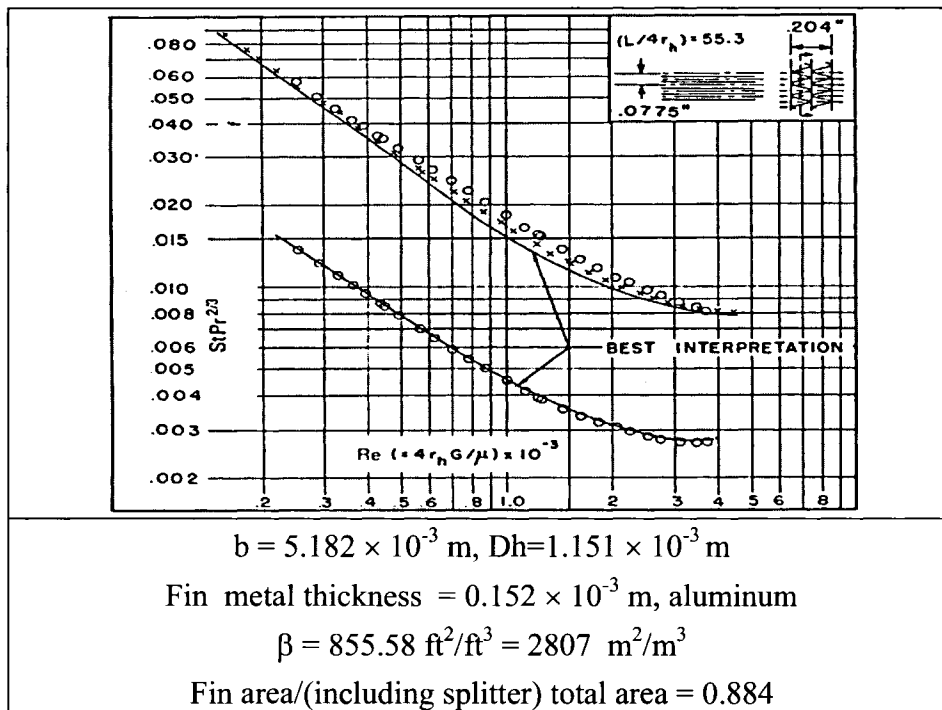
#### 14-Surface 12.00T Plain



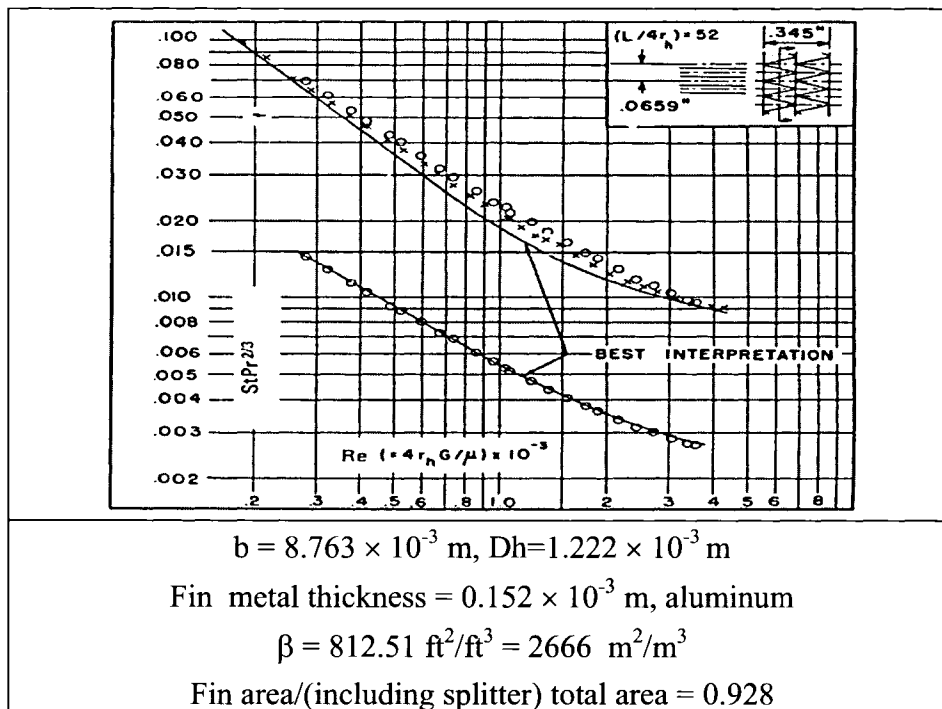
#### 15-Surface 16.96T Plain



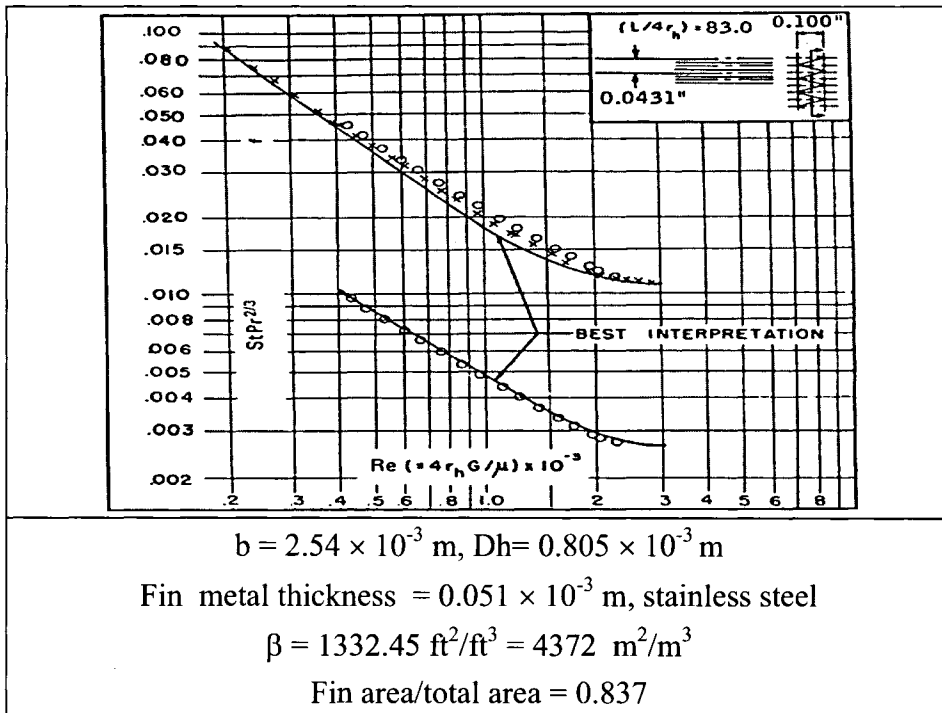
# 16- Surface 25.79T Plain



# 17- Surface 30.33T Plain

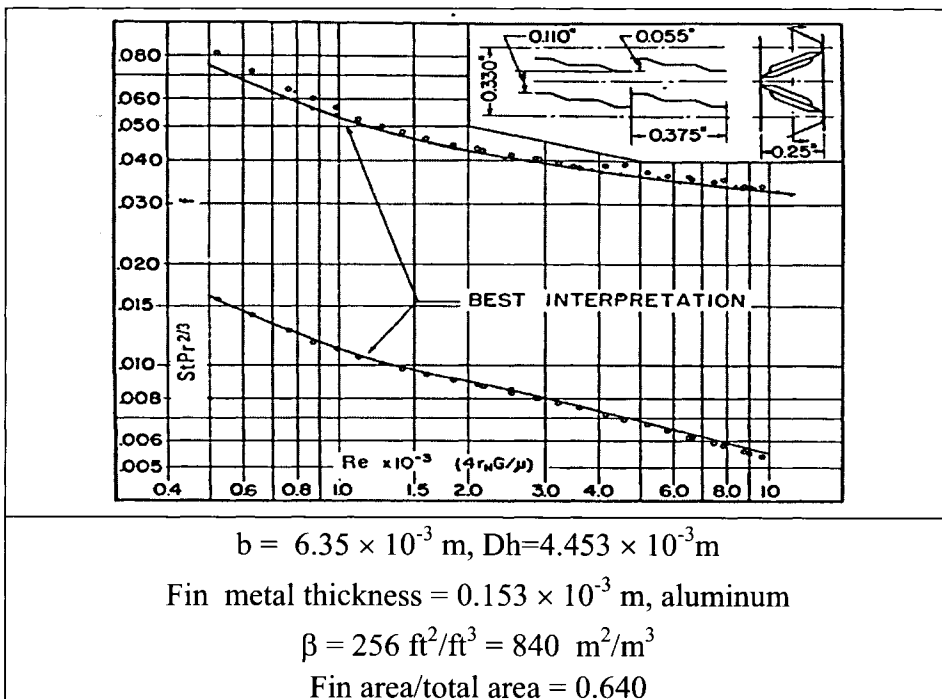


# 18- Surface 46.45T Plain

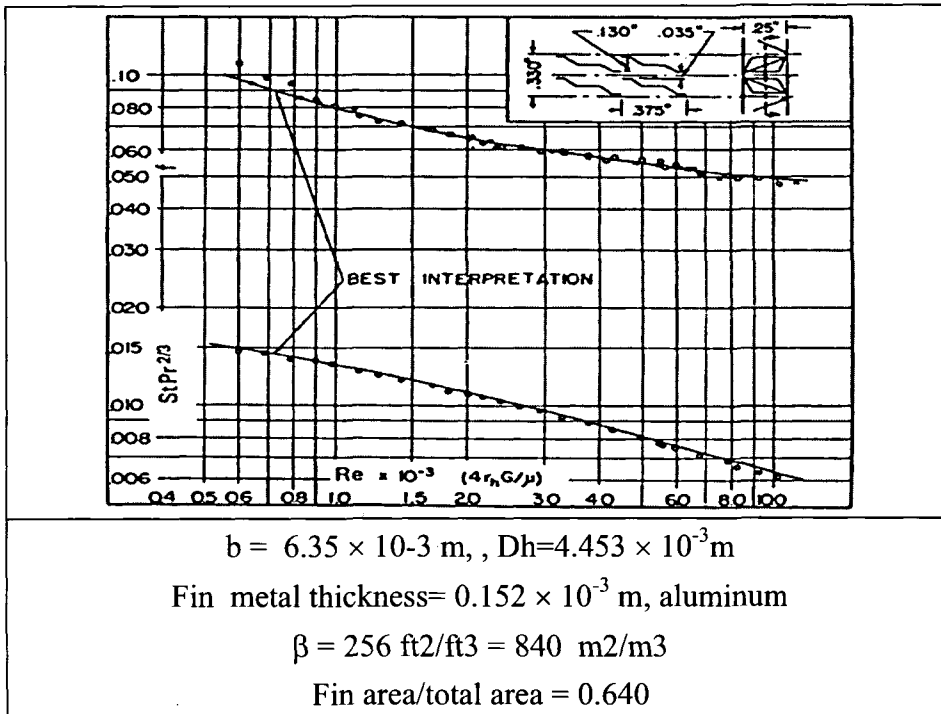


## A-2 Characteristic Curves for Louvered surfaces

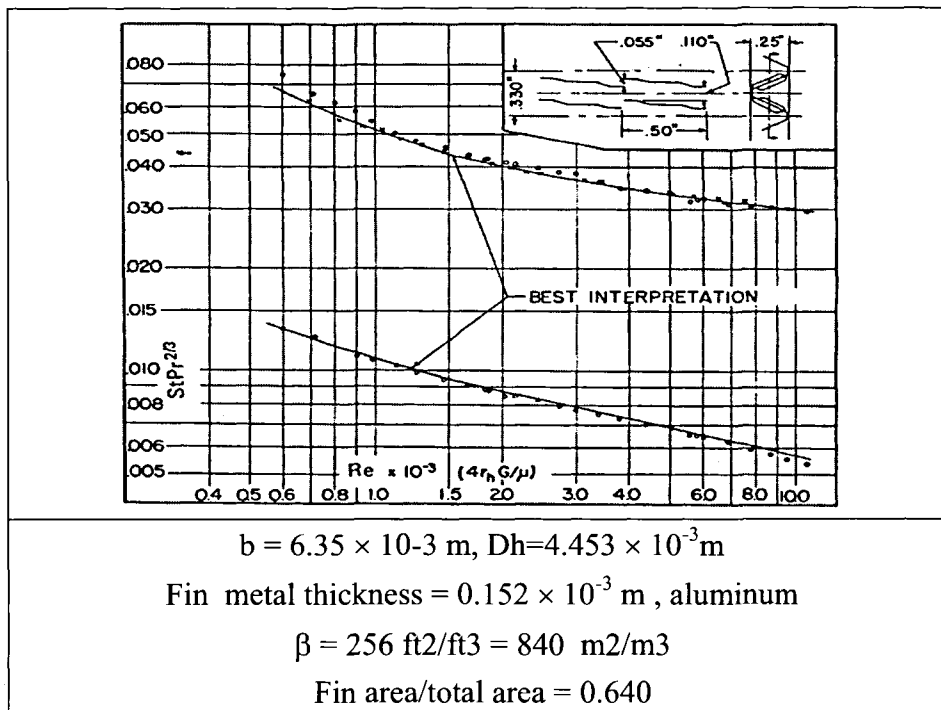
### 1-Surface 3/8-6.06 Louvered



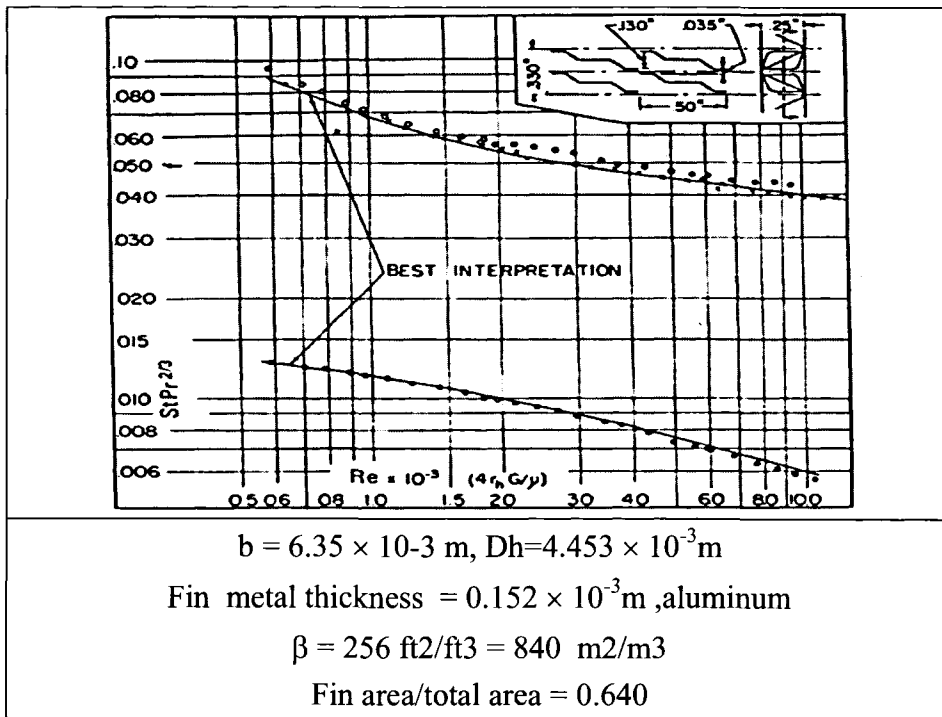
## 2-Surface 3/8(a)-6.06 Louvered



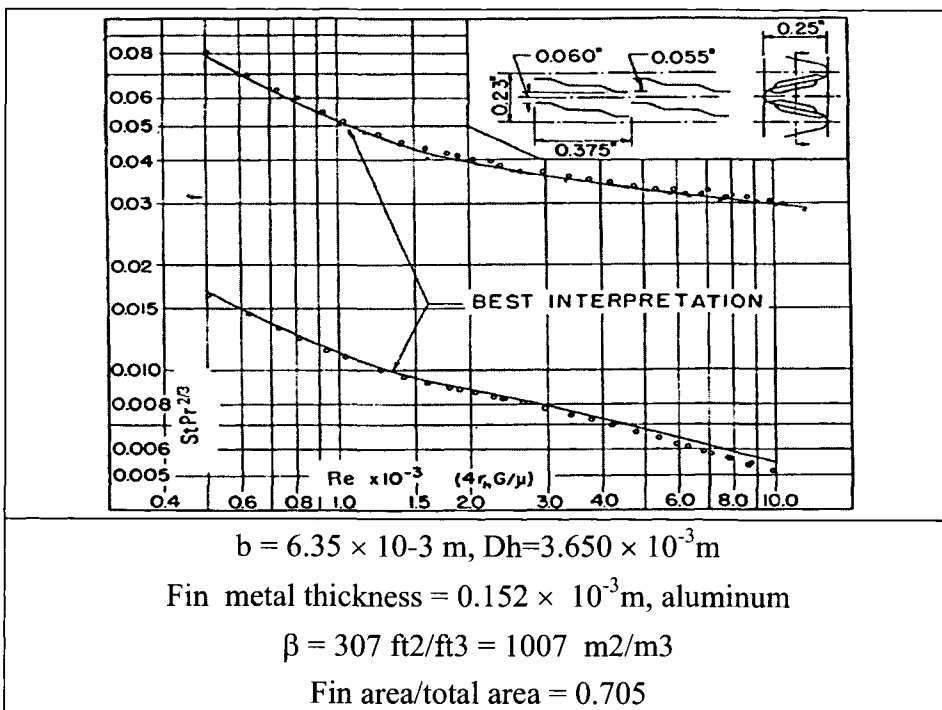
## 3-Surface 1/2-6.06 Louvered



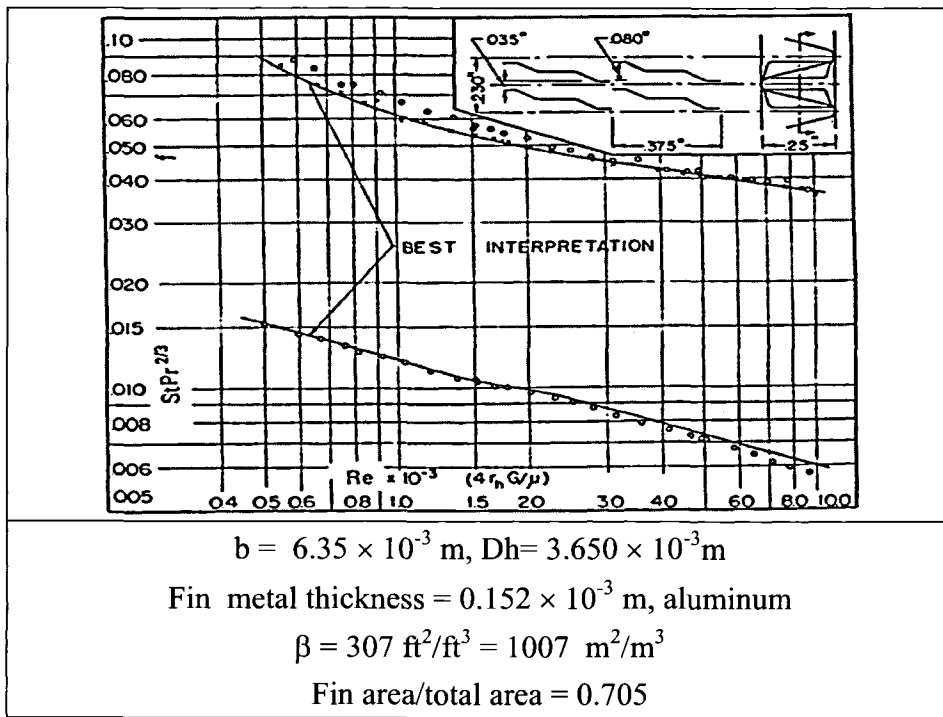
4-Surface 1/2(a)- 6.06



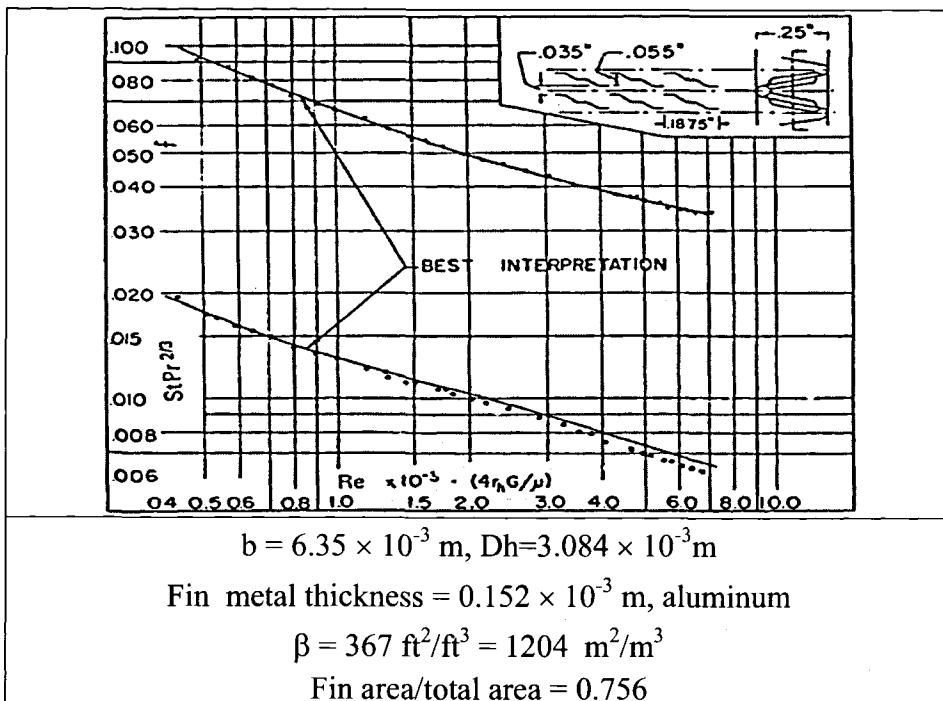
5-Surface 3/8-8.7 Louvered



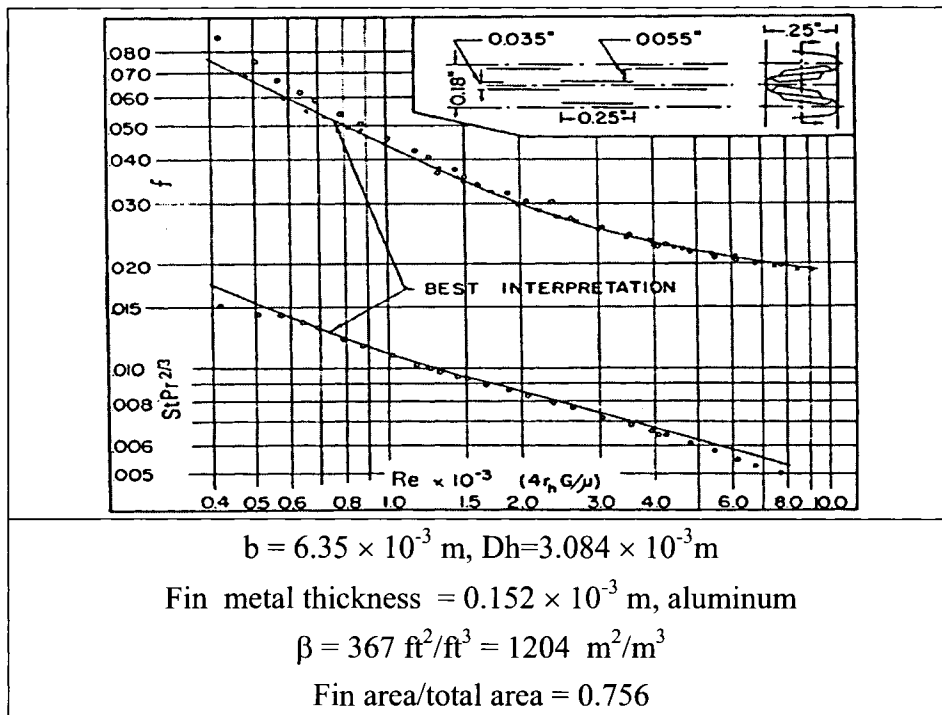
# 6-Surface 3/8(a)-8.7 Louvered



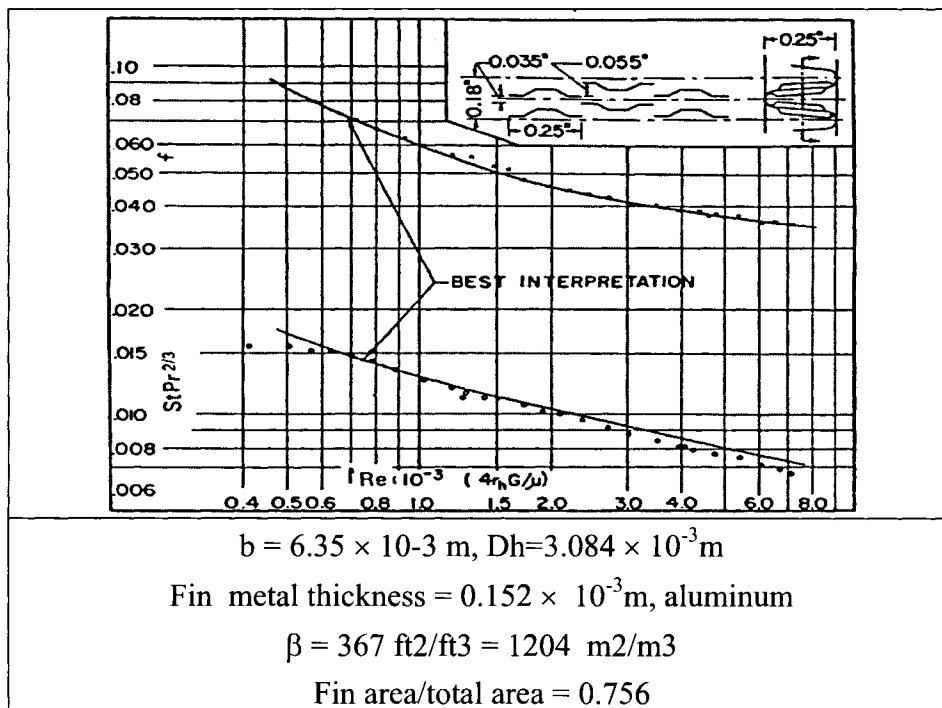
# 7-Surface 3/16-11.1 Louvered



# 8- Surface 1/4-11.1 Louvered

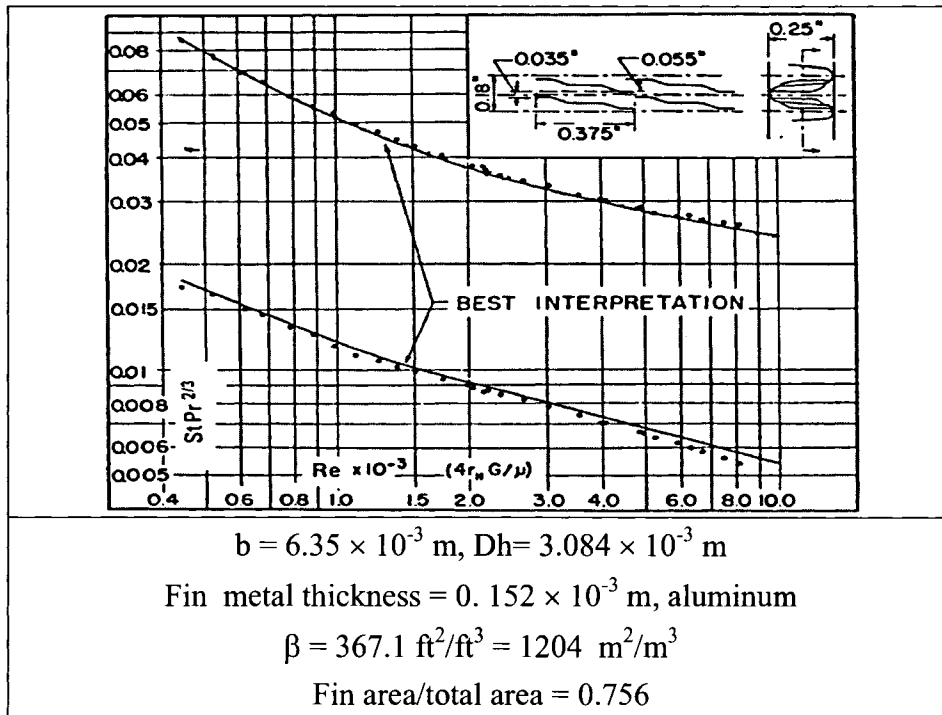


# 9-Surface 1/4(b)-11.1 Louvered

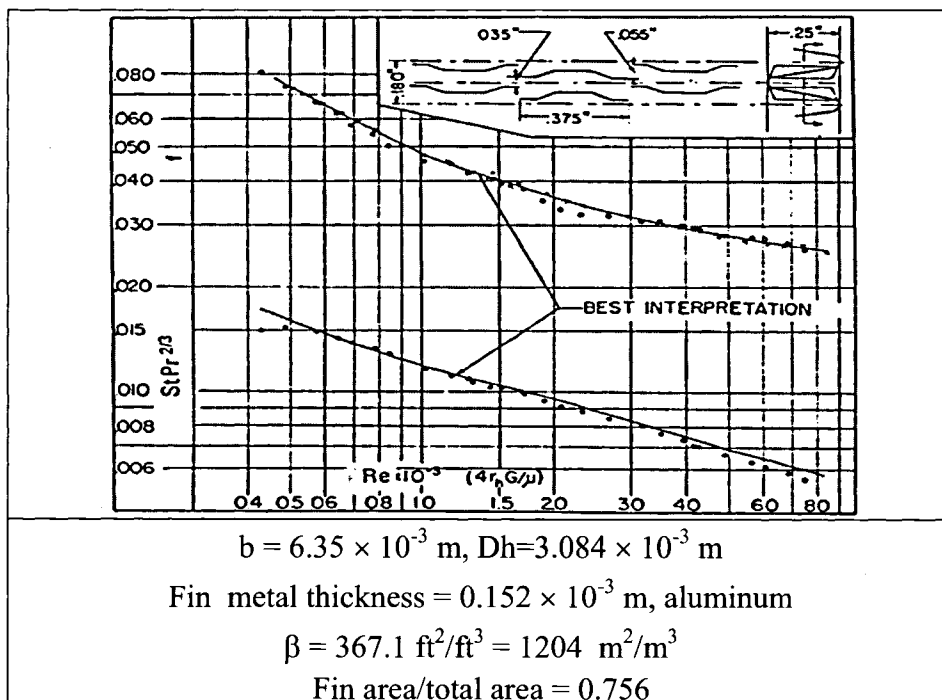




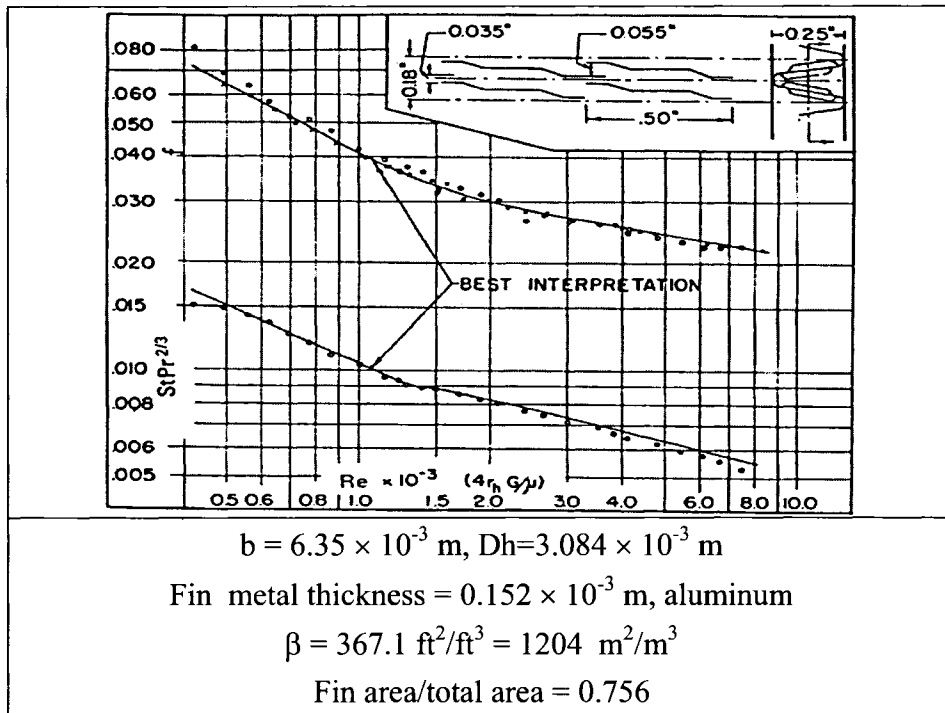
# 10-Surface 3/8-11.1 Louvered



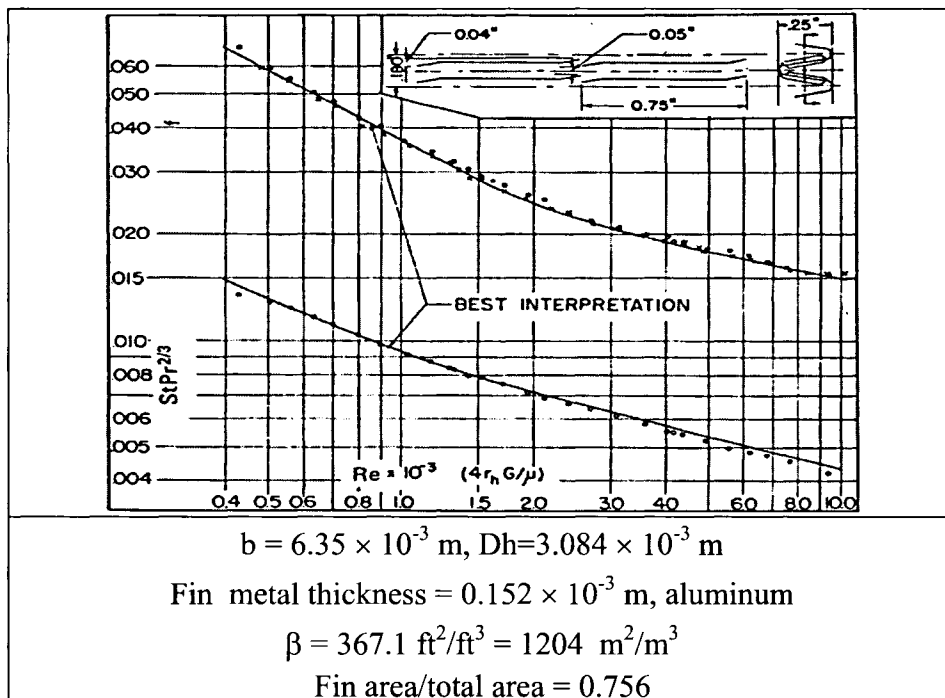
# 11-Surface 3/8(b)-11.1 Louvered



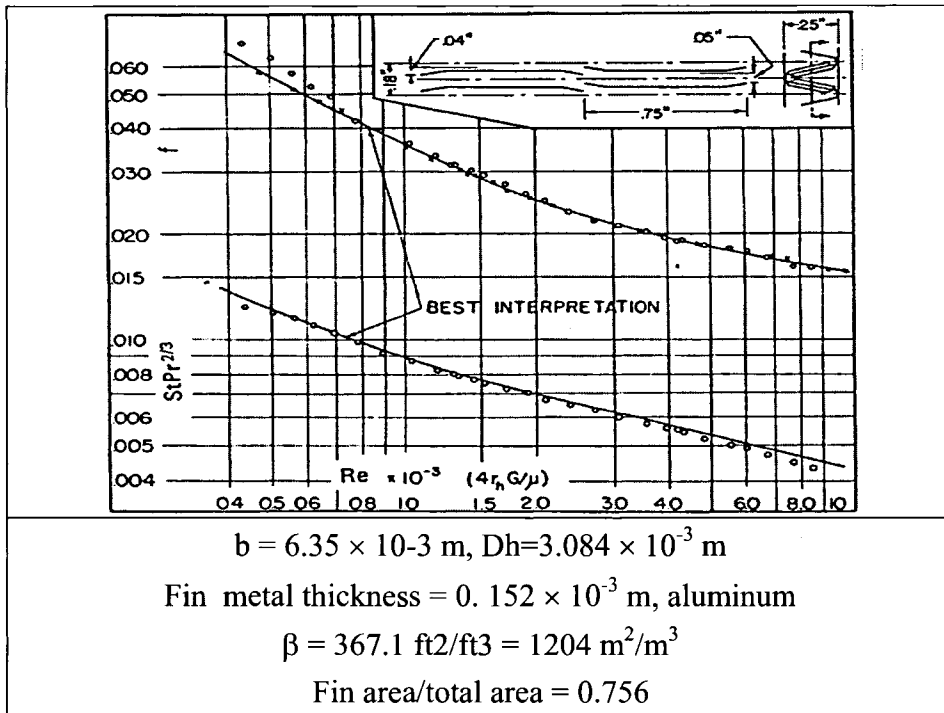
## 12-Surface 1/2-11.1 Louvered



## 13-Surface 3/4-11.1 Louvered

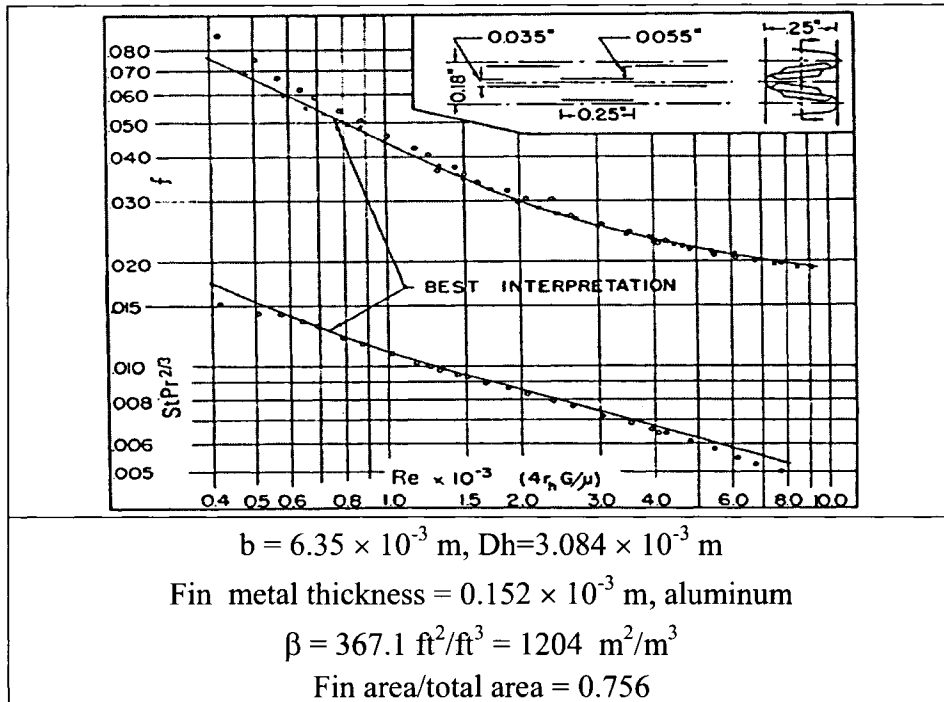


14-Surface 3/4(b)-11.1

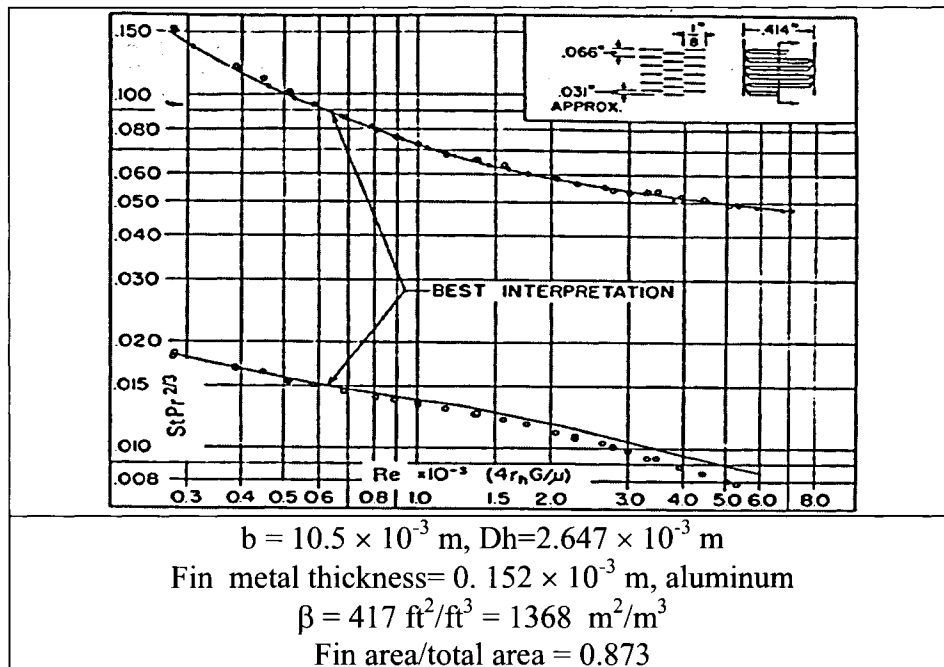


### A-3 Characteristic Curves for Strip Surfaces

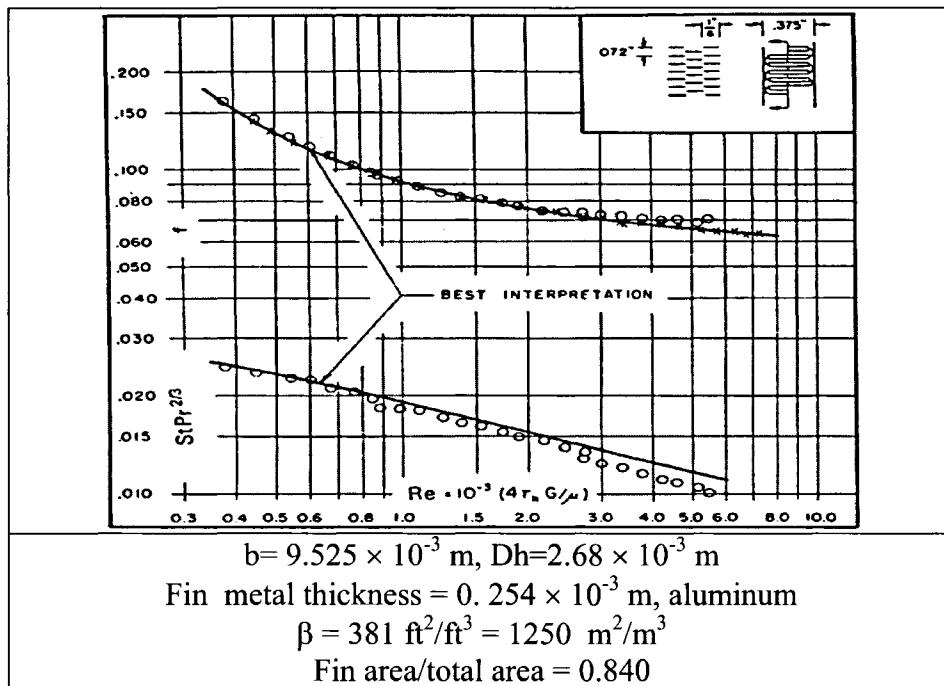
#### 1-Surface 1/4(s)-11.1 Strip



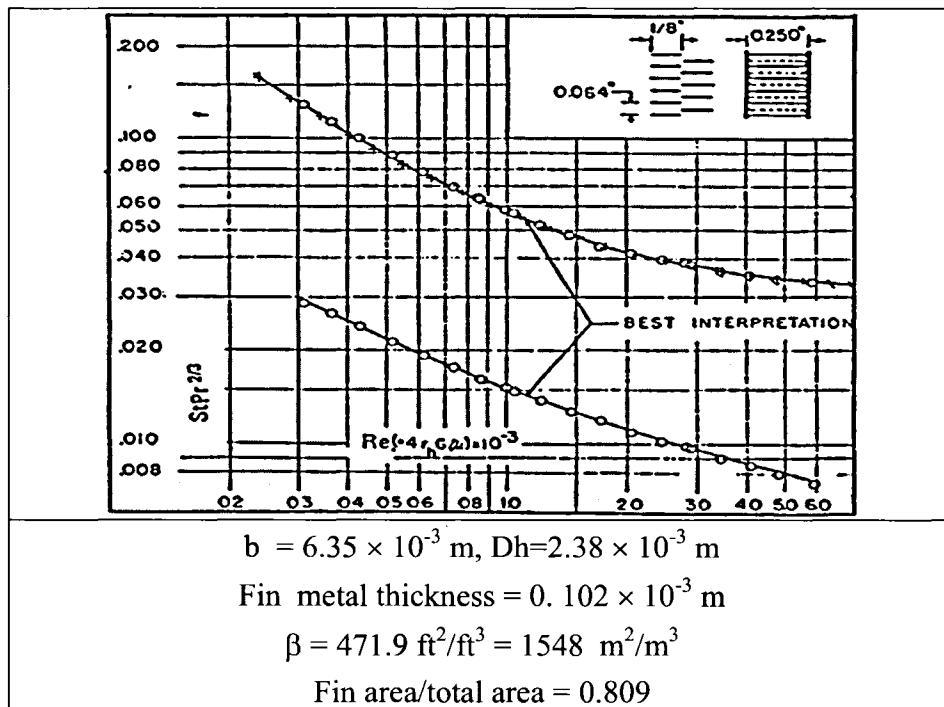
#### 2-Surface 1/8-15.2 Strip



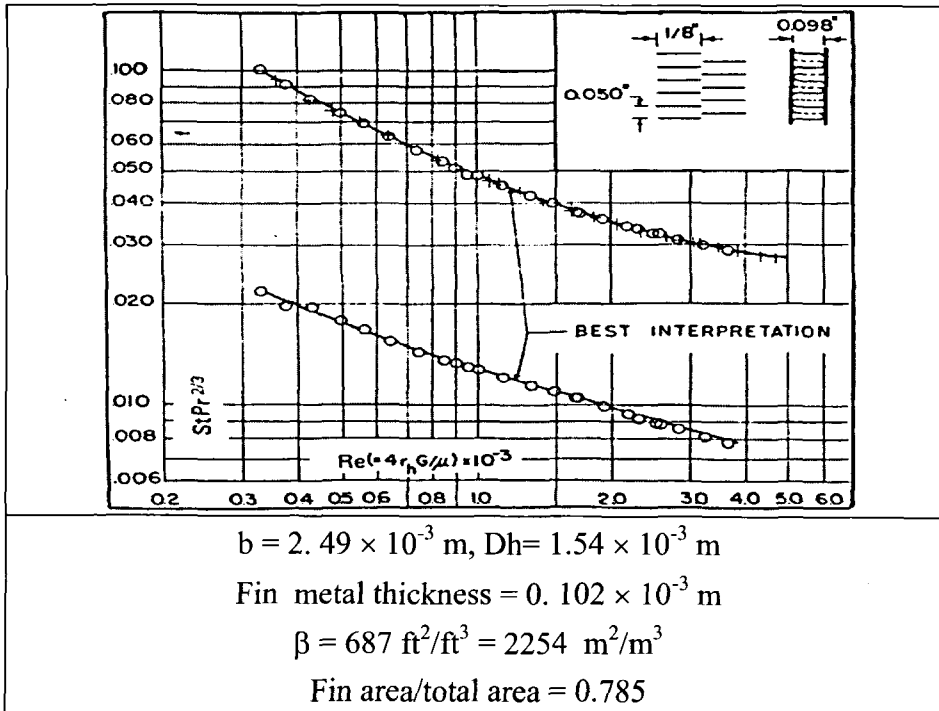
### 3-Surface 1/8-13.95 Strip



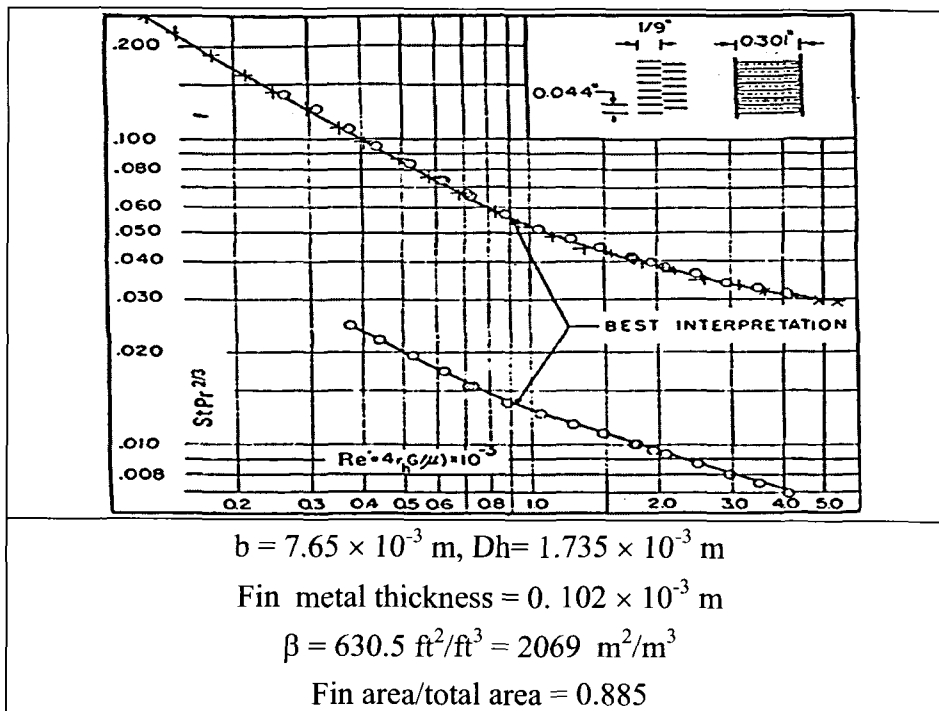
### 4-Surface 1/8-15.61 Strip



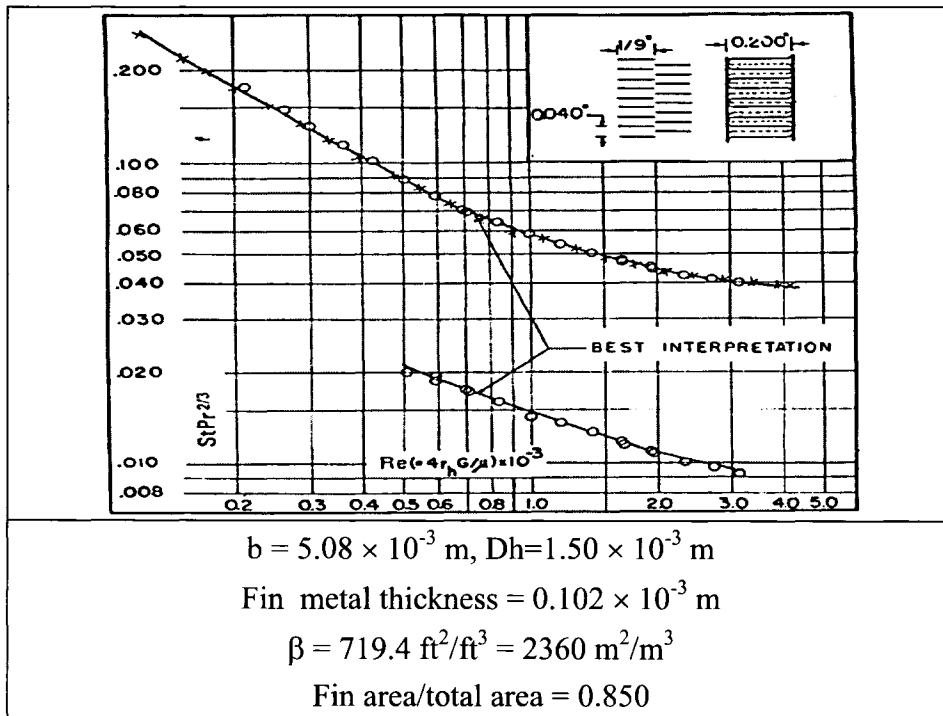
### 5-Surface 1/8-19.86 Strip



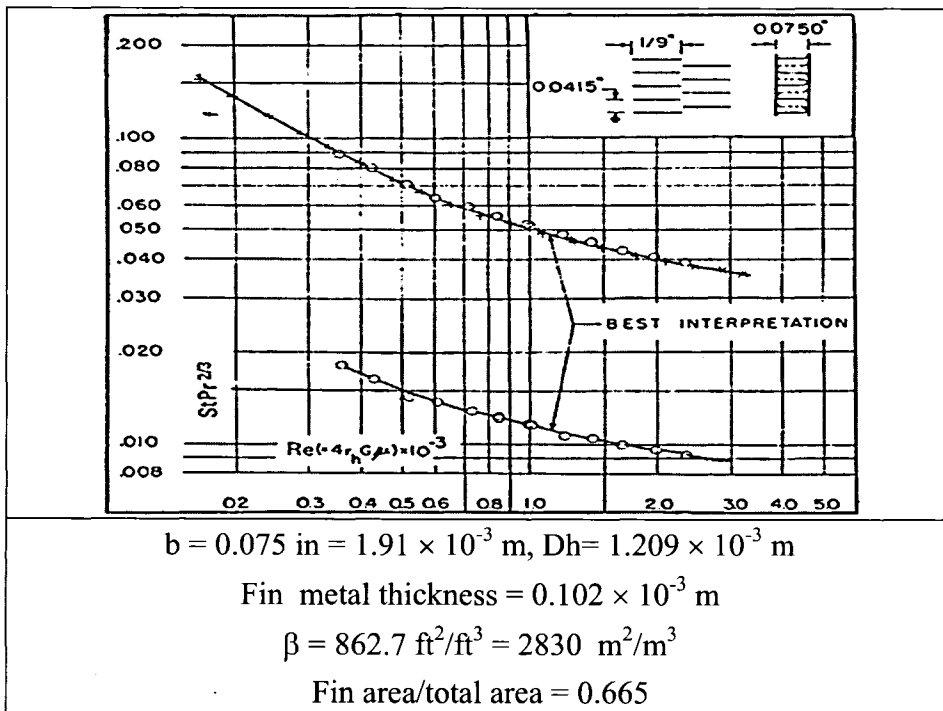
### 6-Surface 1/9-22.68 Strip



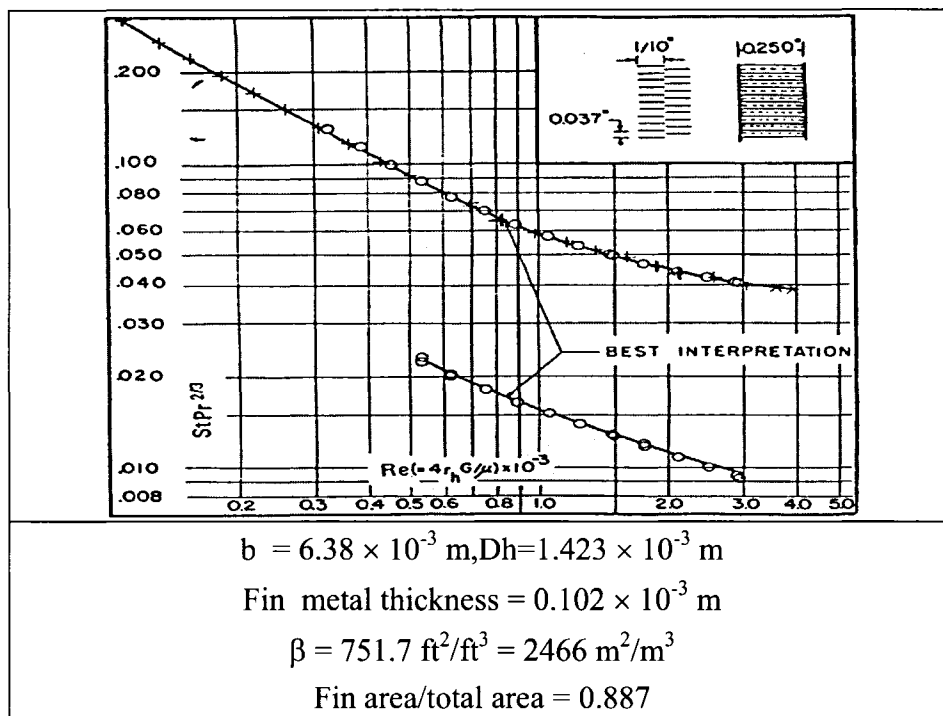
# 7-Surface 1/9-25.01 Strip



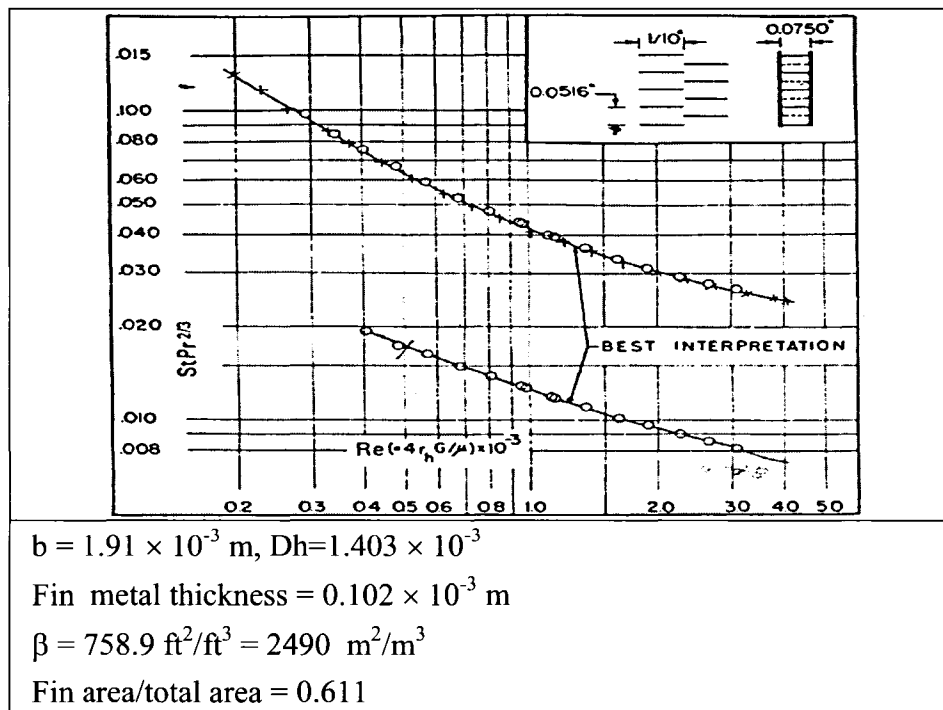
# 8-Surface 1/9-24.12 Strip



### 9-Surface 1/10-27.03 Strip

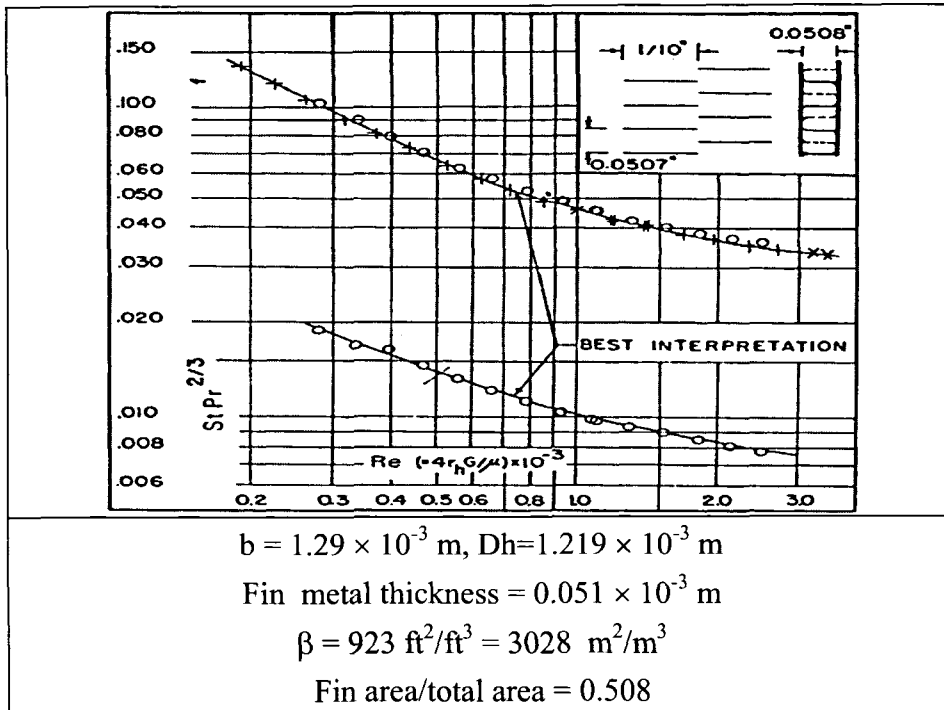


### 10-Surface 1/10-19.35 Strip

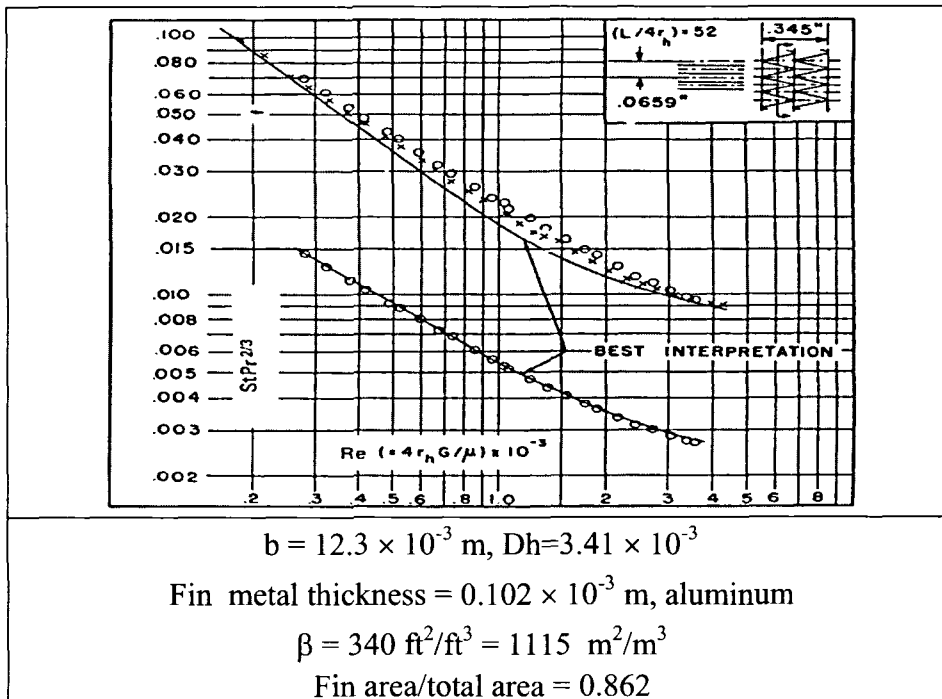




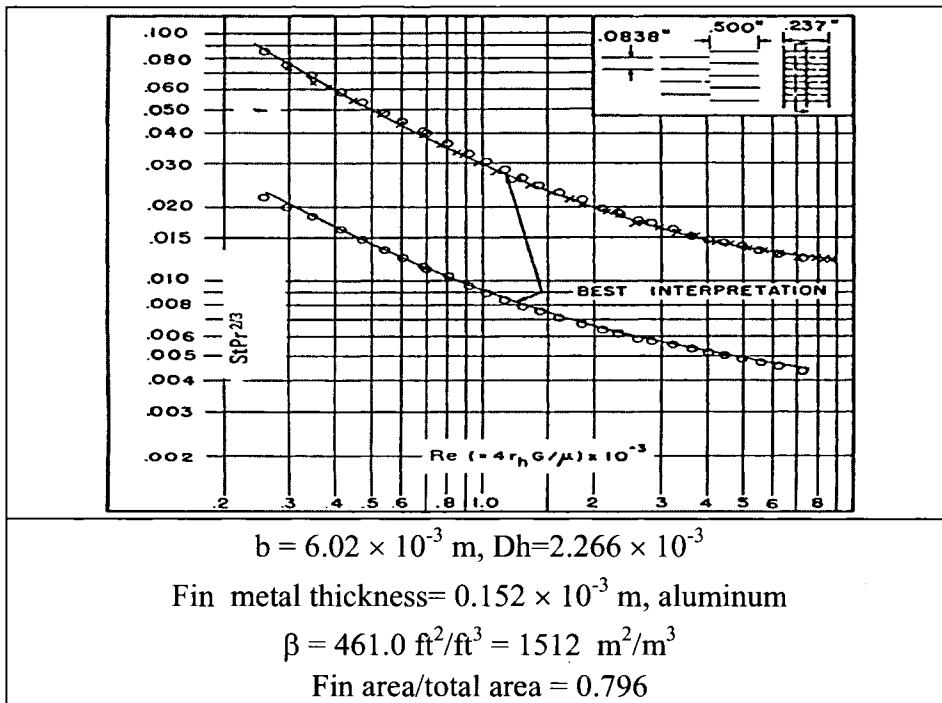
# 11-Surface 1/10-19.74 Strip



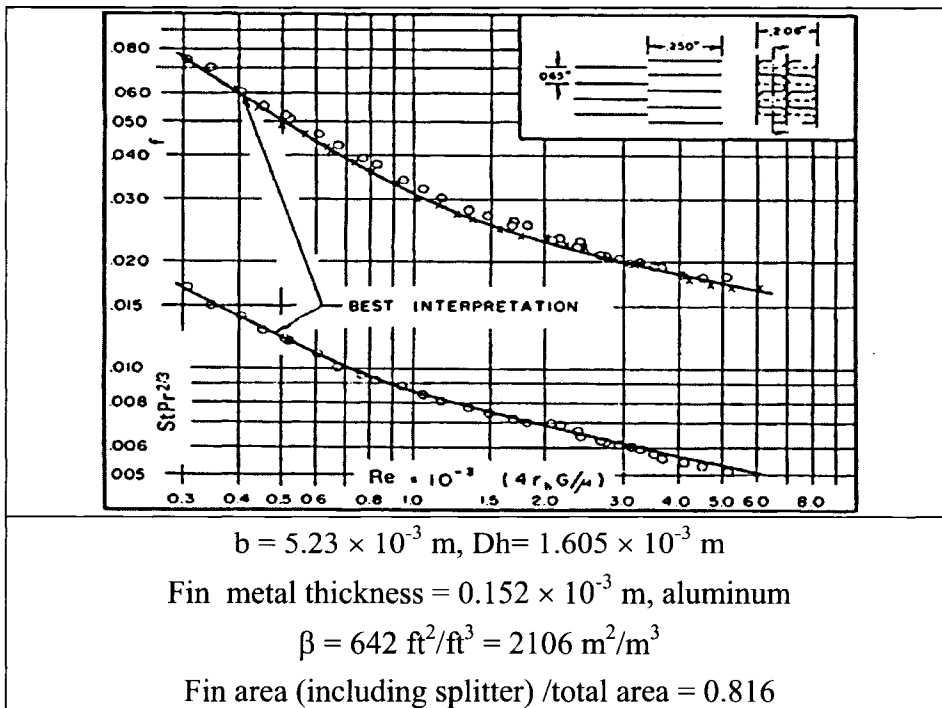
# 12-Surface 3/32-12.22



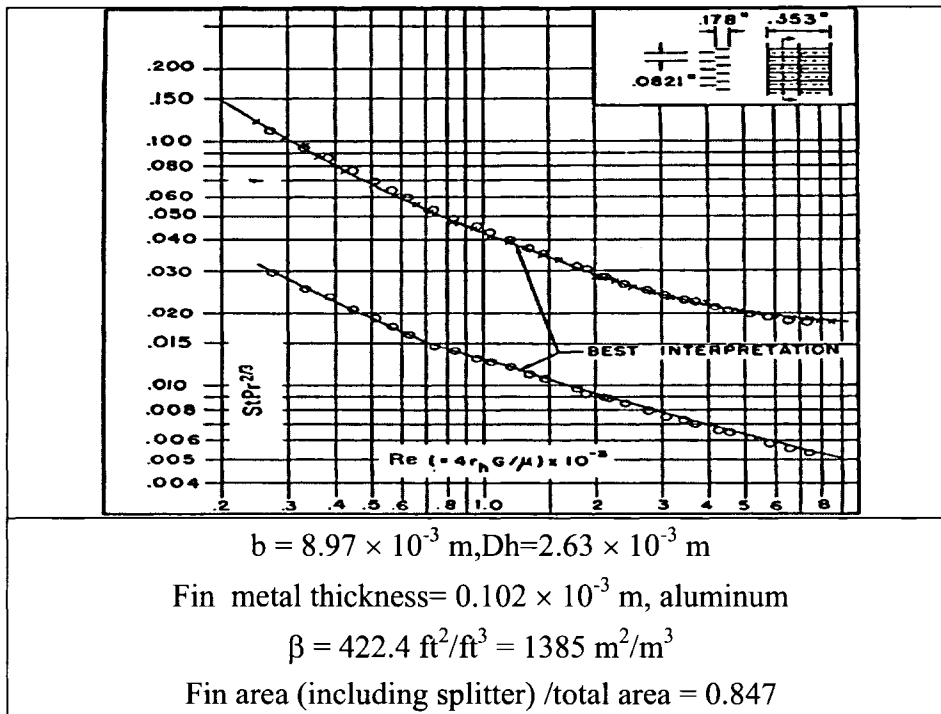
13-Surface 1/2-11.94(D) Strip



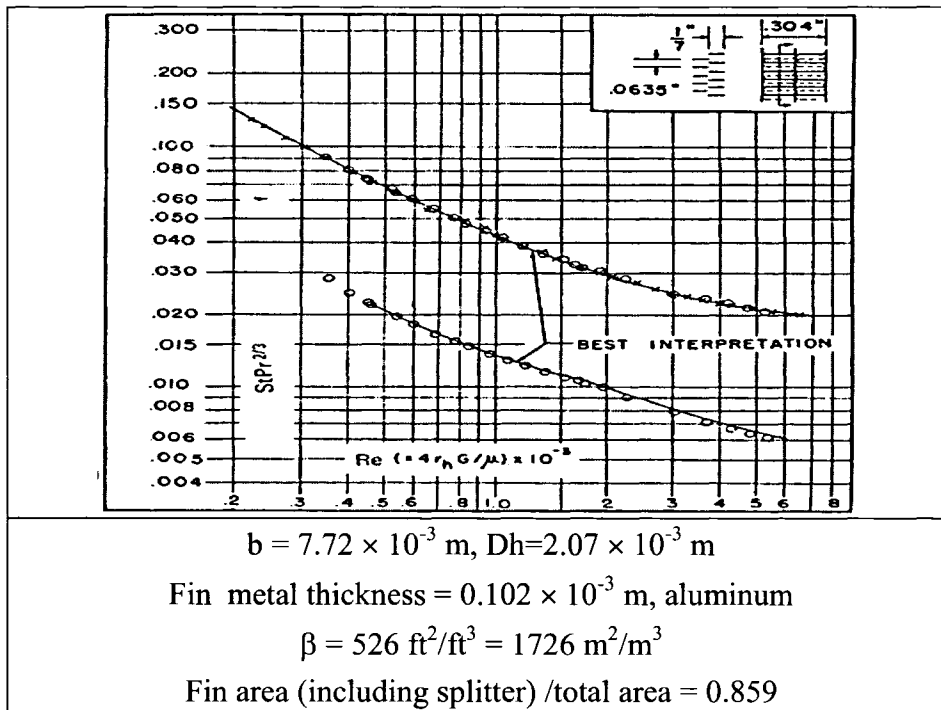
14-Surface 1/4-15.4(D) Strip



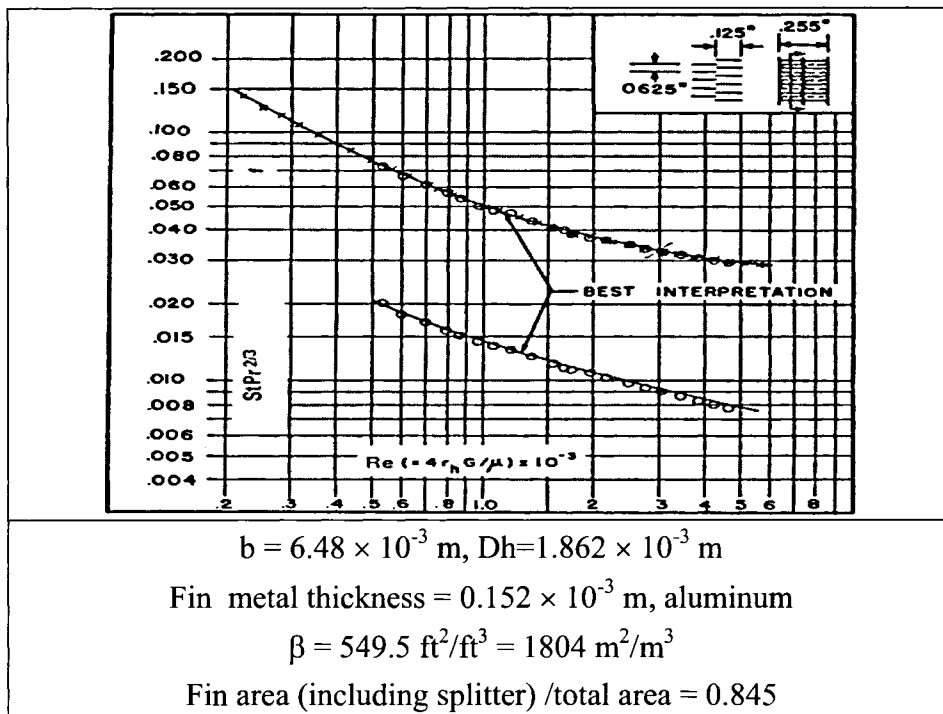
15-Surface 1/6-12.18(D) Strip



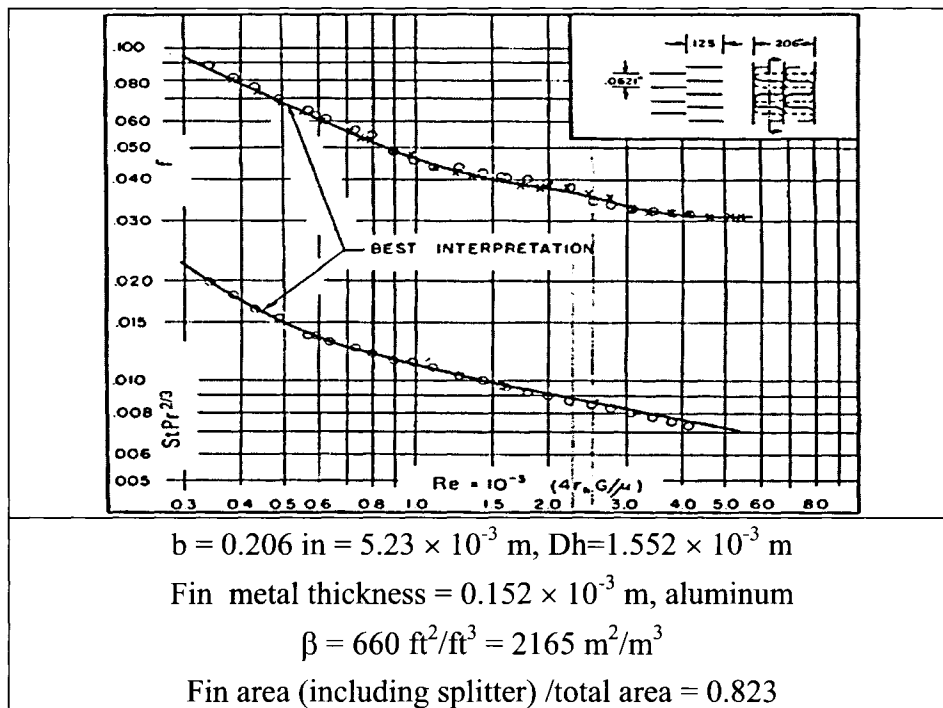
16-Surface 1/7-15.75(D) Strip



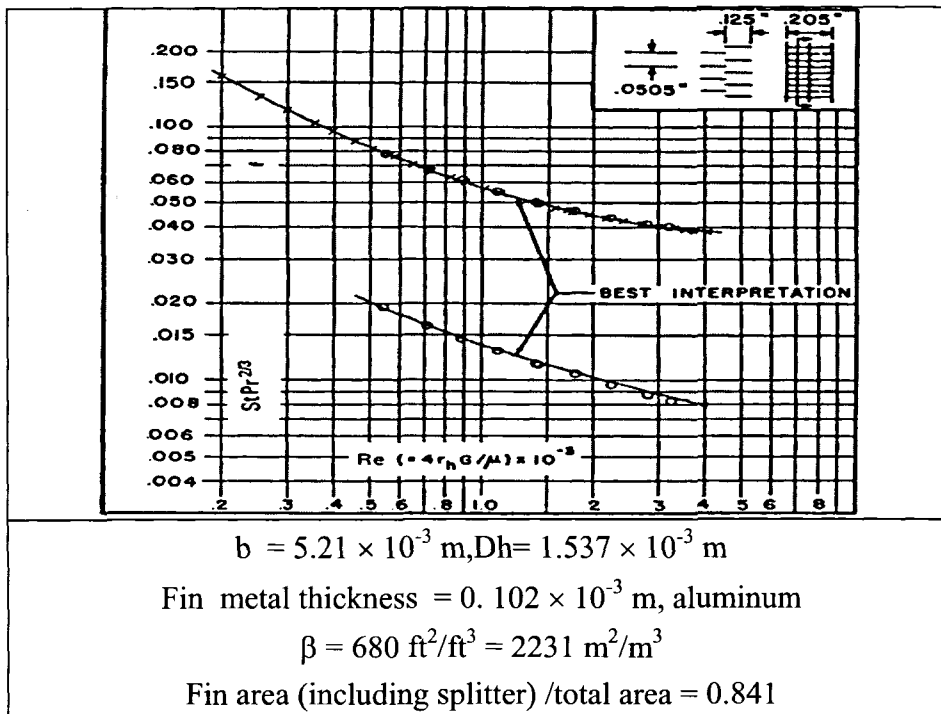
### 17-Surface 1/8-16.00(D) Strip



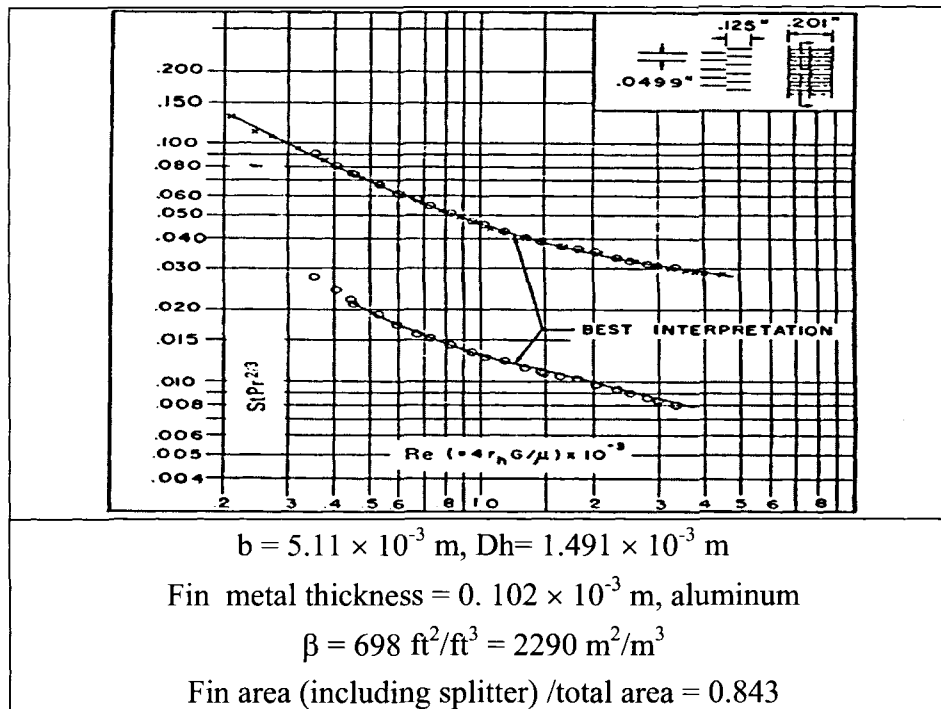
### 18-Surface 1/8-16.12(D) Strip



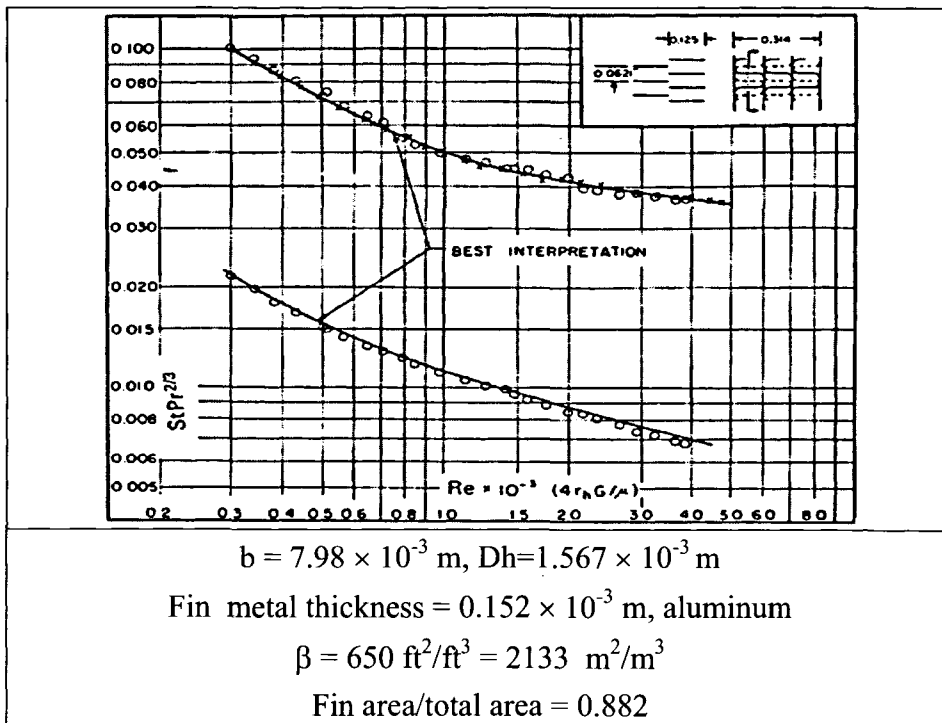
19-Surface 1/8-19.82(D) Strip



20-Surface 1/8-20.06(D) Strip

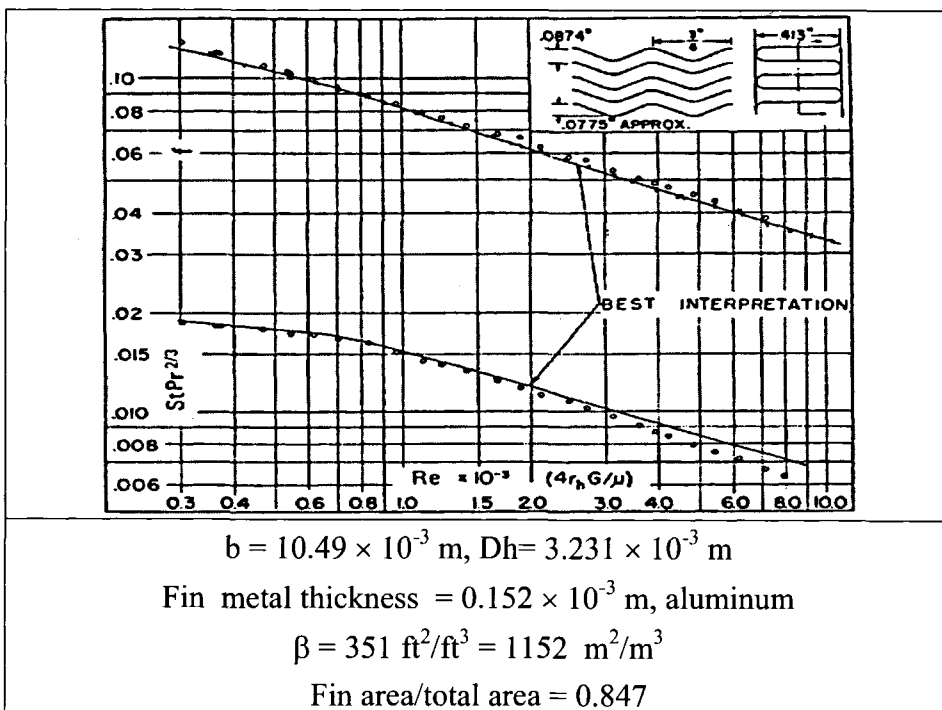


## 21-Surface 1/8-16.12(T) Strip

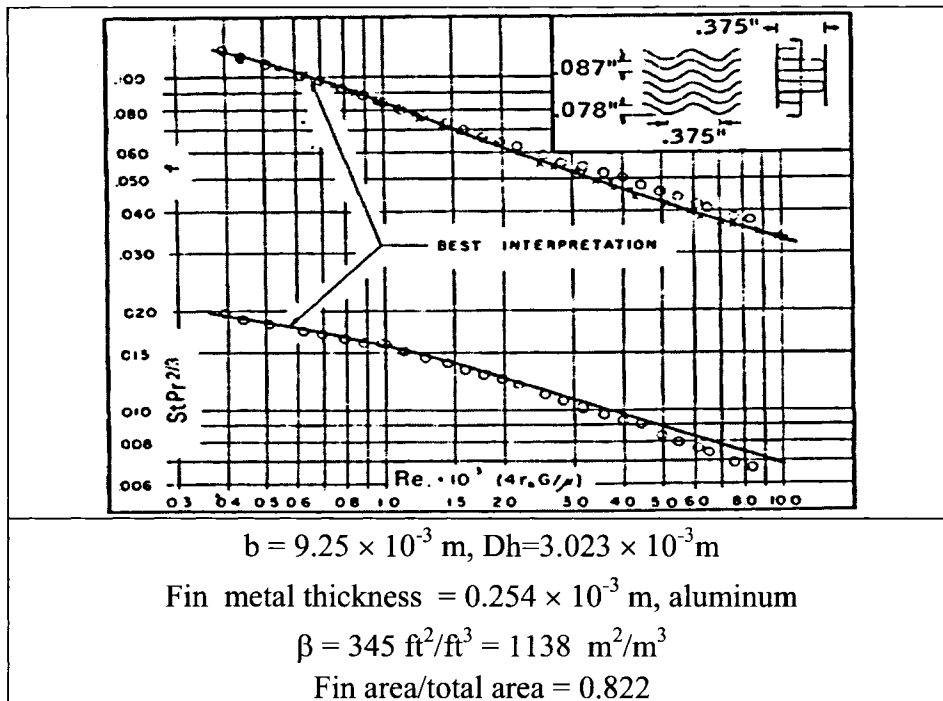


## A-4 Characteristic Curves for Wavy Surfaces

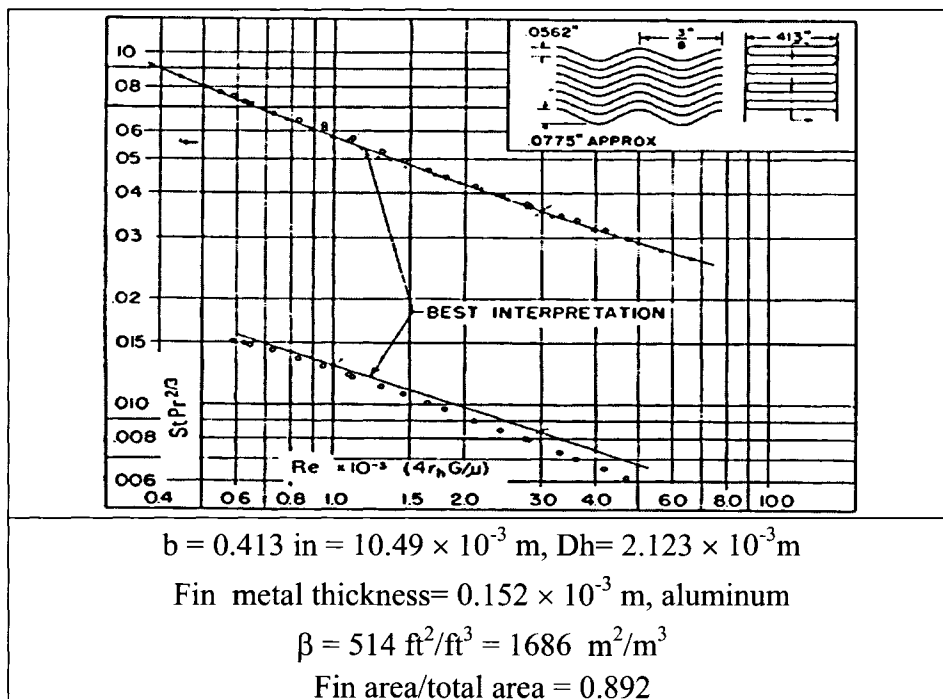
### 1-Surface 11.44-3/8 Wavy



## 2-Surface 11.5-3/8 Wavy

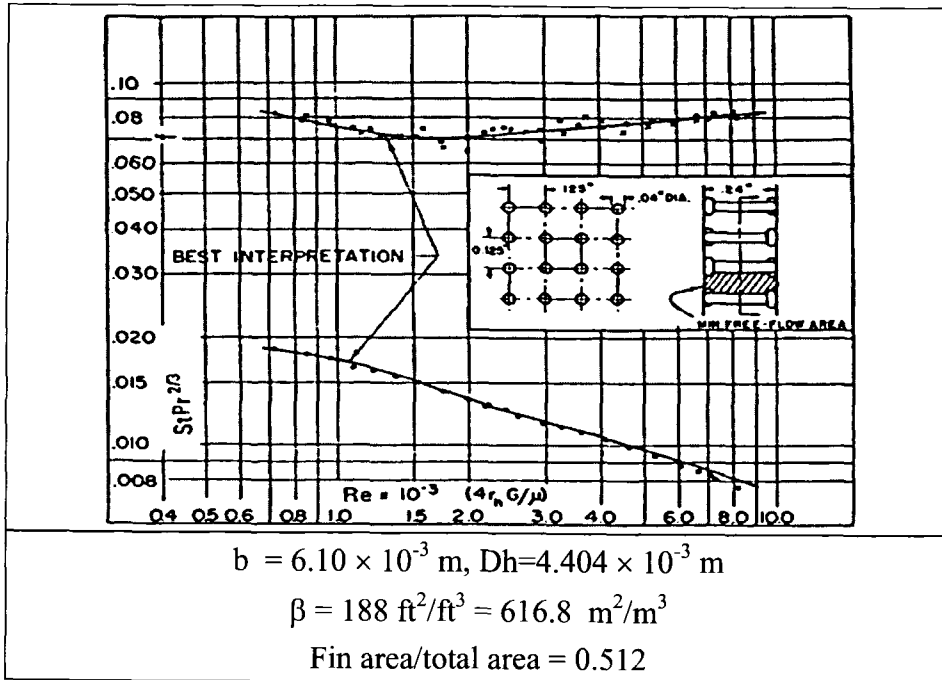


## 3-Surface 17.8-3/8 Wavy

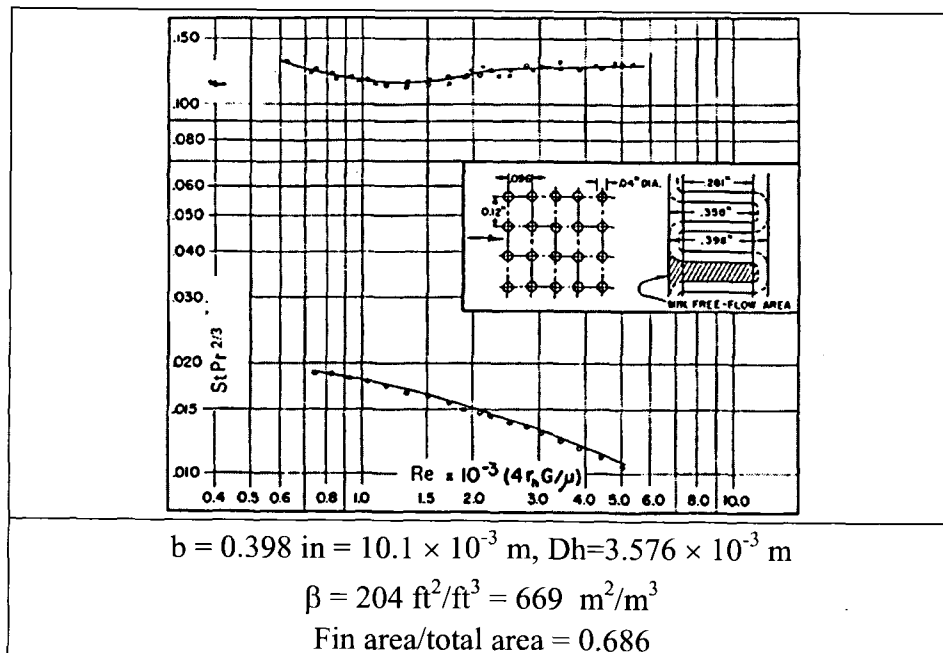


## A-5 Characteristic Curves for Pin Surfaces

### 1-Surface AP-1 Pin

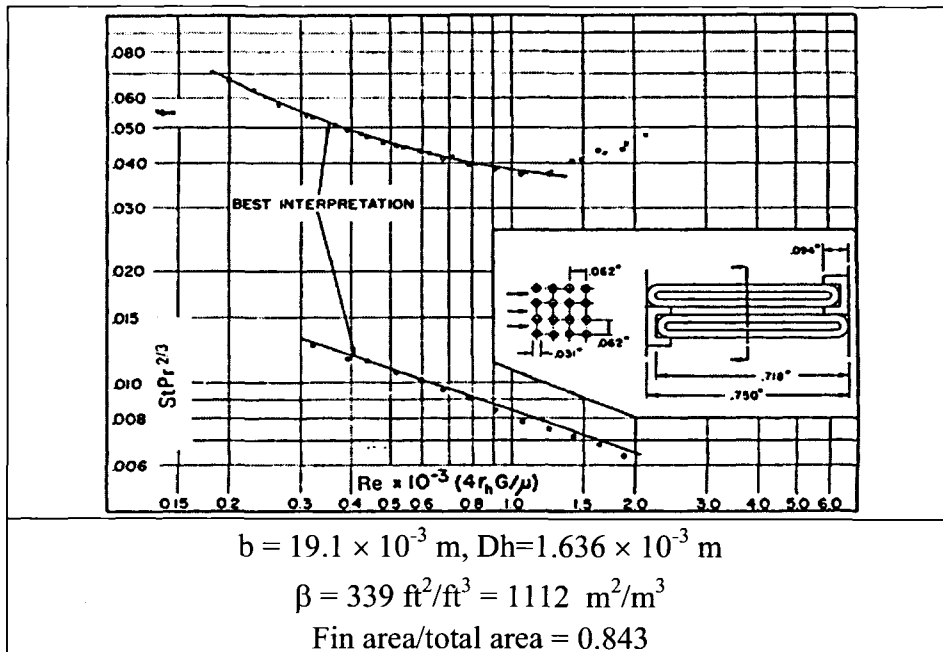


### 2-Surface AP-2 Pin

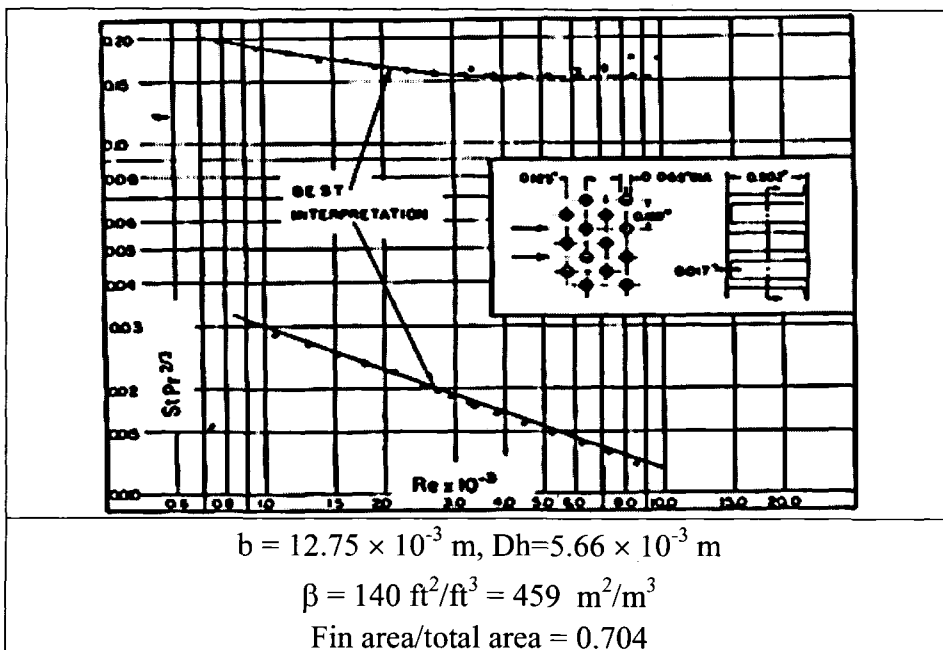




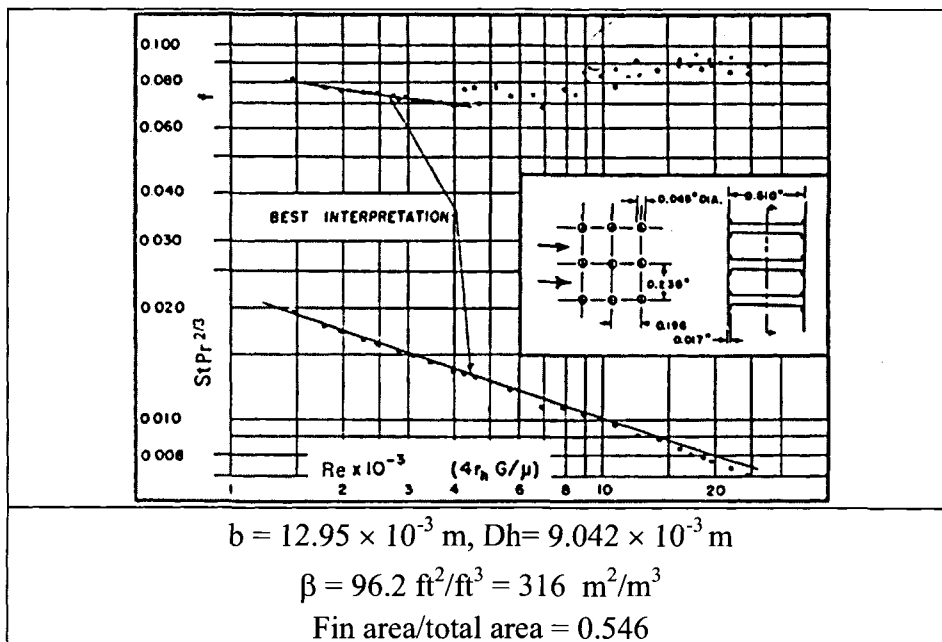
### 3-Surface PF-3 Pin



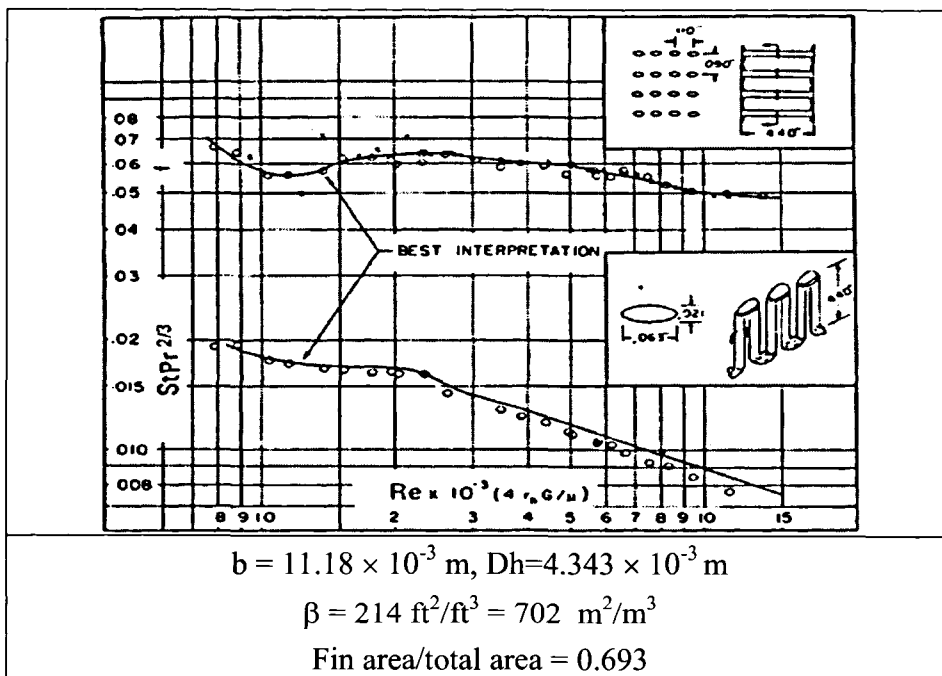
### 4-Surface PF-4(F) Pin



### 5-Surface PF-9(F) Pin

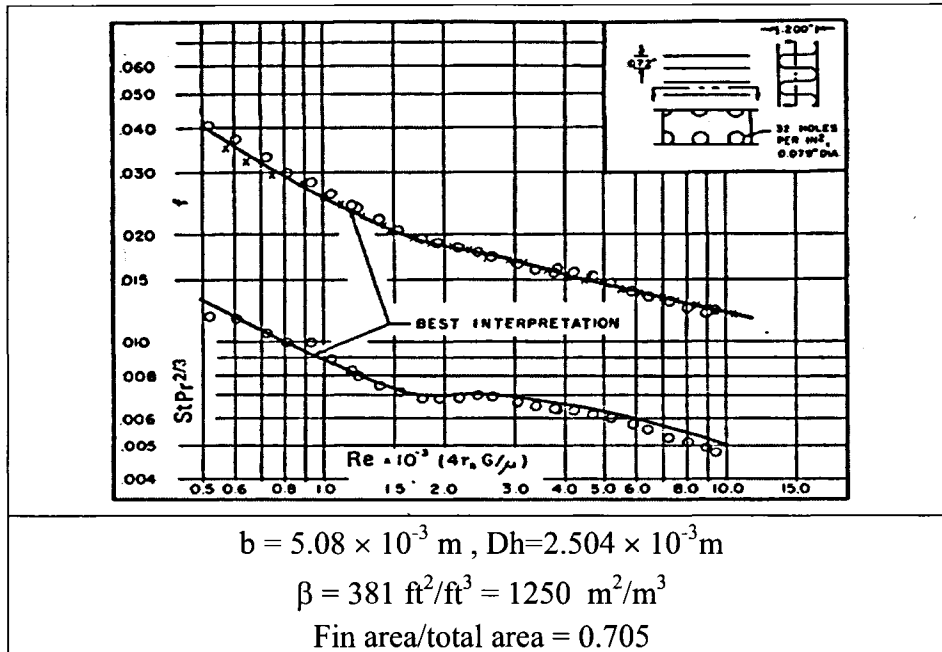


### 6-Surface PF-10(F) Pin

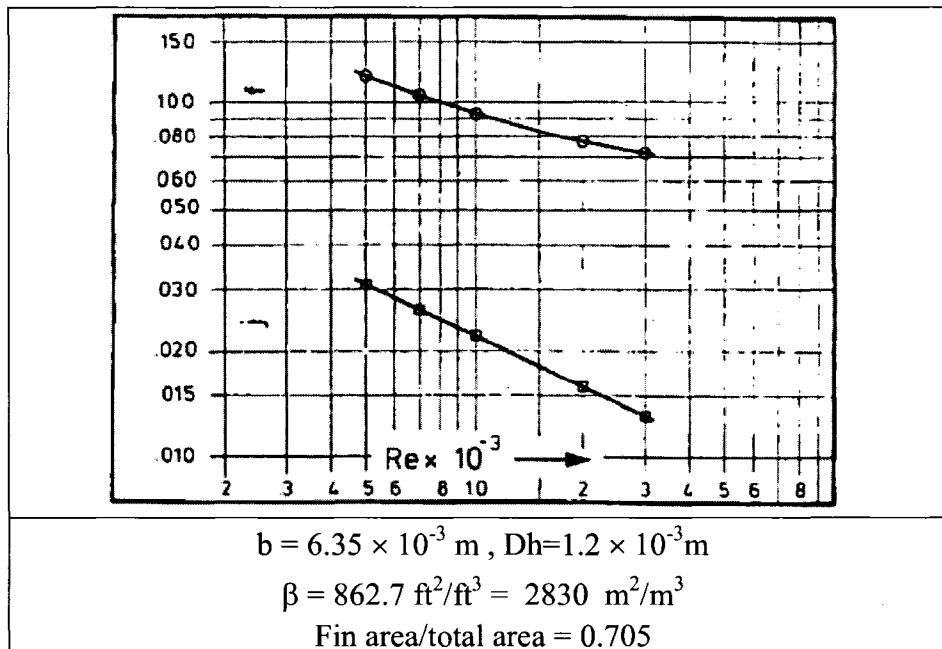


## A-6 Characteristic Curve for Perforated Surface

1-Surface 13.95(P) Perforated

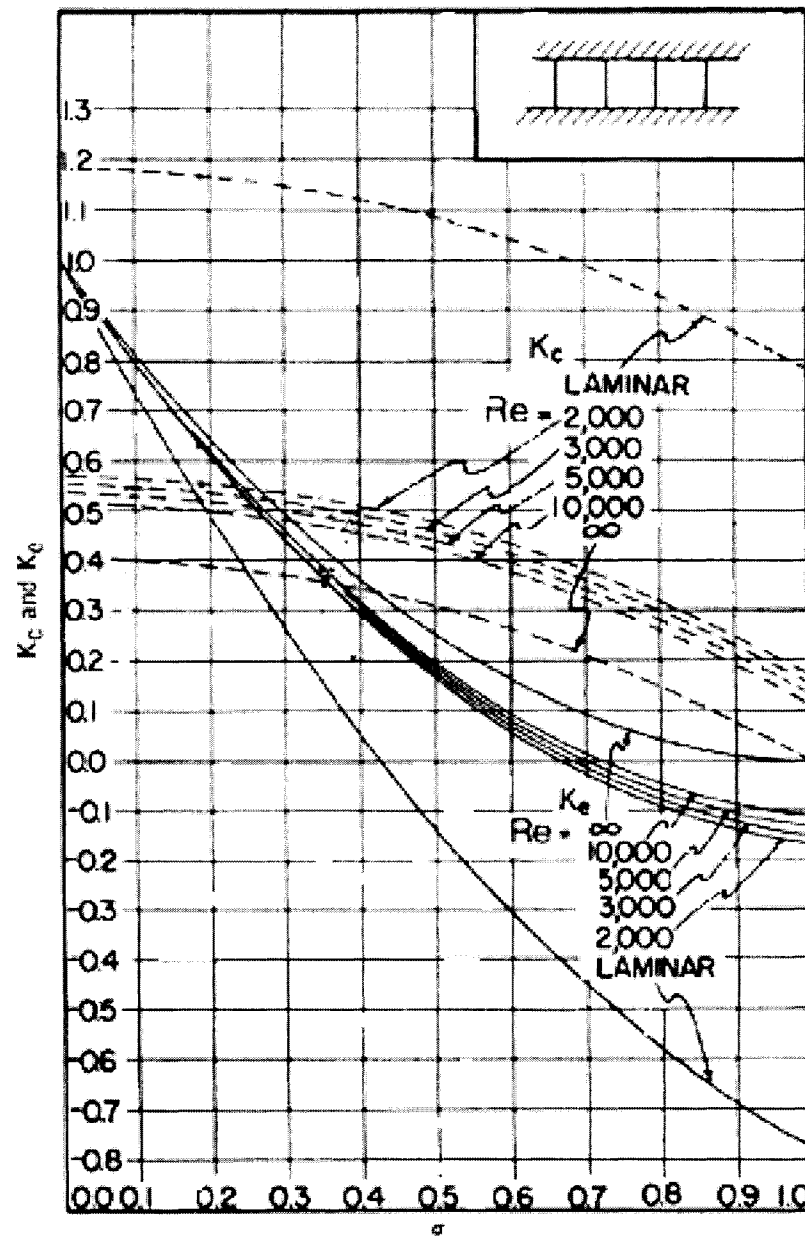


## A-7 Characteristic Curve for Vortex Generator Surface (Brockmeier, 1993)



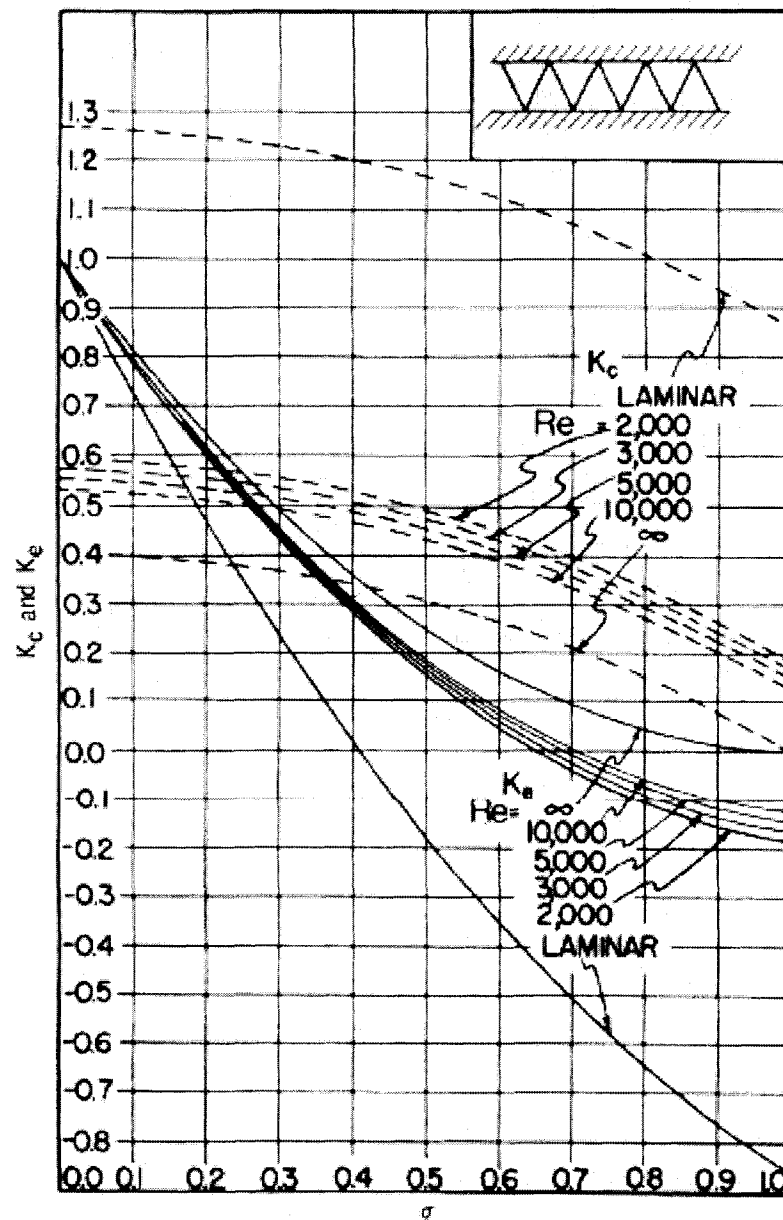
## A.8 Entrance and Exit Losses

### 1-Parallel Passages Entrance and Exit



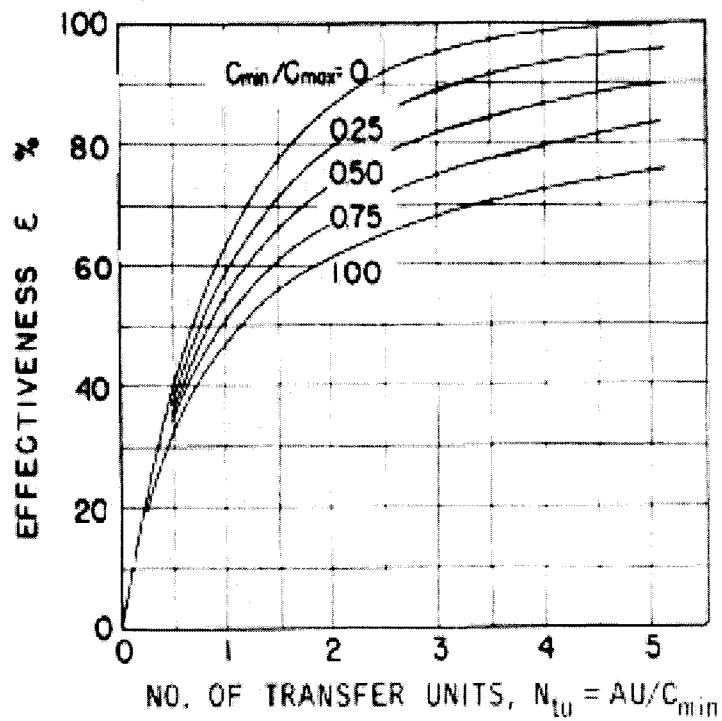
Entrance and Exit Pressure-loss Coefficients for a Multiple Square-Tube Heat Exchanger Core with Abrupt Contraction Entrance and Abrupt Expansion Exit (Kays and London, 1984, Figure 5.4)

## 2-Triangular Passages Entrance and Exit



Entrance and Exit Pressure-loss Coefficients for a Multiple Angular-Tube Heat Exchanger Core with Abrupt Contraction Entrance and Abrupt Expansion Exit (Kays and London, 1984, Figure 5.5)

## A.9 Effectiveness Curve



Heat Transfer Effectiveness as a Function of Number of Transfer Units and Capacity Rate Ratios for Crossflow Exchanger with Fluids Unmixed (Kays and London, 1984, Figure 2-16)

## APPENDIX B – MATHCAD CODE

### B.1 Sizing of Surface 11.94 T Plain

#### Sizing of Compact heat exchanger

##### Surface 11.94T Plain

Given  $T_{ci} := 500$      $T_{hi} := 700$      $T_{co} := 620$      $P_{ci} := 500 \cdot 10^3$

$$\Delta P_c := 5 \cdot 10^3 \quad \Delta P_h := 4 \cdot 10^3 \quad \Phi_i := 100 \cdot 10^3$$

$$T_{cref} := \frac{T_{ci} + T_{co}}{2} \quad m_c := 20 \quad m_h := 20$$

$$T_{cref} = 560 \quad T_{href} := 700$$

$$C_{pc} := 1.041 \quad C_{ph} := 1.075 \quad +$$

$$C_c := m_c \cdot C_{pc}$$

$$C_c := m_c \cdot C_{pc}$$

$$C_c = 20.82$$

$$C_h := m_h \cdot C_{ph}$$

$$C_h = 21.5$$

$$C1 := \frac{C_c}{C_h}$$

$$C1 = 0.968$$

$$\varepsilon := \frac{T_{co} - T_{ci}}{T_{hi} - T_{ci}}$$

$$\varepsilon = 0.6$$

$$T_{ho} := T_{ci} + (1 - C1 \cdot \varepsilon) \cdot (T_{hi} - T_{ci})$$

$$T_{ho} = 583.795$$

$$T_{href} := \frac{T_{hi} + T_{ho}}{2}$$

$$T_{href} = 641.898$$

$$C_{ph} := 1.061$$

$$Ch := m_h \cdot C_{ph}$$

$$Ch = 21.22$$

$$C1 := \frac{C_c}{Ch}$$

$$C1 = 0.981$$

$$\varepsilon := \frac{T_{co} - T_{ci}}{T_{hi} - T_{ci}}$$

$$\varepsilon = 0.6$$

$$T_{ho} := T_{ci} + (1 - C1 \cdot \varepsilon) \cdot (T_{hi} - T_{ci})$$

$$T_{ho} = 583.795$$

$$T_{href} := \frac{T_{hi} + T_{ho}}{2}$$

$$T_{href} = 641.898$$

$$C_{ph} := 1.061$$



$$Ch := mh \cdot Cph$$

$$Ch = 21.22$$

$$C1 := \frac{Cc}{Ch}$$

$$C1 = 0.981$$

$$\varepsilon := \frac{Tco - Tci}{Thi - Tci}$$

$$\varepsilon = 0.6$$

$$Tho := Tci + (1 - C1 \cdot \varepsilon) \cdot (Thi - Tci)$$

$$Tho = 582.262$$

$$NTU := 1.811$$

$$UA := NTU \cdot Cc$$

$$UA = 37.705$$

$$\mu_c := 28.95 \cdot 10^{-6}$$

$$\mu_h := 31.67 \cdot 10^{-6}$$

$$kc := 4.32 \cdot 10^{-2}$$

$$Pr_c := 0.698$$

$$Pr_h := 0.699$$

$$\rho_{ci} := 3.484$$

$$\rho_{hi} := 0.498$$

$$\rho_{co} := 2.782$$

$$\rho_{ho} := 0.572$$

$$\rho_{cm} := \left[ 0.5 \cdot \left( \frac{1}{\rho_{ci}} + \frac{1}{\rho_{co}} \right) \right]^{-1}$$

$$\rho_{cm} = 3.094$$

$$\rho_{hm} := \left[ 0.5 \cdot \left( \frac{1}{\rho_{hi}} + \frac{1}{\rho_{ho}} \right) \right]^{-1}$$

$$\rho_{hm} = 0.532$$

$$NTU1 := 2 \cdot NTU$$

$$NTU1 = 3.622$$

$$NTU2 := C1 \cdot NTU1$$

$$NTU2 = 3.554$$

### **Matching Geometric Criteria**

#### **Selection of Plain fin surface 11.94T**

$$nf := 470$$

$$b := 6.325 \cdot 10^{-3}$$

$$Dh := 2.87 \cdot 10^{-3}$$

$$\delta := 0.152 \cdot 10^{-3} \quad \eta_{oc} := 0.9 \quad \eta_{oh} := 0.9$$

$$\beta := 1289 \quad S := 0.286404$$

$$a := 2 \cdot 10^{-3}$$

$$G_c := \left[ (S) \cdot \frac{\Delta P_c}{P_{ci}} \cdot \frac{2 \cdot \rho_{cm} \cdot \eta_{oc} \cdot P_{ci}}{NTU1 \cdot Pr_c^{0.66}} \right]^{0.5}$$

$$G_c = 52.833$$

$$G_h := \left[ (S) \cdot \frac{\Delta P_h}{P_{hi}} \cdot \frac{2 \cdot \rho_{hm} \cdot \eta_{oh} \cdot P_{hi}}{NTU2 \cdot Pr_h^{0.66}} \right]^{0.5}$$

$$G_h = 19.782$$

$$Re_c := \frac{G_c \cdot Dh}{\mu_c}$$

$$\text{Rec} = 5.238 \times 10^3$$

$$\text{Reh} := \frac{\text{Gh} \cdot \text{Dh}}{\mu \text{h}}$$

$$\text{Reh} = 1.793 \times 10^3$$

$$\text{jc} := 3.228 \cdot 10^{-3}$$

$$\text{jh} := 3.497 \cdot 10^{-3}$$

$$\text{fc} := 0.012$$

$$\text{fh} := 8.472 \cdot 10^{-3}$$

$$\frac{\text{jc}}{\text{fc}} = 0.269$$

$$\frac{\text{jh}}{\text{fh}} = 0.413$$

$$\text{Gc} := \left[ \left( \frac{\text{jc}}{\text{fc}} \right) \cdot \frac{\Delta \text{Pc}}{\text{Pci}} \cdot \frac{2 \cdot \rho_{\text{pcm}} \cdot \eta_{\text{oc}} \cdot \text{Pci}}{\text{NTU1} \cdot \text{Pr}_{\text{c}}^{0.66}} \right]^{0.5}$$

$$\text{Gc} = 51.202$$

$$\text{Gh} := \left[ \left( \frac{\text{jh}}{\text{fh}} \right) \cdot \frac{\Delta \text{Ph}}{\text{Phi}} \cdot \frac{2 \cdot \rho_{\text{phm}} \cdot \eta_{\text{oh}} \cdot \text{Phi}}{\text{NTU2} \cdot \text{Pr}_{\text{h}}^{0.66}} \right]^{0.5}$$

$$\text{Gh} = 23.749$$

$$\text{Rec} := \frac{\text{Gc} \cdot \text{Dh}}{\mu \text{c}}$$

$$\text{Rec} = 5.076 \times 10^3$$

$$\text{Reh} := \frac{\text{Gh} \cdot \text{Dh}}{\mu \text{h}}$$

$$\text{Reh} = 2.152 \times 10^3$$

$$\text{jc} := 3.229 \cdot 10^{-3}$$

$$f_c := 8.532 \cdot 10^{-3}$$

$$j_h := 3.272 \cdot 10^{-3}$$

$$f_h := 0.011$$

$$\frac{j_c}{f_c} = 0.378$$

$$\frac{j_h}{f_h} = 0.297$$

$$G_c := \left[ \left( \frac{j_c}{f_c} \right) \cdot \frac{\Delta P_c}{P_{ci}} \cdot \frac{2 \cdot \rho_{cm} \cdot \eta_{oc} \cdot P_{ci}}{NTU1 \cdot Pr_c^{0.66}} \right]^{0.5}$$

$$G_c = 60.732$$

$$G_h := \left[ \left( \frac{j_h}{f_h} \right) \cdot \frac{\Delta P_h}{P_{hi}} \cdot \frac{2 \cdot \rho_{hm} \cdot \eta_{oh} \cdot P_{hi}}{NTU2 \cdot Pr_h^{0.66}} \right]^{0.5}$$

$$G_h = 20.16$$

$$Re_c := \frac{G_c \cdot D_h}{\mu_c}$$

$$Re_c = 6.021 \times 10^3$$

$$Re_h := \frac{G_h \cdot D_h}{\mu_h}$$

$$Re_h = 1.827 \times 10^3$$

$$j_c := 3.219 \cdot 10^{-3}$$

$$j_h := 3.463 \cdot 10^{-3}$$

$$f_c := 8.182 \cdot 10^{-3}$$

$$f_h := 0.012$$

$$\frac{j_c}{f_c} = 0.393$$

$$\frac{j_h}{f_h} = 0.289$$

$$T_w := \frac{T_{cref} + T_{href}}{2}$$

$$T_w = 600.949$$

$$n := 0.3 - \left( \log \left( \frac{T_w}{T_{cref}} \right) \right)^{0.25}$$

$$n = -0.118$$

$$j_{cc} := j_c \cdot \left( \frac{T_w}{T_{cref}} \right)^n +$$

$$j_{cc} = 3.192 \times 10^{-3}$$

$$j_{hc} := j_h \cdot \left( \frac{T_w}{T_{href}} \right)^0$$

$$j_{hc} = 3.463 \times 10^{-3}$$

$$f_{cc} := f_c \cdot \left( \frac{T_w}{T_{cref}} \right)^{-0.1}$$

$$f_{cc} = 8.124 \times 10^{-3}$$

$$f_{hc} := f_h \cdot \left( \frac{T_w}{T_{href}} \right)^{0.81}$$

$$f_{hc} = 0.011$$

$$h_c := j_{cc} \cdot \frac{G_c \cdot C_{pc}}{P_{rc}} \cdot 10^3$$

$$h_c = 256.483$$

$$h_h := j_{hc} \cdot \frac{G_h \cdot C_{ph}}{P_{rh}} \cdot 10^3$$

$$h_h = 94.046$$

$$l_c := \frac{b}{2} - \delta$$

$$l_c = 3.01 \times 10^{-3}$$

$$mc := \sqrt{\frac{2 \cdot hc}{k \cdot \delta}} \quad +$$

$$mc = 129.899$$

k here is the thermal conductivity of fin Material

$$\eta_{fc} := \frac{\tanh(mc \cdot l_c)}{mc \cdot l_c}$$

$$\eta_{fc} = 0.952$$

$$l_h := \frac{b}{2} - \delta$$

$l_c = l_h$  for the same geometry only

$$l_h = 3.01 \times 10^{-3}$$

$$mh := \sqrt{\frac{2 \cdot hh}{k \cdot \delta}}$$

$$mh = 78.659$$

$$\eta_{fh} := \frac{\tanh(mh \cdot l_h)}{mh \cdot l_h}$$

$$\eta_{fh} = 0.982$$

$$Arc := 0.769$$

$$\eta_{oc} := 1 - (1 - \eta_{fc}) \cdot Arc$$

$$\eta_{oc} = 0.963$$

$$\eta_{oh} := 1 - (1 - \eta_{fh}) \cdot Arc$$

$$\eta_{oh} = 0.986$$

$$U := \left( \frac{1}{\eta_{oc} \cdot h_c} + \frac{1}{\eta_{oh} \cdot h_h} \right)^{-1}$$

$$U = 67.417$$

$$Ac := \frac{20 \cdot C_{pc} \cdot NTU}{U} \cdot 10^3$$

$$Ac = 559.284$$

$$Ah := 559.284$$

$$A_{oc} := \frac{20}{G_c}$$

A<sub>oc</sub> is the free flow area in the cold side  
A<sub>oh</sub> is the free flow area on the hot side

$$A_{oc} := \frac{20}{G_c}$$

$$A_{oc} = 0.329$$

$$A_{oh} := \frac{20}{G_h}$$

$$A_{oh} = 0.992$$

$$\sigma_c := \frac{b \cdot \beta \cdot Dh}{8(b + a)}$$

$$\sigma_c = 0.351$$

$$\sigma_h := 0.351$$

$$A_{fc} := \frac{A_{oc}}{\sigma_c}$$

$$A_{fc} = 0.937$$

$$A_{fh} := \frac{A_{oh}}{\sigma_h}$$

$$A_{fh} = 2.826$$

$$L_c := \frac{D_h \cdot A_c}{4 \cdot A_{oc}}$$

$$L_c = 1.219$$

$$L_h := \frac{D_h \cdot A_h}{4 \cdot A_{oh}}$$

$$L_h = 0.404$$

$$L_{stack} := \frac{A_{frc}}{L_h}$$

$$L_{stack} = 2.317$$

$$r_h := \frac{D_h}{4}$$

### Pressure Drop Calculation

$$K_{ec} := 0.45$$

$$K_{cc} := 0.51$$

$$K_{ch} := 1.22$$

$$K_{eh} := 0.2$$

$$P_c := \frac{G_c^2}{2 \cdot P_{ci} \cdot \rho_{ci}} \cdot \left[ \left( 1 - \sigma_c^2 + K_{cc} \right) + f_{cc} \cdot \frac{L_c \cdot \rho_{ci}}{r_h \cdot \rho_{cm}} + 2 \cdot \left( \frac{\rho_{ci}}{\rho_{co}} - 1 \right) - \left( 1 - \sigma_c^2 - K_{ec} \right) \cdot \frac{\rho_{ci}}{\rho_{co}} \right]$$

$$P_c = 0.018$$

$$\Delta P_{ac} := P_c \cdot P_{ci}$$

$$\Delta P_{ac} = 8.944 \times 10^3$$

$$P_h := \frac{G_h^2}{2 \cdot P_{hi} \cdot \rho_{hi}} \cdot \left[ \left( 1 - \sigma_h^2 + K_{ch} \right) + f_{hc} \cdot \frac{L_h \cdot \rho_{hi}}{r_h \cdot \rho_{hm}} + 2 \cdot \left( \frac{\rho_{hi}}{\rho_{ho}} - 1 \right) - \left( 1 - \sigma_h^2 - K_{eh} \right) \cdot \frac{\rho_{hi}}{\rho_{ho}} \right]$$

$$P_h = 0.03$$

$$\Delta P_{ah} := P_h \cdot P_{hi}$$

$$\Delta P_{ah} = 2.957 \times 10^3$$



The hot side satisfied the pressure drop constraints but the cold side did not satisfy the pressure drop constraints 5 kpa  
we will recalculate  $G_c$  and recalculate the  $j$  colburn factor due to different  $Re$

$$G_c := \frac{[(2 \cdot P_{ci} \cdot \rho_{ci}) \cdot 0.01]^{0.5}}{\left[ \left( 1 - \sigma_c^2 + K_{cc} \right) + f_{cc} \cdot \frac{L_c \cdot \rho_{ci}}{r_h \cdot \rho_{cm}} + 2 \cdot \left( \frac{\rho_{ci}}{\rho_{co}} - 1 \right) - \left( 1 - \sigma_c^2 - K_{ec} \right) \cdot \frac{\rho_{ci}}{\rho_{co}} \right]^{0.5}}$$

$$G_c = 45.41$$

$$G_h := \frac{[(2 \cdot \Phi_{hi} \cdot \rho_{hi}) \cdot 0.04]^{0.5}}{\left[ \left( 1 - \sigma_h^2 + K_{ch} \right) + f_{hc} \cdot \frac{L_h \cdot \rho_{hi}}{r_h \cdot \rho_{hm}} + 2 \cdot \left( \frac{\rho_{hi}}{\rho_{ho}} - 1 \right) - \left( 1 - \sigma_h^2 - K_{eh} \right) \cdot \frac{\rho_{hi}}{\rho_{ho}} \right]^{0.5}}$$

$$G_h = 23.446$$

$$Re_c := \frac{G_c \cdot D_h}{\mu_c}$$

$$Re_c = 4.502 \times 10^3$$

$$Re_h := \frac{G_h \cdot D_h}{\mu_h}$$

$$Re_h = 2.125 \times 10^3$$

$j_{cf}$  is the final value  $j_{hf}$  is the final value for hot fluid

$$j_{cf} := 3.265 \cdot 10^{-3}$$

$$j_{hf} := 3.275 \cdot 10^{-3}$$

$$f_{cf} := 8.704 \cdot 10^{-3}$$

$$f_{hf} := 0.011$$

$$\frac{j_{cf}}{f_{cf}} = 0.375$$

$$\frac{j_{hf}}{f_{hf}} = 0.298$$

$$R_h := \frac{1}{\eta_{oh} \cdot h_h \cdot A_h}$$

$$R_h = 1.928 \times 10^{-5}$$

$$R_c := \frac{1}{\eta_{oh} \cdot h_c \cdot A_c}$$

$$R_c = 7.071 \times 10^{-6}$$

$$T_{wf} := \frac{T_{href} + \left( \frac{R_h}{R_c} \right) \cdot T_{cref}}{1 + \frac{R_h}{R_c}}$$

$$T_{wf} = 581.973$$

$$n := 0.3 - \left( \log \left( \frac{T_{wf}}{T_{cref}} \right) \right)^{0.25}$$

$$n = -0.06$$

$$j_{cfc} := j_{cf} \cdot \left( \frac{T_{wf}}{T_{cref}} \right)^n$$

$$j_{cfc} = 3.258 \times 10^{-3}$$

$$m := -0.1$$

$$f_{cfc} := f_{cf} \cdot \left( \frac{T_{wf}}{T_{cref}} \right)^m$$

$$f_{cfc} = 8.671 \times 10^{-3}$$

$$fh_{fc} := fh_f \cdot \left( \frac{T_{wf}}{T_{href}} \right)^{0.81}$$

$$fh_{fc} = 0.01$$

$$hc := jcf_c \cdot \frac{G_c \cdot C_{pc}}{Pr_c^{0.66666}} \cdot 10^3$$

$$+ \quad hc = 195.696$$

$$Gh = 23.446$$

$$hh := jhf \cdot \frac{G_h \cdot C_{ph}}{Pr_h^{0.66666}} \cdot 10^3$$

$$hh = 103.437$$

$$lc := \frac{b}{2} - \delta$$

$$lc = 3.01 \times 10^{-3} \quad k := 200$$

$$mc := \sqrt{\frac{2 \cdot hc}{k \cdot \delta}}$$

$$mc = 113.467$$

k here is the thermal conductivity of fin Material

$$\eta_{fc} := \frac{\tanh(mc \cdot lc)}{mc \cdot lc}$$

$$\eta_{fc} = 0.963$$

lc=lh for the same geometry only

$$lh := \frac{b}{2} - \delta$$

$$lh = 3.01 \times 10^{-3}$$

$$mh := \sqrt{\frac{2 \cdot hh}{k \cdot \delta}}$$

$$mh = 82.493$$

$$\eta_{fh} := \frac{\tanh(mh \cdot lh)}{mh \cdot lh}$$

$$\eta_{fh} = 0.98$$

$$Arc := 0.769$$

$$\eta_{oc} := 1 - (1 - \eta_{fc}) \cdot Arc$$

$$\boxed{\eta_{oc} = 0.971}$$

$$\eta_{oh} := 1 - (1 - \eta_{fh}) \cdot Arc$$

$$\boxed{\eta_{oh} = 0.985}$$

$$U := \left( \frac{1}{\eta_{oc} \cdot hc} + \frac{1}{\eta_{oh} \cdot hh} \right)^{-1}$$

$$\boxed{U = 66.315}$$

$$Ac := \frac{20 \cdot C_{pc} \cdot NTU}{U} \cdot 10^3$$

$$\boxed{Ac = 568.572}$$

$$\boxed{Ah := 568.572}$$

$$A_{oc} := \frac{20}{G_c}$$

$$\boxed{A_{oc} = 0.44}$$

$$G_h = 23.446$$

$$A_{oh} := \frac{20}{G_h}$$

$$\boxed{A_{oh} = 0.853}$$

$$\sigma_c := \frac{b \cdot \beta \cdot Dh}{8(b + a)}$$

+

$$\boxed{\sigma_c = 0.351}$$

$$\sigma_h := 0.351$$

$$A_{frc} := \frac{A_{oc}}{\sigma_c}$$

$$A_{frc} = 1.254$$

$$A_{fth} := \frac{A_{oh}}{\sigma_h}$$

$$A_{fth} = 2.43$$

$$L_c := \frac{D_h \cdot A_c}{4 \cdot A_{oc}}$$

$$L_c = 0.926$$

$$L_h := \frac{D_h \cdot A_h}{4 \cdot A_{oh}}$$

$$L_h = 0.478$$

$$L_{stack} := \frac{A_{frc}}{L_h}$$

$$L_{stack} = 2.621$$

### Pressure drop Check

$$K_{ec} := 0.38$$

$$K_{cc} := 0.5$$

$$K_{ch} := 0.52$$

$$K_{eh} := 0.35$$

$$P_c := \frac{G_c^2}{2 \cdot P_{ci} \cdot \rho_{ci}} \left[ \left( 1 - \sigma_c^2 + K_{cc} \right) + f_{cfc} \cdot \frac{L_c \cdot \rho_{ci}}{r_h \cdot \rho_{cm}} + 2 \cdot \left( \frac{\rho_{ci}}{\rho_{co}} - 1 \right) - \left( 1 - \sigma_c^2 - K_{ec} \right) \cdot \frac{\rho_{ci}}{\rho_{co}} \right]$$

$$P_c = 8.206 \times 10^{-3}$$

$$\Delta P_{ac} := P_c \cdot P_{ci}$$

$$\Delta P_{ac} = 4.103 \times 10^3$$

$$Ph := \frac{Ch^2}{2 \cdot Phi \cdot phi} \left[ \left( 1 - \sigma h^2 + Kch \right) + fhfc \cdot \frac{Lh \cdot phi}{rh \cdot phm} + 2 \cdot \left( \frac{phi}{rho} - 1 \right) - \left( 1 - \sigma h^2 - Keh \right) \cdot \frac{phi}{rho} \right]$$

$$Ph = 0.039$$

$$Ph = 0.039$$

$$\Delta P_{ah} := Ph \cdot Phi$$

$$\Delta P_{ah} = 3.871 \times 10^3$$

$$Vf := Lc \cdot Lh \cdot Lstack$$

$$Vf = 1.161$$

$$P_{cc} := \frac{\Delta P_{ac} \cdot mc}{\rho cm}$$

$$P_{cc} = 1.505 \times 10^5$$

$$Phh := \frac{\Delta P_{ah} \cdot mh}{\rho hm}$$

$$Phh = 5.998 \times 10^5$$

**Very Good Geometry**

## BIBLIOGRAPHY

- [1] Kays, W.M., & London, A.L. (1984). Compact Heat Exchangers (3<sup>rd</sup> ed). McGraw Hill.
- [2] Hesselgreaves, J.E.(2001).Compact Heat Exchangers Selection, Design and Operation (1<sup>st</sup> ed.). Pergamon.
- [3] Sekulic, D.P.(2006).Heat Transfer Calculations, ed. Kurtz, M., Chapter 29, McGraw Hill.
- [4] Picon-Nunez, M., Polley, G.T., Torres-Reyes, E., Gallegos-Munoz, A. (1999) Surface Selection and Design of Plate Fin Heat Exchangers. *Journal of Applied Thermal Engineering*, Vol.19, pp. 917-931.
- [5] Shah, R., Sekulic, D.P.(2003). Fundamentals of Heat Exchangers Design.(1<sup>st</sup> ed.). John Wiley & Sons, Inc.
- [6] Jacobi, A.M., Shah,R.K. (1995). Heat Transfer Surface Enhancement through the use of Longitudinal Vortices: A Review of Recent Progress. *Experimental Thermal and Fluid Science*, Vol.11, pp. 295-309.
- [7] Brockmeier, U., Guentermann, TH., Fiebig, M.(1993). Performance Evaluation of Vortex Generator Heat Transfer Surface and Comparison with Different High Performance Surfaces. *Int. Journal of Heat and Mass Transfer*, Vol.36 (10), pp.2575-2587.
- [8] Webb, R.L. (1981). Performance Evaluation Criteria for the Use of Enhanced Heat Transfer Surface in Heat Transfer Design. *Int. Journal of Heat and Mass Transfer*, Vol.24, pp.715-726.
- [9] Webb, R.L. (1987). Enhancement of Single Phase Heat Transfer. *Handbook of Single Phase Convective Heat Transfer*, ed. Kakac, S., John Wiley & Sons, New York, Chapter 17.
- [10] Webb, R.L. (1994). Principles of Enhanced Heat Transfer. (1<sup>st</sup> ed.) John Wiley & Sons.

- [11] Hesselgreaves, J.E. (1993). Fin Thickness Optimization of Plate-Fin Heat Exchangers, 1<sup>st</sup>. *Int. Conf. on Aerospace Heat Exchangers Technology*, Palo Alto; Elsevier, New York.
- [12] Cowell, T.A., (1990). A General Method for the Comparison of Compact Heat Transfer Surfaces. *Journal of Heat Transfer*, Vol.112, pp. 289-294.
- [13] Tagliafico, L., Tanda, G., (1996). A Thermodynamic Method for the Comparison of Plate Fin Heat Exchangers Performance. *Journal of Heat Transfer*, Vol.118, pp. 805-809.
- [14] Shah, R.K., (1978). Compact Heat Exchangers Surface Selection Methods. *Int. Heat Transfer Conf.*, Toronto, Vol.4, pp.193-199.
- [15] Sekulic, D.P., (1990). The Second Law Quality of Energy Transformation in a Heat Exchanger. *ASME Journal of Heat Transfer*, Vol.112, pp.295-300.
- [16] Bejan, A., (1982). Entropy Generation Through Heat and Fluid Flow. John Wiley, New York, pp.119-134.
- [17] Bejan, A., (1987). The Thermodynamic Design of Heat and Mass Transfer Processes and Devices. *Int. Journal of Heat Fluid Flow*, Vol.8, pp. 258-276.
- [18] Schenone, C., Tagliafico, L., and Tanda, G., (1991). Second Law Performance Analysis for Offset Strip Fin Heat Exchangers. *Heat Transfer Engineering*, Vol.12, pp.19-27.
- [19] London, A.L., (1982). Economics and Second Law: an Engineering view and Methodology. *Int. Journal of Heat Mass Transfer*, Vol.25, pp. 743-751.
- [20] Cowell, T.A., Heikal, M.R., and Achaichia, A., (1995). Flow and Heat Transfer in Compact Louvered Fin Surfaces. R.K., Shah, and A.Hashemi (Eds.), in: *Aerospace Heat Exchanger Technology*, Elsevier Science Publ. Amsterdam, pp.549-560.
- [21] Bergeles, A.E., Blumenkrantz, A.R., and Taborek, J., (1974). Performance Evaluation Criteria for Selection of Enhanced Heat Transfer Surfaces. *Int. Heat Transfer Conf.*, Tokyo, Vol.11, pp. 239-243.
- [22] Dahlgren, A.I., Jenssen, S.K., (1970). Comparison of Heat Exchangers Surfaces. Chemical and Process Engineering, Heat Transfer Survey, pp.31-33.
- [23] Soland, J.G., Mack, W.M., and Rohsenow, (1978). Performance Ranking of Plate Fin Heat Exchangers Surfaces. *ASME Journal of Heat Transfer*, Vol.100, pp.514-519.
- [24] Sunden, B., Svantesson, J., (1992). Correlations of  $j$  and  $f$  factors for Multi louvered Heat Transfer Surfaces. *Proc., 3<sup>rd</sup> UK Natl. Heat Transfer Conf.*, pp.805-811.



- [25] Sahnoun, A., Webb, R.L., (1992). Prediction of Heat Transfer and Friction for the Louver Fin Geometry," *ASME Journal of Heat Transfer*, Vol.114, pp.893-900.
- [26] Taylor, M.A., (1987). Plate Fin Heat Exchangers: Guide to their Specifications and use, 1<sup>st</sup> Edition, HTFS.
- [27] Shah, R.K., (1988). Plate Fin and Tube Fin Heat Exchangers Design Procedures. In R.K., Shah, E.C., Subbarao, R.A., Mashelkar (Eds.), *Heat Transfer Equipment Design*, Publishing Corporation, Washington, DC, PP.255-265.
- [28] Shah, R.K., (1997). Compact Heat Exchangers and Enhancement Technology for the Process Industries: *Proceedings of the International Conference on Compact Heat Exchangers and Process Industries* Held at the cliff Lodge Center.
- [29] Shah, R.K., (1999). Compact Heat Exchangers and Enhancement Technology for the Process Industries: *Proceedings of the International Conference on Compact Heat Exchangers and Process Industries* Held at the Banff Center.
- [30] Smith, E.M., (1994). Direct Thermal Sizing of Plate Fin Heat Exchangers, in: *Proceedings of the 10<sup>th</sup> International Heat Transfer Conference*, Brighton, UK, pp.55-66.
- [31] Campbell, J.F., Roshnow, W.M., (1992). Gas Turbine Regenerators: A Method for Selecting the optimum Plate Finned Surface Pair for Minimum Core Volume. *Int. Journal of Heat and Mass Transfer*, 35 912 pp.3441-3450.
- [32] Bejan, A., (1978). General Criterion for Rating Heat Exchanger Performance. *Int. Journal of Heat and Mass Transfer*, 21 (5) pp.655-658.
- [33] Andrews, M.J., Fletcher, L.S., (1996). Comparison of Several Heat Transfer Enhancement Technologies for Gas Heat Exchangers. *Journal of Heat Transfer*, 118 (4), pp.897-902.
- [34] Bergeles, A.E., Bunn, R.L., Junkhan, G.H., (1974). Extended Performance Evaluation Criteria for Enhanced Heat Transfer Surfaces. *Letters Heat Mass Transfer*, 1, pp.113-120.
- [35] Kakac, S., Liu, H., (1997). Heat Exchangers Selection, Rating, and thermal Design.(1<sup>st</sup> ed.) pp.115-133, CRC Press, New York.
- [36] Raju, K.S.N., Bansal, J.C., (1981). Design of Plate Heat Exchangers. *Low Reynolds Number in Forced Convection in channels and Bundles*, ASI proceedings, Ankara pp.597-616.
- [37] Sekulic, D., (1990). A Reconsideration of the Definition of Heat Exchangers. *Int. Journal of Heat Mass Transfer*, Vol.33, No.12, pp2748-2750.

- [38] Shah, R.K., (1983). Compact Heat Exchangers Surface Selection, Optimization, and Computer-Aided Thermal Design. In: S. Kakac, R.K. Shah and A.E. Bergles (Eds.), *Low Reynolds Number Flow Heat Exchangers*, Hemisphere, Washington, DC, pp. 845–874.
- [39] Shah, R.K., (1983). Heat Exchanger Basic Design Methods. In: S. Kakac, R.K. Shah and A.E. Bergles (Eds.), *Low Reynolds Number Flow Heat Exchangers*, Hemisphere, Washington, DC, pp. 21–72.
- [40] London, A.L., (1983). Compact Heat Exchangers Design Methodology. In: S. Kakac, R.K. Shah and A.E. Bergles (Eds.), *Low Reynolds Number Flow Heat Exchangers*, Hemisphere, Washington, DC, pp. 815–844.
- [41] Song, D., (1990). The Optimization Analysis Calculation for High Performance Heat Exchanger. S.J. Deng, T.N. Veziroglu, Y.K. Tan, and L.Q. Chen (Eds.) *Heat Transfer Enhancement and Energy Conservation*, pp. 535-542. New York
- [42] Sparrow, E.M., Liu, (1979). Heat-Transfer, Pressure Drop and Performance Relationships for In-Line, Staggered, and Continuous Plate Heat Exchangers. *International Journal of Heat and Mass Transfer*, 22 (12), pp. 1613-1625.
- [43] Wen, J., Li, Y., Zhou, A., Zhang, K., (2006). An Experimental and Numerical Investigation of Flow Patterns in the Entrance of Plate Fin Heat Exchangers. *International Journal of Heat and Mass Transfer*, Vol.49, pp.1667-1678.
- [44] Fiebig, M., (1995). Vortex Generators for Compact Heat Exchangers. *Journal of Enhanced Heat Transfer*, Vol.2, pp.43-61.
- [45] Brckmeier, U., Fiebig, M., Guntermann, T., and Mitra, N.K. (1989). Heat Transfer Enhancement in Fin-Plate Heat Exchangers by Wing Type Vortex Generators. *Chemical Engineering Technology*, Vol.12, pp.288-294.
- [46] Guntermann, T., (1992). Dreidimensionale Stationäre und Selbst-erschwingende Strömungs- und Temperaturfelder in Hochleistungswärmeübertragern mit Wirbelerzeugern. Dissertation, Ruhr University.
- [47] Brckmeier, U., Guntermann, T., and Fiebig, M., (1993). Performance Evaluation of a Vortex Generator Heat Transfer Surfaces. *International Journal of Heat and Mass Transfer*, Vol.36, pp.2575-2587.
- [48] Jacobi, A.M, Shah, R.K., (1998). Air Side Flow and Heat Transfer in Compact Heat Exchangers; A Discussion of Enhancement Mechanisms. *Heat Transfer Engineering*, Vol.19 (4), pp.29-41.

- [49] Stevens A., Adderley, CI and Cool, T., (2001). Using Genetic Algorithms to Optimize Heat Exchange. *Proceedings of UKSIM Conference*.
- [50] Zhao, H., Qian, Y., Gao, F., Wang, F., (2003). Simulation on thermal integrity of the fin/tube brazed joint of heat exchangers. *Journal of Materials Science and Technology*. Volume 19,PP. 71-72.
- [51] Incropera, F.P., Dewitt, D.P., (2002). *Introduction to Heat Transfer*. 4<sup>th</sup> Edition pp.637-642. John Wiley & Sons.
- [52] Hewitt, G.F., Shires, G.L., Bott, R.L., (1994). *Process Heat Transfer*. pp. 11-42.

VITA  
Graduate College  
University of Nevada, Las Vegas

Ibrahim Mohamed Khalil

Local Address:

4320 Escondido Street  
Apartment # 15  
Las Vegas, Nevada 89119

Permanent Address:

Hallabo, Street 94  
Fifth Floor  
El-Gomrok, Alexandria  
Egypt

Degree:

Bachelor of Science, Mechanical Engineering, 2000  
Alexandria University, Alexandria

Publications:

Khalil, Ibrahim, Sham A., Boehm R.F ., "Wet or Dry Cooling" *Proceedings of ISCE* , July 08-13, 2006, Denver, CO.

Thesis Title:

Performance of Plate Fin Compact Heat Exchangers

Thesis Examination Committee:

Chairperson, Dr. Robert F. Boehm, Ph. D.  
Committee Member, Dr. Yitung Chen, Ph. D.  
Committee Member, Dr. Samir Moujaes, Ph. D.  
Graduate Faculty Representative, Dr. Moses Karakouzian, Ph. D.